NASA Technical Paper 1562

Elastic Constants for Superplastically Formed/Diffusion-Bonded Corrugated Sandwich Core

William L. Ko

MAY 1980

19960319 054

NASA

NASA Technical Paper 1562

Elastic Constants for Superplastically Formed/Diffusion-Bonded Corrugated Sandwich Core

William L. Ko
Dryden Flight Research Center
Edwards, California

ELASTIC CONSTANTS FOR SUPERPLASTICALLY

FORMED/DIFFUSION-BONDED CORRUGATED SANDWICH CORE

William L. Ko
Dryden Flight Research Center

INTRODUCTION

Since the first successful application of the sandwich structure in the British all-wood-constructed Mosquito fighter-bomber aircraft during World War II, the use of sandwich structural technology (mainly metallic) has become widespread in aerospace design (for example, for wings, wall panels, webs of beams, tails, and so forth).

The typical sandwich structure consists of two relatively thin high strength face sheets separated by and bonded to a relatively thick, low density, low strength core. Thus, the sandwich structure is characterized by light weight and high flexural stiffness.

The most extensively used sandwich structure in aerospace technology is the honeycomb core sandwich structure, which is usually made of aluminum face sheets and an aluminum or titanium honeycomb core. In this structure, the honeycomb cell generatrix is perpendicular to the face sheet and, therefore, the bonding between the honeycomb core and the face sheet can be achieved only by line contact. This is the major drawback of this type of sandwich structure, because the line-contact bonding between the honeycomb cross section and the face sheet can easily lose its bonding integrity as a result of corrosion.

In recent years, an entirely new process known as superplastic forming with concurrent diffusion bonding (SPF/DB) has emerged (ref. 1). This process involves the fabrication of sandwich structures by using superplastic materials, such as the titanium alloys. The SPF/DB process capitalizes on two natural characteristics of titanium alloys. The first is superplasticity, which is the ability of a material to undergo large plastic deformations (up to 1000 percent strain) at high temperatures without localized thinning (or necking). Second, the alloys have the capacity for

solid state diffusion bonding, which is the joining of the superplastic alloys under pressure at elevated temperatures without melting or the use of bonding agents.

Utilizing the above two characteristics, an SPF/DB sandwich structure can be fabricated by diffusion bonding at least three superplastic alloy sheets at selected areas and then superplastically expanding apart the face sheets by pressure inside the containment (or die cavity) to give the desired configuration. This new process eliminates the use of bonding agents, and allows surface-contact bonding instead of line-contact bonding as in the case of honeycomb sandwich structures. Through this new technique, a number of new shapes and symmetries for the sandwich core become possible. These include corrugated cores, truss cores (the limit case of corrugated core), dimpled cores, and sine-wave cores (where the axis of corrugation is sinusoidal in shape), which are described in reference 1; and egg-carton-like cores, which have projections that are shaped like hollow truncated cones, hollow truncated squares, or hexagonal pyramids and are arranged in square or hexagonal arrays (refs. 2 and 3).

The corrugated, the truss, and the sine-wave cores have relatively high out-of-plane bending stiffness in the direction of the corrugation axis, but they have very low out-of-plane bending stiffness in the direction transverse to the corrugation axis. The egg-carton-like cores have relatively low flexural stiffness in any in-plane direction. However, if these cores are joined with face sheets, the overall stiffness of the sandwich structure is greatly enhanced.

In most of the SPF/DB sandwich structures, the sandwich cores are relatively flexible in the thickness direction, and there is usually a sharp angle at the juncture of the face sheet and core. Thus, if the swelling modes of vibration (that is, the oscillation of the two face sheets in opposite directions) should occur under aerospace service conditions (for example, engine noise, high frequency flutter, and so forth), these vibration modes could create situations favorable to the formation of fatigue cracks at the face sheet/core junction sites, resulting in possible damage to the face sheet/core bond.

In order to study this problem, the assumption that the sandwich core is rigid in the thickness direction (which is the conventional approach to the analysis of sandwich plates) must be abandoned, and the sandwich core must be treated as it is or as an equivalent homogeneous elastic solid. For the latter case, the effective elastic constants for the sandwich core are needed.

The purpose of this paper is to present formulae and graphs for evaluating the effective elastic constants for the SPF/DB corrugated sandwich core. The paper also discusses the relative structural advantages and disadvantages of this sandwich core as compared with the conventional honeycomb sandwich core.

2

SYMBOLS

B	nondimensional parameter associated with displacement (δ)
b	one-half of horizontal projected length of circular arcs and straight diagonal segments of corrugation leg
D	bending stiffness per unit width
d	one-half of the length of straight diagonal segment of corrugation leg
E	modulus of elasticity
F	vertical load in sandwich thickness direction, per unit width in x-direction, concentrated at end points of corrugation leg
f	length of corrugation flat segment
G	shear modulus
H	horizontal load (in y-direction), per unit width in x-direction, concentrated at end points of corrugation leg
h_c	corrugated core thickness (vertical distance between upper and lower corrugation flat segment centerlines)
ℓ	length of one corrugation leg
M	bending moment
p	one-half of corrugation pitch (or half wave length of corrugation)
R	radius of circular arc segments of corrugation leg
s	distance measured along corrugation centerline
t	thickness
x, y, z	Cartesian coordinates
γ	effective shear strain of corrugated core in yz-plane
δ	displacement
ε	strain
θ	corrugation angle (angle between centerline of straight diagonal segment and that of corrugation flat segment)

ν   Poisson ratio

ρ   density

σ   stress

τ $= \dfrac{F}{h_c} = \dfrac{H}{p}$, averaged shear stress in corrugated core in yz-plane

ψ   angle between tangent to corrugation leg centerline and a horizontal line

GEOMETRY OF SANDWICH PLATE

Figure 1 shows an SPF/DB corrugated core sandwich plate. This structure is formed by diffusion bonding three superplastic alloy sheets (two face sheets and one core sheet) in selected areas (ref. 2) and then superplastically expanding the multiple sheet pack inside a die cavity by using gas pressure. This structure is slightly different from the conventional corrugated core sandwich structure because the corrugation leg does not have uniform thickness. Because of superplastic expansion, the diagonal segment of the corrugation leg is always thinner than the flat segment (crest or trough) of the corrugation leg, which has a thickness that is nearly the preexpansion thickness. Thus, the results given by reference 4, which are for the corrugation leg of uniform thickness, cannot be used to evaluate the present structure without considerable modification.

This report analyzes only a symmetric corrugation (that is, a corrugation symmetric with respect to the middle surface of the sandwich plate). The element of the corrugation referred to as the corrugation leg is assumed to be made up of circular arc and straight diagonal segments of thickness t_c and of flat segments of thickness t_f (the preexpansion thickness of the core sheet).

ELASTIC CONSTANTS FOR SUPERPLASTICALLY FORMED/DIFFUSION-BONDED CORRUGATED SANDWICH CORE

The elastic constants evaluated in the following discussion are the effective (or averaged) elastic constants for a homogeneous sandwich core equivalant to the actual sandwich core. This idealization can be adequate when the sandwich plate width (normal to the corrugation axis) is many times the corrugation pitch. The analysis assumes that deformation is infinitesimal and that there is no local buckling of the sandwich structure.

4

Evaluation of Effective Modulus of Elasticity E_x

and Effective Shear Moduli G_{xy} and G_{zx}

The modulus of elasticity in the x-direction, E_x, and the shear moduli in the xy- and zx-planes, G_{xy} and G_{zx}, respectively, may be obtained by modifying the results given in reference 4 by applying the rule of mixture to account for the nonuniform thickness of the corrugation leg. These elastic constants can be expressed in the forms

$$E_x = E_c \frac{1}{ph_c} \left[ft_f + (\ell - f)t_c \right] = E_c \frac{t_f}{h_c} \tag{1}$$

$$G_{xy} = G_c \frac{p}{\ell^2 h_c} \left[ft_f + (\ell - f)t_c \right] = G_c \frac{p^2 t_f}{\ell^2 h_c} \tag{2}$$

$$G_{zx} = G_c \frac{h_c}{\ell^2 p} \left[ft_f + (\ell - f)t_c \right] = G_c \frac{h_c t_f}{\ell^2} \tag{3}$$

where the last terms in the equations are for constant volume superplastic deformations (neglecting small elastic deformations) for which the condition $ft_f + (\ell - f)t_c = pt_f$ holds and

E_c modulus of elasticity of the corrugated core material

G_c shear modulus of the corrugated core material

p one-half of corrugation pitch (or one-half of a wave length of corrugation)

h_c corrugated core thickness (vertical distance between centerlines of the upper and lower corrugation flat segments)

ℓ length of one corrugation leg

f length of corrugation flat segment

For constant volume superplastic deformations, the superplastic incompressibility condition used in equations (1), (2), and (3) may be used to relate the two corrugation leg thicknesses t_c and t_f in the forms

$$\frac{t_c}{t_f} = \frac{p - f}{\ell - f} = \frac{b}{d + R\theta} \tag{4}$$

or

$$\frac{t_c}{t_f} = \frac{\cos\theta + 2\frac{R}{h_c}(1 - \cos\theta)}{1 + 2\frac{R}{h_c}\left[\theta\sin\theta - (1 - \cos\theta)\right]}$$ (5)

where

b one-half of the horizontal projected length of the circular arc and straight diagonal segments of the corrugation leg

d one-half of the length of the straight diagonal segment of the corrugation leg

R radius of circular arc segment of the corrugation leg

θ corrugation angle (angle between the centerline of the straight diagonal segment and the centerline of the corrugation flat segment)

<center>Evaluation of Modulus of Elasticity E_y</center>

Figure 2 shows a free body diagram of a corrugation leg subjected to a horizontal loading, H (per unit width in the x-direction). Neglecting the Timoshenko beam shear deformation of the corrugation leg because of its thinness, the total horizontal displacement of point 0 with respect to point 0′, δ_y^H, may be expressed as the summation of bending and stretching effects. Thus, one can write

$$\delta_y^H = \underbrace{\int_0^{\ell} \frac{M(-1)z'}{E_c I_i}\,ds}_{\text{(Bending)}} + \underbrace{\int_0^{\ell} \frac{H\cos\psi}{E_c t_i}\cos\psi\,ds}_{\text{(Stretching)}}$$ (6)

where the integrals are taken from point 0 to point 0′ (that is, one corrugation leg) and

s distance measured along the corrugation leg centerline

ψ angle between tangent to the corrugation leg centerline and a horizontal line

M $= H\left(\dfrac{h_c}{2} - z'\right)$, bending moment at a cross section of the corrugation leg

6

z' vertical distance from point 0

I_i $= \frac{1}{12} t_i^3$, moment of inertia of a corrugation leg cross section that is normal to s and parallel to the x-axis. In the region of the corrugation flat segment, $I_i = I_f$; and in the circular arc and straight diagonal segments, $I_i = I_c$

t_i thickness of a corrugation leg. In the region of the corrugation flat segment, $t_i = t_f$; and in the circular arc and straight diagonal segments, $t_i = t_c$

The (-1) in the bending term of equation (6) indicates that the displacement of point 0 with respect to point $0'$ is to the left in figure 2 (ref. 5).

The following relationships between the geometric parameters of the corrugation will be useful in the process of evaluating equation (6) and others to follow:

$$\frac{d}{h_c} = \frac{1}{2 \sin \theta} \left[1 - 2 \frac{R}{h_c} (1 - \cos \theta) \right] \tag{7}$$

$$\frac{f}{h_c} = \frac{p}{h_c} - 2 \frac{d}{h_c} \cos \theta - 2 \frac{R}{h_c} \sin \theta \tag{8}$$

$$\frac{b}{h_c} = \frac{1}{2} \left(\frac{p}{h_c} - \frac{f}{h_c} \right) \tag{9}$$

$$\frac{\ell}{h_c} = \frac{f}{h_c} + 2 \frac{d}{h_c} + 2 \frac{R}{h_c} \theta \tag{10}$$

Making use of the equations (7) to (10) in the integration of equation (6), one obtains

$$\delta_y^H = \frac{H h_c^3}{E_c I_c} B_y^H \tag{11}$$

where

$$B_y^H \equiv \frac{2}{3}\left(\frac{d}{h_c}\right)^3 \sin^2\theta + \frac{1}{2}\left(\frac{R}{h_c}\,\theta + \frac{1}{2}\frac{f}{h_c}\frac{I_c}{I_f}\right)$$

$$- \left(\frac{R}{h_c}\right)^2\left[\left(2 - 3\frac{R}{h_c}\right)(\theta - \sin\theta) + \frac{R}{h_c}\sin\theta\,(1 - \cos\theta)\right]$$

$$+ \frac{I_c}{h_c^2 t_c}\left[\frac{f}{h_c}\frac{t_c}{t_f} + 2\frac{d}{h_c}\cos^2\theta + \frac{R}{h_c}(\theta + \sin\theta\cos\theta)\right] \tag{12}$$

The modulus of elasticity E_y is then given by

$$E_y = \frac{\sigma_y}{\varepsilon_y} = \frac{\dfrac{H}{h_c}}{\dfrac{\delta_y^H}{p}} \tag{13}$$

$$= \frac{E_c}{B_y^H}\frac{I_c p}{h_c^4} \tag{14}$$

where σ_y and ε_y are, respectively, the effective stress and the effective strain of the corrugated core in the y-direction.

Evaluation of Poisson Ratio ν_{zy}

As illustrated by figure 2, again, the vertical dispacement of point 0 with respect to point 0′ under horizontal loading H, δ_z^H, may be written

$$\delta_z^H = \int_0^\ell \frac{M(-1)y'}{E_c I_i}\,ds - \int_0^\ell \frac{H\cos\psi}{E_c t_i}\sin\psi\,ds \tag{15}$$

$$\underbrace{\qquad\qquad}_{\text{(Bending)}} \underbrace{\qquad\qquad}_{\text{(Stretching)}}$$

where y' is the horizontal distance from point 0, and the (−1) in the bending term indicates that the displacement of point 0 with respect to point 0′ is downward (ref. 5).

After integration and making use of relationships (7) to (10), equation (15) becomes

$$\delta_z^H = \frac{H h_c^3}{E_c I_c} B_z^H \tag{16}$$

where

$$B_z^H = \frac{2}{3}\left(\frac{d}{h_c}\right)^3 \sin\theta \cos\theta + \frac{1}{2}\frac{I_c}{I_f}\left[\frac{1}{4}\left(\frac{p}{h_c}\right)^2 - \left(\frac{b}{h_c}\right)^2\right]$$

$$+ \frac{R}{h_c}\left\{\frac{b}{h_c}\theta - 2\frac{Rb}{h_c^2}(\theta - \sin\theta) - \frac{R}{h_c}(1 - \cos\theta)\left[1 - \frac{R}{h_c}(1 - \cos\theta)\right]\right\}$$

$$- \frac{I_c}{h_c^2 t_c}\left(2\frac{d}{h_c}\sin\theta\cos\theta + \frac{R}{h_c}\sin^2\theta\right) \tag{17}$$

The Poisson ratio ν_{zy}, which is associated with loading in the y-direction only, is then given by

$$\nu_{zy} = -\frac{\varepsilon_z}{\varepsilon_y} = \frac{\dfrac{\delta_z^H}{h_c}}{\dfrac{\delta_y^H}{p}} \tag{18}$$

$$= \frac{p}{h_c}\frac{B_z^H}{B_y^H} \tag{19}$$

where ε_z is the average strain in the z-direction of the corrugated core.

Evaluation of Modulus of Elasticity E_z

Figure 3 shows a free body diagram of the corrugation leg subjected to a vertical (sandwich thickness direction) loading, F, per unit width in the x-direction. The loading is concentrated at points 0 and 0′. Neglecting the Timoshenko beam shear deformation, as before, the total vertical displacement, δ_z^F, of point 0 with respect to

9

point 0′ may be written as the summation of the bending and stretching effects. Thus,

$$\delta_z^F = \int_0^\ell \frac{M(-1)y'}{E_c I_i} \, ds + \int_0^\ell \frac{F \sin \psi}{E_c t_i} \sin \psi \, ds \qquad (20)$$

$$\underbrace{\hspace{3.5cm}}_{\text{(Bending)}} \quad \underbrace{\hspace{4cm}}_{\text{(Stretching)}}$$

where the (-1) in the bending term indicates that the movement of point 0 with respect to point 0′ is upward (ref. 5). In this case, $M = F\left(\frac{p}{2} - y'\right)$. Taking equations (7) to (10) in the integration of equation (20), we then obtain

$$\delta_z^F = \frac{F h_c^3}{E_c I_c} \, B_z^F \qquad (21)$$

where

$$B_z^F = \frac{2}{3}\left(\frac{d}{h_c}\right)^3 \cos^2 \theta + \frac{2}{3}\frac{I_c}{I_f}\left[\frac{1}{8}\left(\frac{p}{h_c}\right)^3 - \left(\frac{b}{h_c}\right)^3\right]$$

$$+ \frac{R}{h_c}\left[2\left(\frac{b}{h_c}\right)^2 \theta - 4\frac{Rb}{h_c^2}\,(1 - \cos \theta) + \left(\frac{R}{h_c}\right)^2 (\theta - \sin \theta \cos \theta)\right]$$

$$+ \frac{I_c}{h_c^2 t_c}\left[2\frac{d}{h_c}\sin^2 \theta + \frac{R}{h_c}\,(\theta - \sin \theta \cos \theta)\right] \qquad (22)$$

The modulus of elasticity E_z is then given by

$$E_z = \frac{\sigma_z}{\varepsilon_z} = \frac{\dfrac{F}{p}}{\dfrac{\delta_z^F}{h_c}} \qquad (23)$$

$$= \frac{E_c\, I_c}{B_z^F\, p h_c^2} \qquad (24)$$

where σ_z is the effective stress in the corrugated core in the z-direction.

10

If the vertical loading F is distributed over the corrugation flat segment, then B_z^F in equation (22) will have the form

$$B_z^F = \frac{2}{3}\left(\frac{d}{h_c}\right)^3 \cos^2 \theta + \underline{\frac{1}{4}\frac{f}{h_c}\frac{I_c}{I_f}\left[\left(\frac{p}{h_c}\right)^2 - \frac{7}{6}\frac{pf}{h_c^2} + \frac{3}{8}\left(\frac{f}{h_c}\right)^2\right]}$$

$$+ \frac{R}{h_c}\left[2\left(\frac{b}{h_c}\right)^2 \theta - 4\frac{Rb}{h_c^2}(1 - \cos \theta) + \left(\frac{R}{h_c}\right)^2 (\theta - \sin \theta \cos \theta)\right]$$

$$+ \frac{I_c}{h_c^2 t_c}\left[2\frac{d}{h_c}\sin^2 \theta + \frac{R}{h_c}(\theta - \sin \theta \cos \theta)\right] \tag{25}$$

It is apparent that the only difference between equations (22) and (25) occurs in the second term on the right side of each equation (underlined). Equation (25) will not be used in the subsequent analyses.

Evaluation of Poisson Ratio ν_{yz}

From figure 3, the horizontal displacement, δ_y^F, of point 0 with respect to point 0′ under the concentrated vertical loading, F, is given by

$$\delta_y^F = \underbrace{\int_0^\ell \frac{M(-1)z'}{E_c I_i}\,ds}_{\text{(Bending)}} - \underbrace{\int_0^\ell \frac{F \sin \psi}{E_c t_i}\cos \psi\,ds}_{\text{(Stretching)}} \tag{26}$$

where the (-1) in the integrand of the bending term defines the direction of movement of point 0 with respect to point 0′ to be to the right in figure 3 (ref. 5).

After integration of equation (26), with relationships (7) to (10) taken into account, it follows that

$$\delta_y^F = \frac{Fh_c^3}{E_c I_c} B_y^F \tag{27}$$

where

$$B_y^F = B_z^H \tag{28}$$

11

Then the Poisson ratio ν_{yz}, which is associated with loading in the z-direction only, is given by

$$\nu_{yz} = -\frac{\varepsilon_y}{\varepsilon_z} = \frac{\dfrac{\delta_y^F}{p}}{\dfrac{\delta_z^F}{h_c}} \qquad (29)$$

$$= \frac{h_c}{p} \frac{B_y^F}{B_z^F} \qquad (30)$$

If F is distributed over the corrugation flat segment, then B_y^F in equation (28) is modified to

$$B_y^F = \frac{2}{3}\left(\frac{d}{h_c}\right)^3 \sin\theta\cos\theta + \underline{\frac{1}{4}\frac{f}{h_c}\frac{I_c}{I_f}\left(\frac{p}{h_c} - \frac{2}{3}\frac{f}{h_c}\right)}$$

$$+ \frac{R}{h_c}\left\{\frac{b}{h_c}\theta - 2\frac{Rb}{h_c^2}(\theta - \sin\theta) - \frac{R}{h_c}(1 - \cos\theta)\left[1 - \frac{R}{h_c}(1 - \cos\theta)\right]\right\}$$

$$- \frac{I_c}{h_c^2 t_c}\left(2\frac{d}{h_c}\sin\theta\cos\theta + \frac{R}{h_c}\sin^2\theta\right) \qquad (31)$$

All terms are identical to those in equation (17) except the second term on the right side (underlined). Again, equation (31) will not be used in the subsequent analyses.

For the concentrated vertical loading, F, the following relationship holds:

$$\frac{\nu_{yz}}{E_z} = \frac{\nu_{zy}}{E_y} \qquad (32)$$

However, the relationship does not apply to a distributed vertical loading.

Evaluation of Shear Modulus G_{yz}

Figure 4 shows the transverse shear deformation of a corrugated core unit element $0A0'B$ subjected to shearing stress, τ, at the four edges of the unit element. This is equivalent to the application of concentrated vertical and horizontal loads

12

$(F = \tau h_c$ and $H = \tau p)$ at the two ends of the corrugation leg $00'$. As a result, point 0 is displaced to position 0_{FH} with the vertical and horizontal displacements δ_z and δ_y. If force F is acting alone, point 0 will move to point 0_F with the two displacement components δ_y^F and δ_z^F. Alternatively, if force H is acting alone, point 0 will move to position 0_H with displacements δ_y^H and δ_z^H. Displacements δ_y and δ_z may be expressed

$$\delta_y = \delta_y^H - \delta_y^F \tag{33}$$

$$\delta_z = \delta_z^F - \delta_z^H \tag{34}$$

and the effective shear strain, γ, can be written

$$\gamma = \frac{\delta_y}{h_c} + \frac{\delta_z}{p} \tag{35}$$

Substituting equations (33) and (34) into equation (35) and using equations (11), (16), (21), and (27), the shear modulus G_{yz} can then be written in the form

$$G_{yz} = \frac{\tau}{\gamma} = \frac{E_c I_c}{h_c^3 \left(\dfrac{h_c}{p} B_z^F - 2 B_z^H + \dfrac{p}{h_c} B_y^H \right)} \tag{36}$$

when t_f equals t_c, the expressions B_z^F, B_z^H, and B_y^H in equation (36) reduce respectively to the expressions B_3, B_4, and B_6 in reference 4.

Evaluation of Poisson Ratio ν_{yx}

The Poisson ratio ν_{yx} is associated with loading in the x-direction only. The effective strain of the corrugated core in the x-direction, ε_x, is given by

$$\varepsilon_x = \frac{\sigma_x}{E_x} = \frac{\sigma_{xc}}{E_c} \tag{37}$$

where σ_x is the effective stress in the corrugated core in the x-direction and σ_{xc} is the stress in the corrugation leg in the x-direction. The two stresses σ_x and σ_{xc} are related as follows:

$$\sigma_x = \sigma_{xc} \frac{\ell t_c}{ph_c}\left[1 - \frac{f}{\ell}\left(1 - \frac{t_f}{t_c}\right)\right]$$ (38)

where equation (1) is used.

The effective strain in the y-direction of the sandwich core, ε_y, due to loading in the x-direction can be written

$$\varepsilon_y = -\frac{1}{p}\int_0^\ell \varepsilon_s \cos\psi\, ds$$ (39)

where ε_s is the strain in the s-direction due to loading in the x-direction and is given by

$$\varepsilon_s = \nu_c \varepsilon_x$$ (40)

where ν_c is the Poisson ratio of the sandwich core material.

After the integration of equation (39) with equations (37) and (40) taken into consideration,

$$\varepsilon_y = -\frac{\nu_c \sigma_{xc}}{E_c}$$ (41)

From equations (37) and (41),

$$\nu_{yx} = -\frac{\varepsilon_y}{\varepsilon_x} = \nu_c$$ (42)

Evaluation of Poisson Ratio ν_{xy}

The Poisson ratio ν_{xy} is associated with loading in the y-direction only. Using equation (11), the effective strain in the corrugated core in the y-direction, ε_y, is given by

$$\varepsilon_y = \frac{\delta_y^H}{p} = \frac{H\, h_c^3\, B_y^H}{p\, E_c I_c}$$ (43)

The strain in the s-direction, ε_s^H, due to loading H is given by

$$\varepsilon_s^H = \frac{H \cos \psi}{E_c t_i} \tag{44}$$

The effective strains in the corrugated core, in the x-direction, ε_x, can be obtained from the integral

$$\varepsilon_x = -\frac{1}{\ell} \int_0^\ell \varepsilon_{xc} \, ds \tag{45}$$

where ε_{xc} is the strain in the corrugation leg in the x-direction due to loading H, and is given by

$$\varepsilon_{xc} = \nu_c \, \varepsilon_s^H \tag{46}$$

Substituting equations (44) and (46) into equation (45) and integrating,

$$\varepsilon_x = -\frac{H \nu_c \, p}{\ell \, t_c E_c} \left[1 - \frac{f}{p}\left(1 - \frac{t_c}{t_f}\right) \right] \tag{47}$$

The Poisson ratio ν_{xy} is then given by

$$\nu_{xy} = -\frac{\varepsilon_x}{\varepsilon_y} \tag{48}$$

$$= \frac{p^2}{\ell t_c} \frac{\nu_c \, I_c}{h_c^3 \, B_y^H} \left[1 - \frac{f}{p}\left(1 - \frac{t_c}{t_f}\right) \right] \tag{49}$$

The Poisson ratios ν_{xy} and ν_{yx} are related as follows:

$$\frac{\nu_{xy}}{E_y} = \frac{\nu_{yx}}{E_x} \left[1 - \frac{f}{p}\left(1 - \frac{t_c}{t_f}\right) \right] \left[1 - \frac{f}{\ell}\left(1 - \frac{t_f}{t_c}\right) \right] \tag{50}$$

If t_f equals t_c or if the superplastic deformation is constant volume (that is, if the condition of equation (4) is imposed), then we have the familiar expression

$$\frac{\nu_{xy}}{E_y} = \frac{\nu_{yx}}{E_x} \tag{51}$$

<center>Evaluation of Poisson Ratio ν_{zx}</center>

The Poisson ratio ν_{zx} is associated with loading in the x-direction only. The effective strain of the corrugated core, in the z-direction, ε_z, can be written

$$\varepsilon_z = -\frac{1}{h_c} \int_0^\ell \varepsilon_s \sin \psi \, ds \tag{52}$$

After substituting equations (37) and (40) into equation (52) and integrating,

$$\varepsilon_z = -\frac{\nu_c \, \sigma_{xc}}{E_c} \tag{53}$$

From equations (37) and (53), the Poisson ratio ν_{zx} can be written

$$\nu_{zx} = -\frac{\varepsilon_z}{\varepsilon_x} = \nu_c \tag{54}$$

<center>Evaluation of Poisson Ratio ν_{xz}</center>

The Poisson ratio ν_{xz} is associated with loading in the z-direction only. From equation (21), the corrugated core strain in the z-direction, ε_z, is given by

$$\varepsilon_z = \frac{\delta_z^F}{h_c} = \frac{F \, B_z^F}{h_c E_c I_c} \tag{55}$$

In addition, the corrugated core strain in the x-direction, ε_x, is expressed as

$$\varepsilon_x = -\frac{1}{\ell} \int_0^\ell \tilde{\varepsilon}_{xc} \, ds \tag{56}$$

where $\tilde{\varepsilon}_{xc}$ is the strain in the corrugation leg in the x-direction due to loading in the z-direction, and is given by

$$\tilde{\varepsilon}_{xc} = \nu_c \, \varepsilon_s^F \tag{57}$$

where ε_s^F is the corrugation leg strain in the s-direction due to loading F, and is given by

$$\varepsilon_s^F = \frac{F \sin \psi}{E_c t_i} \tag{58}$$

Integrating equation (56) in the light of equations (57) and (58), we have

$$\varepsilon_x = -\frac{\nu_c F h_c}{\ell t_c E_c} \tag{59}$$

The Poisson ratio ν_{xz} is then given by

$$\nu_{xz} = -\frac{\varepsilon_x}{\varepsilon_z} = \frac{I_c}{\ell t_c h_c} \frac{\nu_c}{B_z^F} \tag{60}$$

The two Poisson ratios ν_{zx} and ν_{xz} can be related by the equation

$$\frac{\nu_{xz}}{E_z} = \frac{\nu_{zx}}{E_x} \left[1 - \frac{f}{\ell} \left(1 - \frac{t_f}{t_c} \right) \right] \tag{61}$$

If t_f equals t_c or if f equals 0, then equation (61) becomes

$$\frac{\nu_{xz}}{E_z} = \frac{\nu_{zx}}{E_x} \tag{62}$$

For the superplastic incompressible deformation, equation (61) can be reduced to

$$\frac{\nu_{xz}}{E_z} = \frac{\nu_{zx}}{E_x} \frac{p}{\ell} \frac{t_f}{t_c} \tag{63}$$

ELASTIC CONSTANTS FOR HONEYCOMB CORE

As shown in figure 5, the honeycomb core is made up of corrugated strips joined together at the corrugation flat segments, with the corrugation axis oriented normal to the sandwich middle surface. Therefore, by taking the coordinate system shown in the figure, the results obtained for the previous case can be applied directly to the honeycomb core if t_c is set equal to t_f.

17

EFFECT OF FACE SHEETS ON MODULUS OF ELASTICITY E_z

The following calculations are presented to evaluate the effect of the face sheets on the stiffness in the z-direction, E_z, when bonded to the corrugated core. Let $\overline{E}_z$ denote the modulus of elasticity in the z-direction when the deformation of the corrugated core is constrained by the face sheets.

As shown in figure 6, if the corrugation leg is not constrained by the two face sheets and is subjected to loading H and F, point 0 will move to 0_1. The horizontal and the vertical components of this displacement are given by equations (27) and (21), respectively.

$$\delta_y^F = \frac{Fh_c^3}{E_c I_c} B_y^F \tag{27}$$

$$\delta_z^F = \frac{Fh_c^3}{E_c I_c} B_z^F \tag{21}$$

If the corrugation leg is constrained by the face sheets, point 0 will move only to point 0_2. This constraint is equivalent to bringing point 0 back from position 0_1 to position 0_2 by means of horizontal force H.

The horizontal and vertical components of the displacement $\overline{0_1 0_2}$ due to H are given by equations (11) and (16), respectively.

$$\delta_y^H = \frac{Hh_c^3}{E_c I_c} B_y^H \tag{11}$$

$$\delta_z^H = \frac{Hh_c^3}{E_c I_c} B_z^H \tag{16}$$

The horizontal component, $\overline{\delta}_y$, of the displacement $\overline{00_2}$ is due to the compression (neglecting buckling) of the face sheets, and can be written

$$\overline{\delta}_y = \frac{Hp}{2t_s E_c} \tag{64}$$

where t_s is the thickness of the face sheets. From the relation

$$\bar{\delta}_y = \delta_y^F - \delta_y^H \tag{65}$$

it is possible to express H in terms of F with the aid of equations (27) and (11) as follows:

$$H = F \frac{B_y^F}{B_y^H} \frac{1}{1 + \dfrac{p I_c}{2 t_s h_c^3 B_y^H}} \tag{66}$$

The vertical component, $\bar{\delta}_z$, of the displacement $\overline{00}_2$ is given by

$$\bar{\delta}_z = \delta_z^F - \delta_z^H \tag{67}$$

which, with reference to equations (21) and (16), becomes

$$\bar{\delta}_z = \frac{F h_c^3}{E_c I_c} B_z^F \left(1 - \frac{B_y^F}{B_y^H} \frac{B_z^H}{B_z^F} \frac{1}{1 + \dfrac{p I_c}{2 t_s h_c^3 B_y^H}} \right) \tag{68}$$

Using equations (19), (24), and (30), the modulus of elasticity $\bar{E}_z$ is then given by

$$\bar{E}_z = \frac{\dfrac{F}{p}}{\dfrac{\bar{\delta}_z}{h_c}} \tag{69}$$

$$= \frac{E_z}{1 - \nu_{yz}\nu_{zy} \dfrac{1}{1 + \dfrac{p I_c}{2 t_s h_c^3 B_y^H}}} \tag{70}$$

indicating that the stiffness of the corrugated core in the z-direction is greatly enhanced when the core is bonded to the face sheets.

CORRUGATED CORE BENDING STIFFNESS

The bending stiffness in the x-direction of the SPF/DB corrugated sandwich core may be written

$$D_x = E_c \bar{I}_c \tag{71}$$

where

D_x bending stiffness in the x-direction per unit width of a beam cut from the SPF/DB corrugated sandwich core

$\bar{I}_c$ moment of inertia taken about the horizontal centroidal axis of the corrugation cross section per unit width of the corrugation cross section parallel to the yz-plane, or

$$\bar{I}_c = \frac{h_c^3 t_c}{p} \left\{ \frac{1}{4} \frac{f}{h_c} \frac{t_f}{t_c} \left(1 + \frac{1}{3} \frac{t_f^2}{h_c^2} \right) + \frac{2}{3} \frac{d^3}{h_c^3} \left(\sin^2 \theta + \frac{1}{4} \frac{t_c^2}{d^2} \cos^2 \theta \right) \right.$$

$$\left. + \frac{R}{h_c} \left[\frac{\theta}{2} - 2 \frac{R^2}{h_c^2} \sin \theta - \frac{R}{h_c} \left(2 - 3 \frac{R}{h_c} \right) (\theta - \sin \theta) \right] \right\} \tag{72}$$

The bending stiffness in the y-direction of the SPF/DB corrugated core is very small and is of the order of $E_c I_i$.

NUMERICAL RESULTS

In obtaining the numerical values for the effective elastic constants of the SPF/DB corrugated core, it was assumed that R was equal to t_f and that the corrugated core material was a titanium alloy 6Al-4V having the following physical properties:

$$E_c = E_{Ti} = 1.1 \times 10^{11} \text{ N/m}^2 \ (16 \times 10^6 \text{ psi})$$

$$G_c = G_{Ti} = 4.3 \times 10^{10} \text{ N/m}^2 \ (6.2 \times 10^6 \text{ psi})$$

20

$$\nu_c = \nu_{Ti} = 0.33$$

$$\rho_c = \rho_{Ti} = 4.47 \text{ gr/cm}^3 \ (0.16 \text{ lb/in}^3)$$

where ρ_c is the density of the core material.

Figure 7 shows the variation of the corrugation angle, θ, with the thickness of the diagonal segment, t_c, after superplastic expansion. It is apparent that t_c is insensitive to changes in t_f/h_c.

Figures 8 to 16 present graphs for evaluating the major effective elastic constants for the SPF/DB corrugated core. The elastic constants are plotted against p/h_c, with t_f/h_c and θ as parameters. Envelopes of optimum points or envelopes of limit points are also shown in the figures. These envelopes correspond to the case when $f = 0$ (that is, triangular truss core).

Figure 8 shows that E_y is sensitive to the values of t_f and θ, but relatively insensitive to the change of p (or f), and that E_y is very small. This indicates that the corrugated core has negligible stiffness in the y-direction.

Figure 9 shows that E_z is also very small, and is sensitive to the changes of both t_f and p, but is insensitive to the change of θ. For a given θ, E_z reaches its maximum (or optimum) value at $f = 0$. As will be seen later, the lateral (that is, y-direction) constraint provided by the face sheets will increase the value of E_z by several orders of magnitude.

The shear modulus G_{xy} shown in figure 10 is also sensitive to θ. As is expected, G_{xy} increases with increasing values of p (or f).

Figure 11 shows that G_{yz} is very sensitive to the values of p (or f). For a given θ, G_{yz} reaches maximum value at $f = 0$. Because of the steepness of the curves, a slight increase of f above 0 drastically reduces the value of G_{yz}.

Figure 12 shows that G_{zx} decreases with increasing values of p (or f) and that maximum value for a given θ occurs when the corrugation degenerates into a triangular truss core.

The value of Poisson ratio ν_{xy}, shown in figure 13, is small. It is sensitive to the values of t_f and θ, and increases as p increases.

Figure 14 shows the plots of Poisson ratios ν_{yz} and ν_{zy}. It is apparent that ν_{yz} is greater than unity. This is quite common in the truss type of structure, which is not a continuum. For example, if a square truss is pulled diagonally into a rhombic shape, the Poisson ratio will be greater than unity. Both ν_{yz} and ν_{zy} are sensitive to both p and θ, but insensitive to the value of t_f.

Figure 15 shows that the value of Poisson ratio ν_{xz} is also small. It is quite sensitive to the change of t_f and less sensitive to the values of p and θ.

Figure 16 presents graphs for evaluating the modulus of elasticity $\overline{E}_z$. Because of the constraint of the face sheets, $\overline{E}_z$ is several orders of magnitude larger than E_z. $\overline{E}_z$ is sensitive to the change of p at low values of t_f.

Figure 17 shows plots of the bending stiffness, D_x, of the SPF/DB corrugated core. In the plots, D_x is normalized by $D_c = \dfrac{E_c h_c^3}{12}$ (bending stiffness per unit width of the solid core with height h_c). For given values of θ and t_f, the triangular truss core has the lowest bending stiffness.

For comparison, corresponding graphs evaluating the elastic constants for the honeycomb core are also presented (figs. 18 to 26). All the elastic constants have been normalized and may be used for any material, except for G_{yz}, ν_{xy}, and ν_{xz}, which are for titanium only. For a material other than titanium, G_{yz}, ν_{xy}, and ν_{xz} (figs. 22, 24, and 26) must be multiplied by $\dfrac{E}{G}\dfrac{G_{Ti}}{E_{Ti}}$, $\dfrac{\nu}{\nu_{Ti}}$, and $\dfrac{\nu}{\nu_{Ti}}$, respectively.

COMPARISON WITH HONEYCOMB CORE

This section compares the stiffness of the SPF/DB titanium alloy corrugated core with that of the honeycomb (aluminum or titanium) core when both types of sandwich core have the same density.

Let $(\ )_{SP}$ and $(\ )_{HC}$ denote, respectively, the quantities associated with the SPF/DB corrugated core and the honeycomb core. The densities, ρ, of these two types of sandwich core may be written

$$\rho_{SP} = \left(\frac{t_f}{h_c}\right)_{SP} \rho_{Ti} \tag{73}$$

$$\rho_{HC} = \left(\frac{t_c \ell}{ph_c}\right)_{HC} \rho_c \tag{74}$$

where ρ_c is the density of the honeycomb core material. From the condition $\rho_{SP} = \rho_{HC}$, equations (73) and (74) may be related to find the geometric parameter t_f/h_c for the SPF/DB core as follows:

$$\left(\frac{t_f}{h_c}\right)_{SP} = \left(\frac{t_c \ell}{ph_c}\right)_{HC} \frac{\rho_c}{\rho_{Ti}} \tag{75}$$

A typical honeycomb core for application to high speed aircraft is characterized by the following geometric parameters:

$$t_c = t_f \approx R, \quad \theta \approx 60° \tag{76}$$

$$\left(\frac{f}{h_c}\right)_{HC} = 0.4053 \tag{77}$$

$$\left(\frac{\ell}{h_c}\right)_{HC} = 1.5600 \tag{78}$$

$$\left(\frac{t_c}{h_c}\right)_{HC} = 0.0147 \tag{79}$$

$$\left(\frac{p}{h_c}\right)_{HC} = 0.9825 \tag{80}$$

For the aluminum honeycomb core, the material properties are:

$$E_c = E_{Al} = 6.8948 \times 10^{10} \text{ N/m}^2 \ (10 \times 10^6 \text{ psi})$$

$$G_c = G_{Al} = 2.7579 \times 10^{10} \text{ N/m}^2 \ (4 \times 10^6 \text{ psi})$$

$$\nu_c = \nu_{Al} = 0.36$$

$$\rho_c = \rho_{Al} = 2.77 \text{ gr/cm}^3 \ (0.100 \text{ lb/in}^3)$$

Using the numerical values given above, equation (75) yields the following geometric parameters for the SPF/DB corrugated core corresponding to $\left(\dfrac{t_f}{h_c}\right)_{HC}$ = 0.0147. When the honeycomb core is aluminum,

$$\left(\frac{t_f}{h_c}\right)_{SP} = 0.0146 \tag{81}$$

When the honeycomb core is titanium,

$$\left(\frac{t_f}{h_c}\right)_{SP} = 0.02334 \tag{82}$$

From figures 18, 21, and 23 the three major elastic constants for the honeycomb core, E_x, G_{xy}, and G_{zx}, may be replotted against t_f/h_c for $\theta = 60°$ and $p/h_c = 0.9825$ (eq. (80)). This is shown in figure 27.

Likewise, from figures 16, 11, and 12, the optimum values of the corresponding elastic constants for the SPF/DB corrugated core, $\bar{E}_z$, G_{yz}, and G_{zx}, may be replotted against t_f/h_c for $\theta = 60°$ (fig. 28).

Because of the different orientations of the coordinate axes of the two types of sandwich cores, E_x, G_{xy}, and G_{zx} (honeycomb core moduli) should be compared respectively with their counterparts, $\bar{E}_z$, G_{yz}, and G_{zx} (SPF/DB corrugated core moduli).

Because $\left(E_x\right)_{HC}$ is insensitive to the existence of the face sheets, it is used to compare with $\left(\bar{E}_z\right)_{SP}$, which is insensitive to the change of thickness of the face sheets.

Given that $E_c = E_{Al}$ and $G_c = G_{Al}$ for the aluminum honeycomb core and that $E_c = E_{Ti}$ and $G_c = G_{Ti}$ for the titanium honeycomb core, figures 27 and 28 allow the comparisons between the elastic constants as shown in tables 1 and 2.

From the tables, it becomes apparent that the stiffness in the sandwich thickness direction of the SPF/DB corrugated core is lower than that of the honeycomb core (aluminum or titanium). The transverse shear stiffness of the SPF/DB corrugated core is greater than that of the honeycomb core.

24

CONCLUDING REMARKS

In this report the formulae and related graphs are developed to evaluate the major effective elastic constants for a superplastically formed/diffusion-bonded (SPF/DB) corrugated sandwich core. Assuming uniform thickness of the corrugation leg, the formulae were used to evaluate the effective elastic constants for a honeycomb sandwich core.

A comparison of the stiffness of the two types of sandwich core was made under conditions of equal sandwich core density. It was found that the stiffness in the thickness direction of the optimum SPF/DB corrugated core (that is, triangular truss core) was lower than that of the honeycomb core, and that the former had a higher transverse shear stiffness than the latter. Alternatively, for the same transverse shear stiffness, the SPF/DB corrugated core had lower core density than the honeycomb core, but its thickness stiffness was lower than that of the honeycomb core.

For the SPF/DB corrugated sandwich core, it was found that increasing the length of the crest or trough increased the bending stiffness but reduced the transverse shear stiffness.

Dryden Flight Research Center
National Aeronautics and Space Administration
Edwards, Calif., June 27, 1979

REFERENCES

1. Pulley, John: Evaluation of Low-Cost Titanium Structure for Advanced Aircraft. NASA CR-145111, 1976.

2. Ueng, Charles E. S.: Superplastically Formed New Sandwich Cores. Transportation Eng. J., American Soc. Civil Eng., vol. 104, July 1978, pp. 437-447.

3. Ueng, C. E. S.; Underwood, E. E.; and Liu, T. L.: Shear Modulus of Superplastically Formed Sandwich Cores. Trends in Computerized Structural Analysis and Synthesis. Pergamon Press, 1978, pp. 393-397.

4. Libove, Charles; and Hubka, Ralph E.: Elastic Constants for Corrugated-Core Sandwich Plates. NACA TN 2289, 1951.

5. Roark, Raymond J.: Formulas for Stress and Strain. Third ed. McGraw-Hill Book Co., Inc., 1954.

TABLE 1.—COMPARISON BETWEEN ELASTIC CONSTANTS FOR
ALUMINUM HONEYCOMB CORE AND SPF/DB TITANIUM CORRUGATED CORE
$$[\rho_{SP} = \rho_{HC}]$$

Aluminum honeycomb core	SPF/DB titanium corrugated core	$()_{SP}/()_{HC}$
$\dfrac{t_f}{h_c} = 0.0147, \ \theta = 60°$	$\dfrac{t_f}{h_c} = 0.0146, \ \theta = 60°, \ f = 0$	----
$E_x = 14.4790 \times 10^8 \ \text{N/m}^2$ $(2.1 \times 10^5 \ \text{psi})$	$\overline{E}_z = 8.2737 \times 10^8 \ \text{N/m}^2$ $(1.2 \times 10^5 \ \text{psi})$	0.57
$G_{xy} = 2.4821 \times 10^8 \ \text{N/m}^2$ $(3.6 \times 10^4 \ \text{psi})$	$G_{yz} = 2.7358 \times 10^8 \ \text{N/m}^2$ $(3.968 \times 10^4 \ \text{psi})$	1.10
$G_{zx} = 2.5924 \times 10^8 \ \text{N/m}^2$ $(3.76 \times 10^4 \ \text{psi})$	$G_{zx} = 4.7022 \times 10^8 \ \text{N/m}^2$ $(6.82 \times 10^4 \ \text{psi})$	1.81

TABLE 2.—COMPARISON BETWEEN ELASTIC CONSTANTS FOR
TITANIUM HONEYCOMB CORE AND SPF/DB TITANIUM CORRUGATED CORE
$$[\rho_{SP} = \rho_{HC}]$$

Titanium honeycomb core	SPF/DB titanium corrugated core	$()_{SP}/()_{HC}$
$\dfrac{t_f}{h_c} = 0.0147, \ \theta = 60°$	$\dfrac{t_f}{h_c} = 0.02334, \ \theta = 60°, \ f = 0$	----
$E_x = 23.1664 \times 10^8 \ \text{N/m}^2$ $(3.36 \times 10^5 \ \text{psi})$	$\overline{E}_z = 13.4586 \times 10^8 \ \text{N/m}^2$ $(1.9520 \times 10^5 \ \text{psi})$	0.58
$G_{xy} = 3.8473 \times 10^8 \ \text{N/m}^2$ $(5.58 \times 10^4 \ \text{psi})$	$G_{yz} = 4.5740 \times 10^8 \ \text{N/m}^2$ $(6.8340 \times 10^4 \ \text{psi})$	1.22
$G_{zx} = 4.0182 \times 10^8 \ \text{N/m}^2$ $(5.8280 \times 10^4 \ \text{psi})$	$G_{zx} = 7.5663 \times 10^8 \ \text{N/m}^2$ $(1.0974 \times 10^5 \ \text{psi})$	1.88
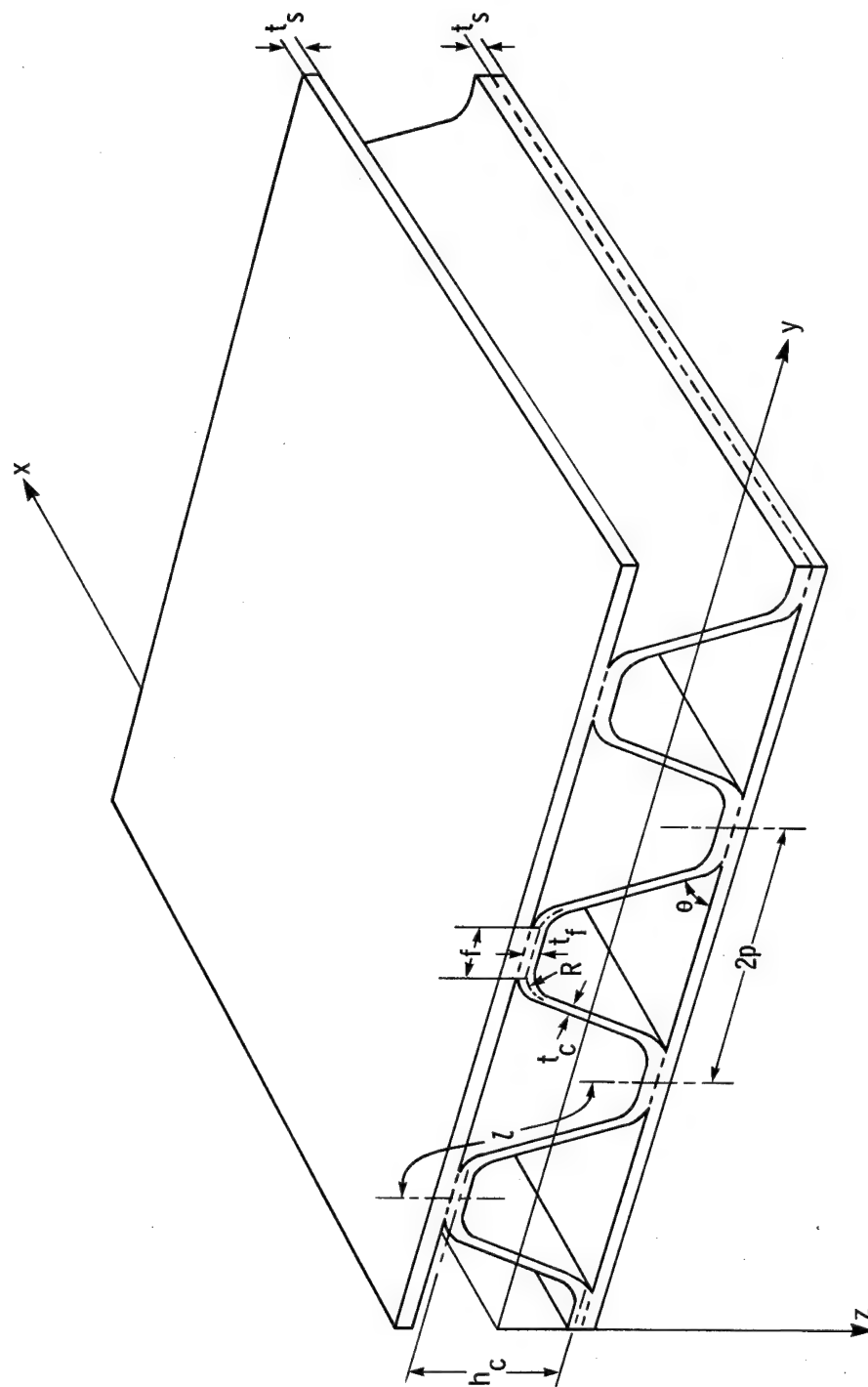
Figure 1. Geometry of superplastically formed/diffusion-bonded corrugated core sandwich plate.
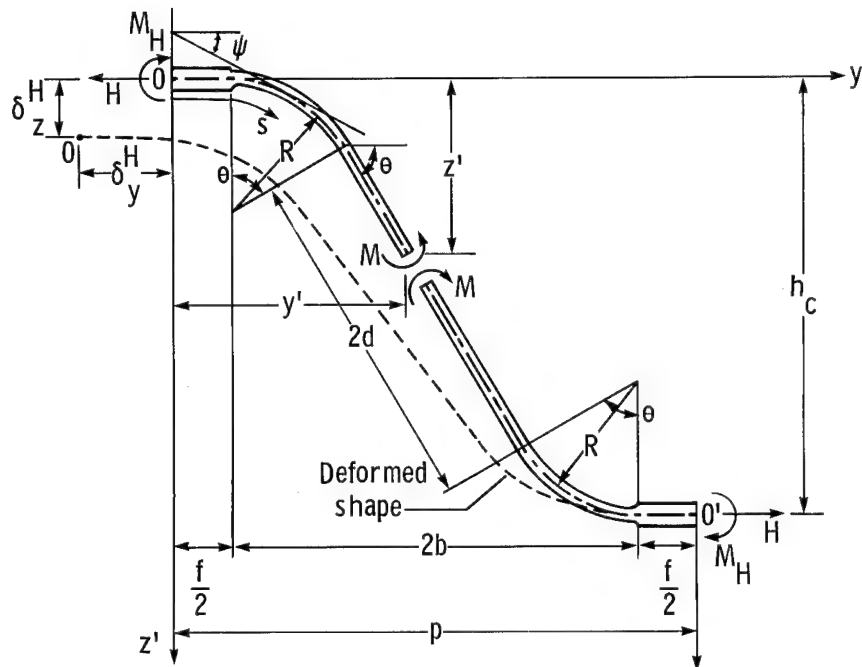
Figure 2. Free body diagram of corrugation leg under horizontal loading. $M_H = \frac{1}{2} H h_c$.
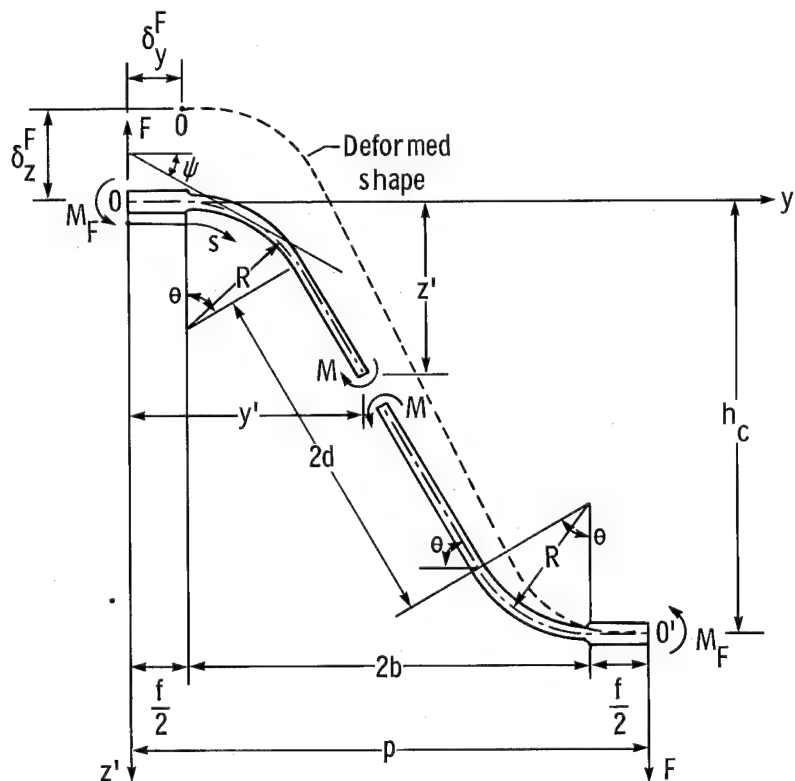
Figure 3. Free body diagram of corrugation leg under vertical loading. $M_F = \frac{1}{2} Fp$.
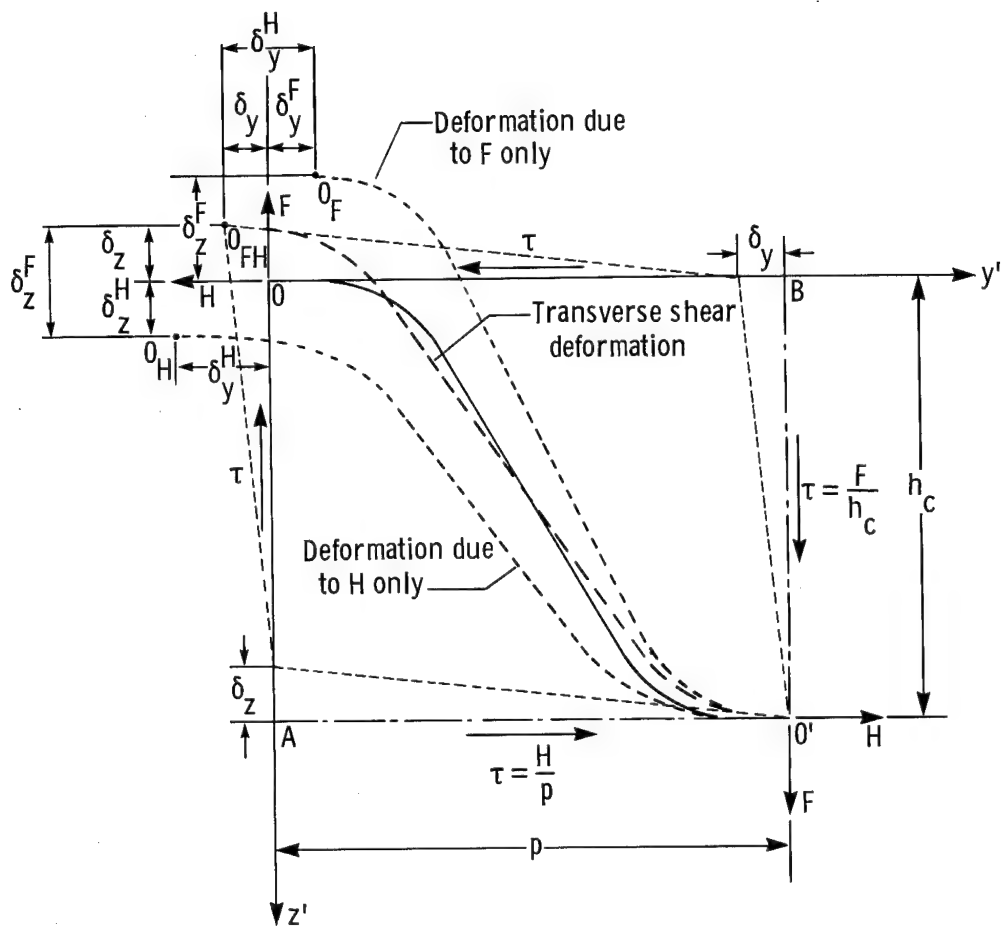
*Figure 4. Transverse shear deformation of the
corrugated core unit element.*
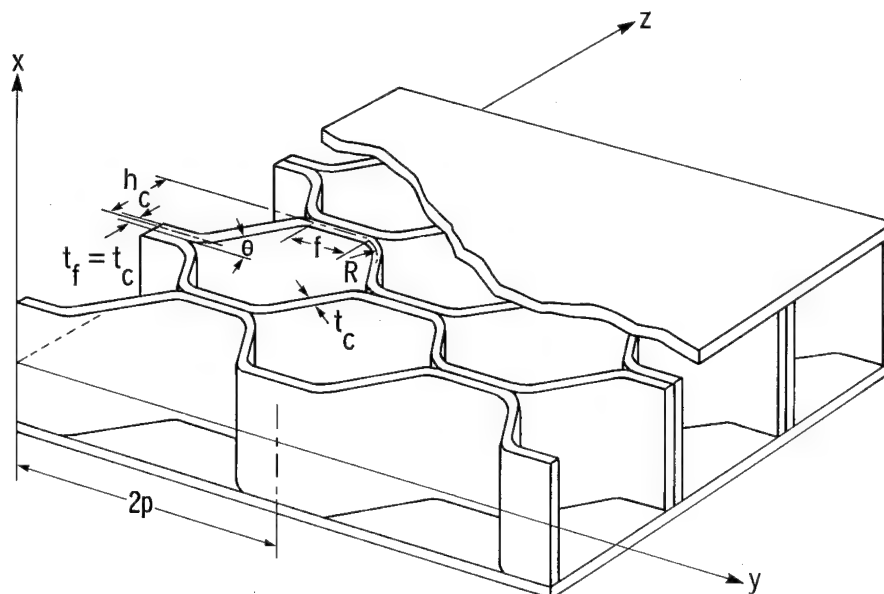
Figure 5. Geometry of honeycomb core sandwich plate.
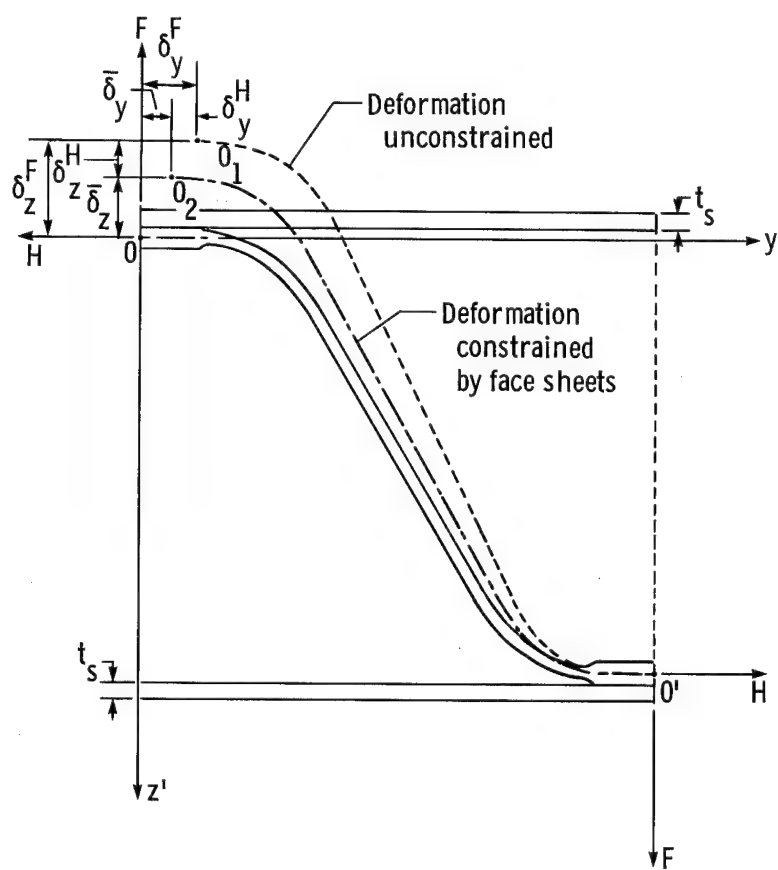
Figure 6. Constrained deformation of
corrugation leg.
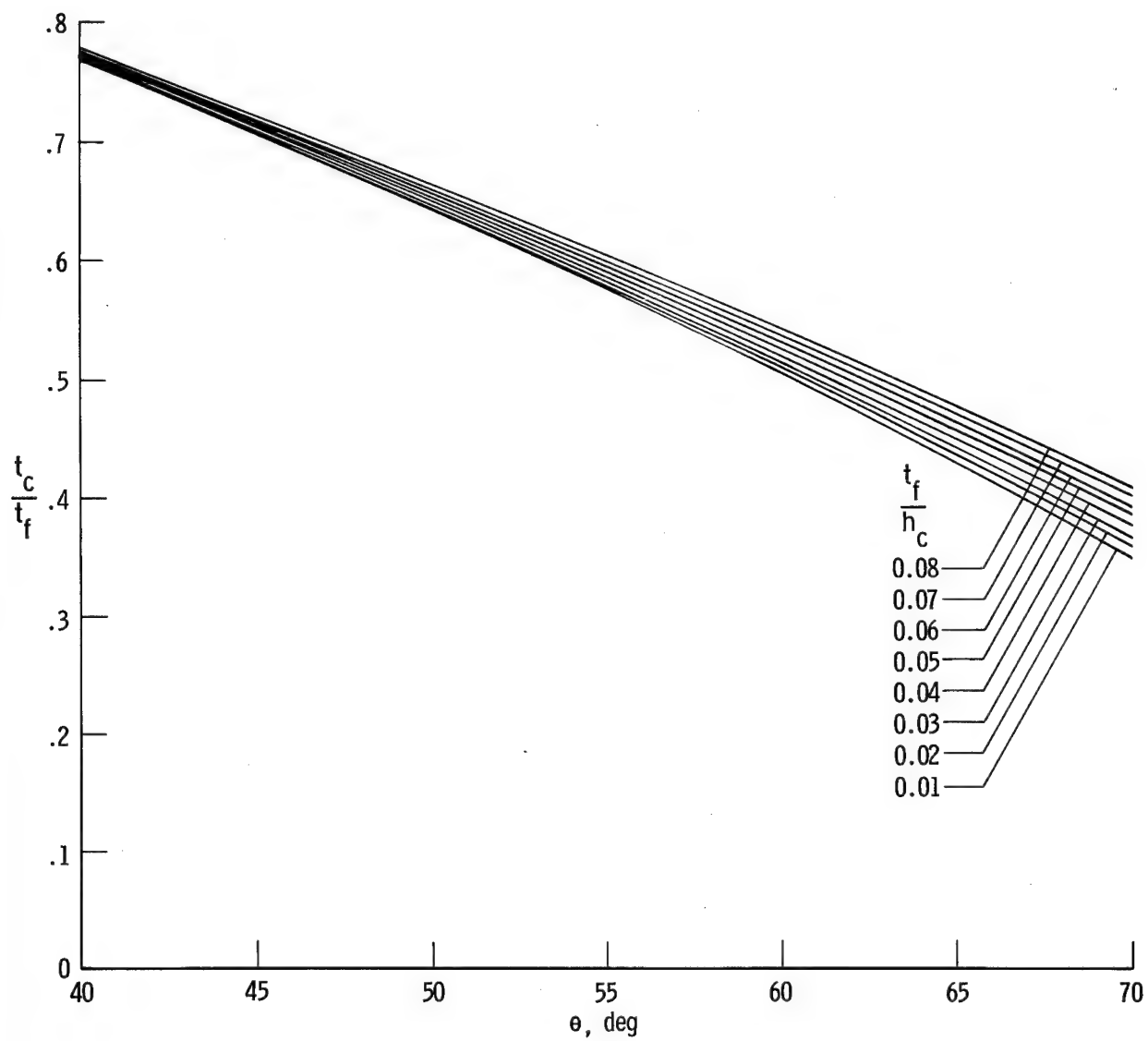
Figure 7.   Corrugation leg straight diagonal segment thickness versus corrugation angle.   R = t_f.
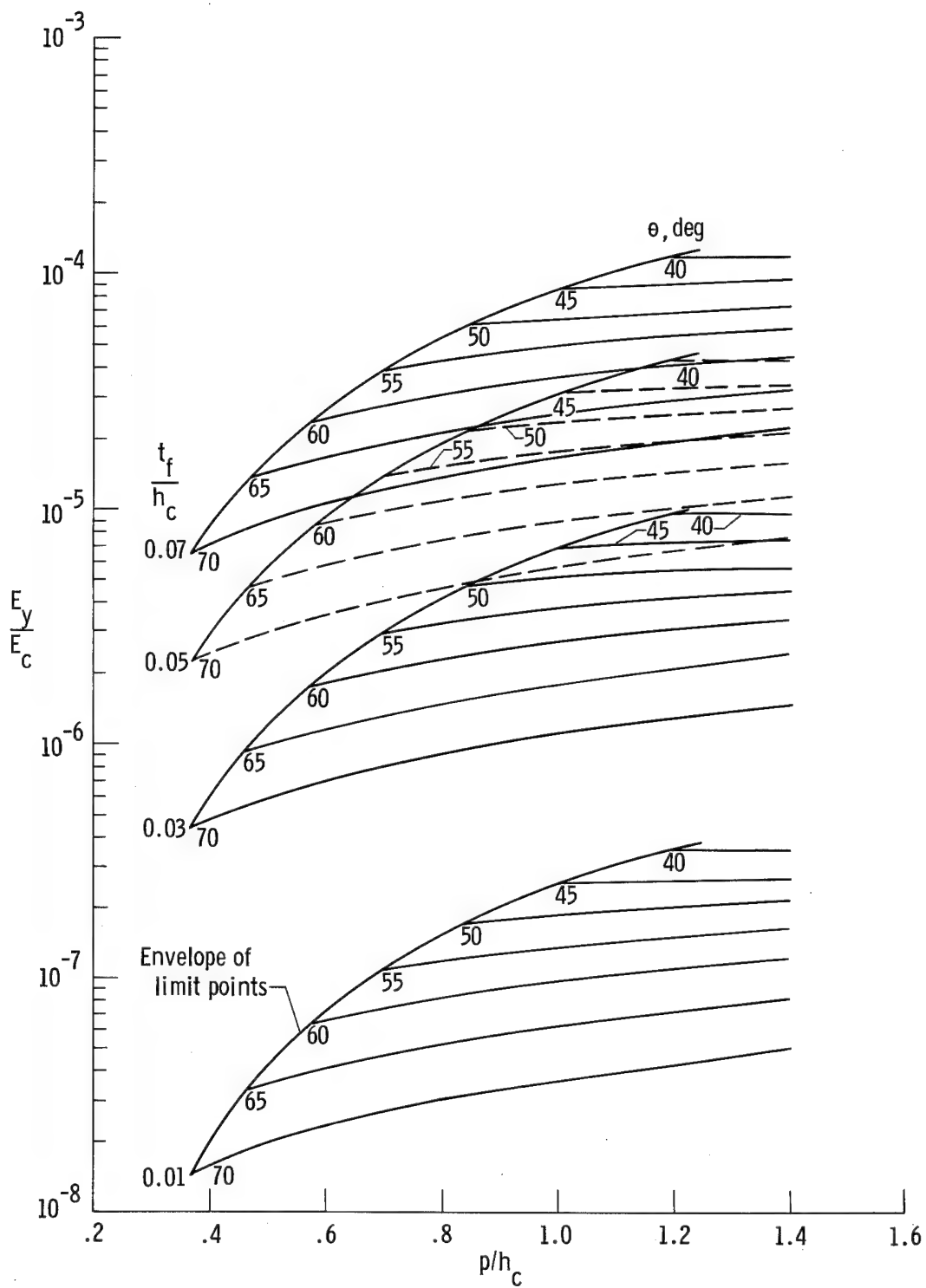
Figure 8. Modulus of elasticity E_y for SPF/DB
corrugated core. $R = t_f$.
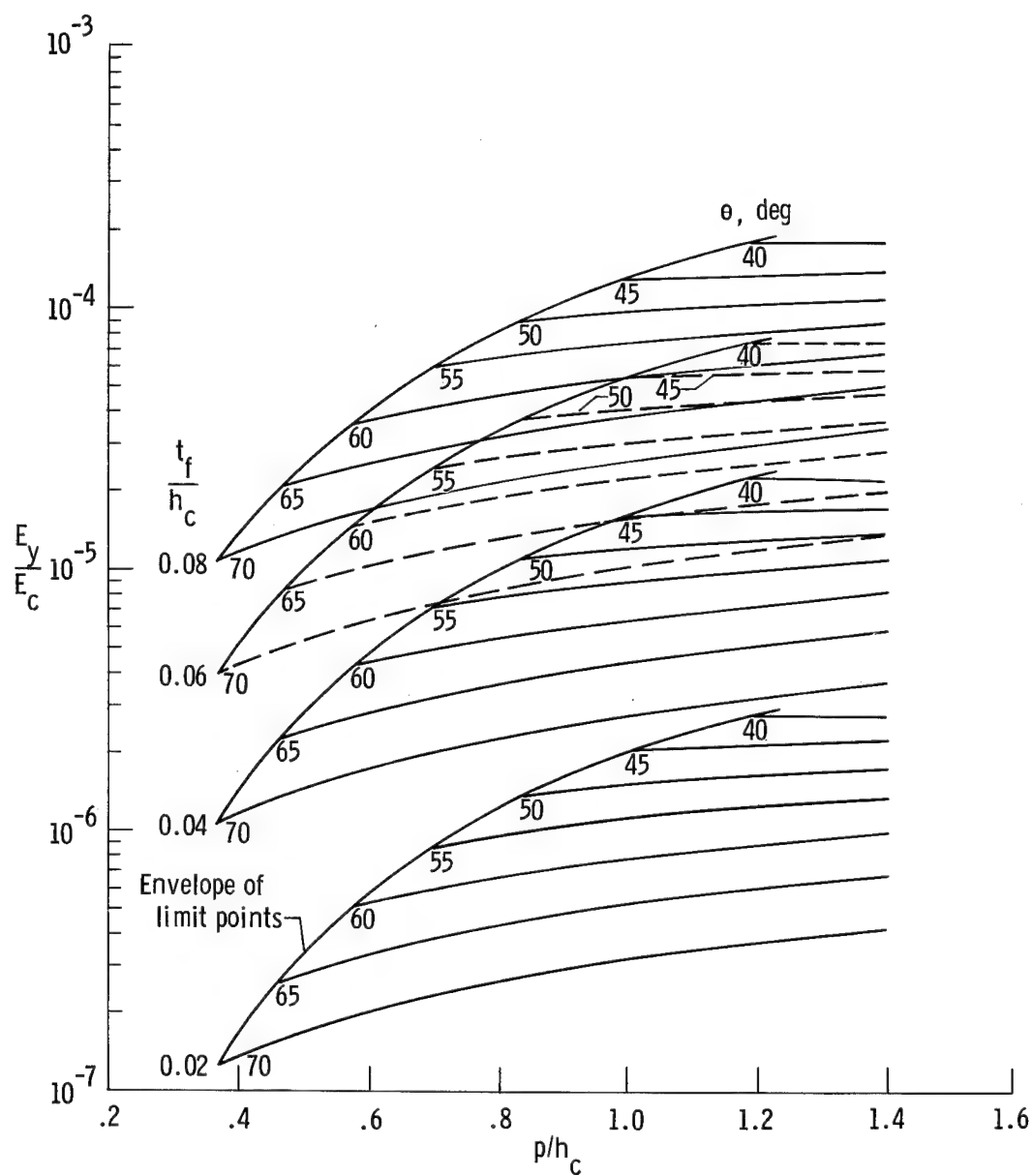
Figure 8. Concluded.
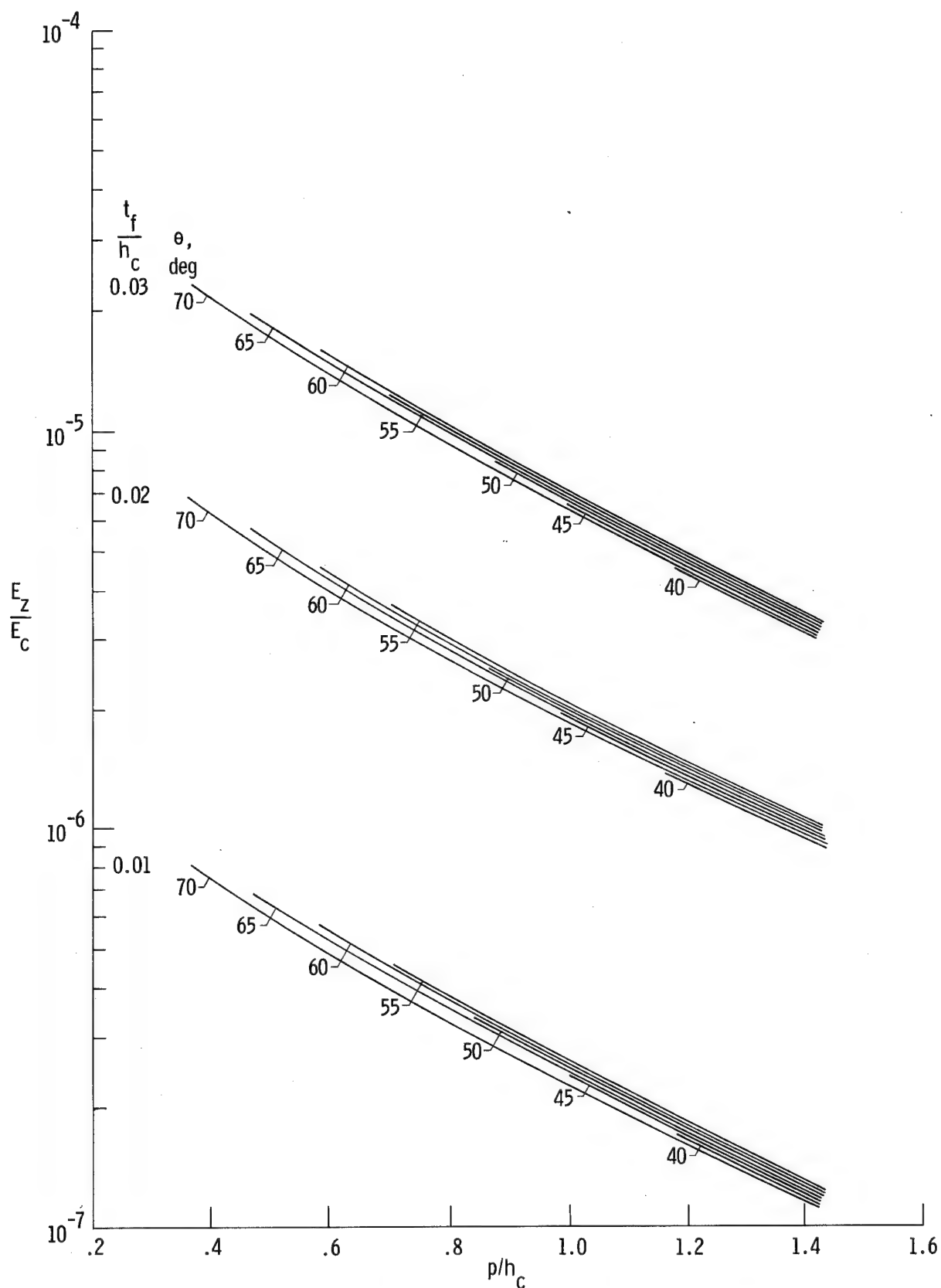
Figure 9. *Modulus of elasticity E_z for SPF/DB corrugated core. $R = t_f$.*
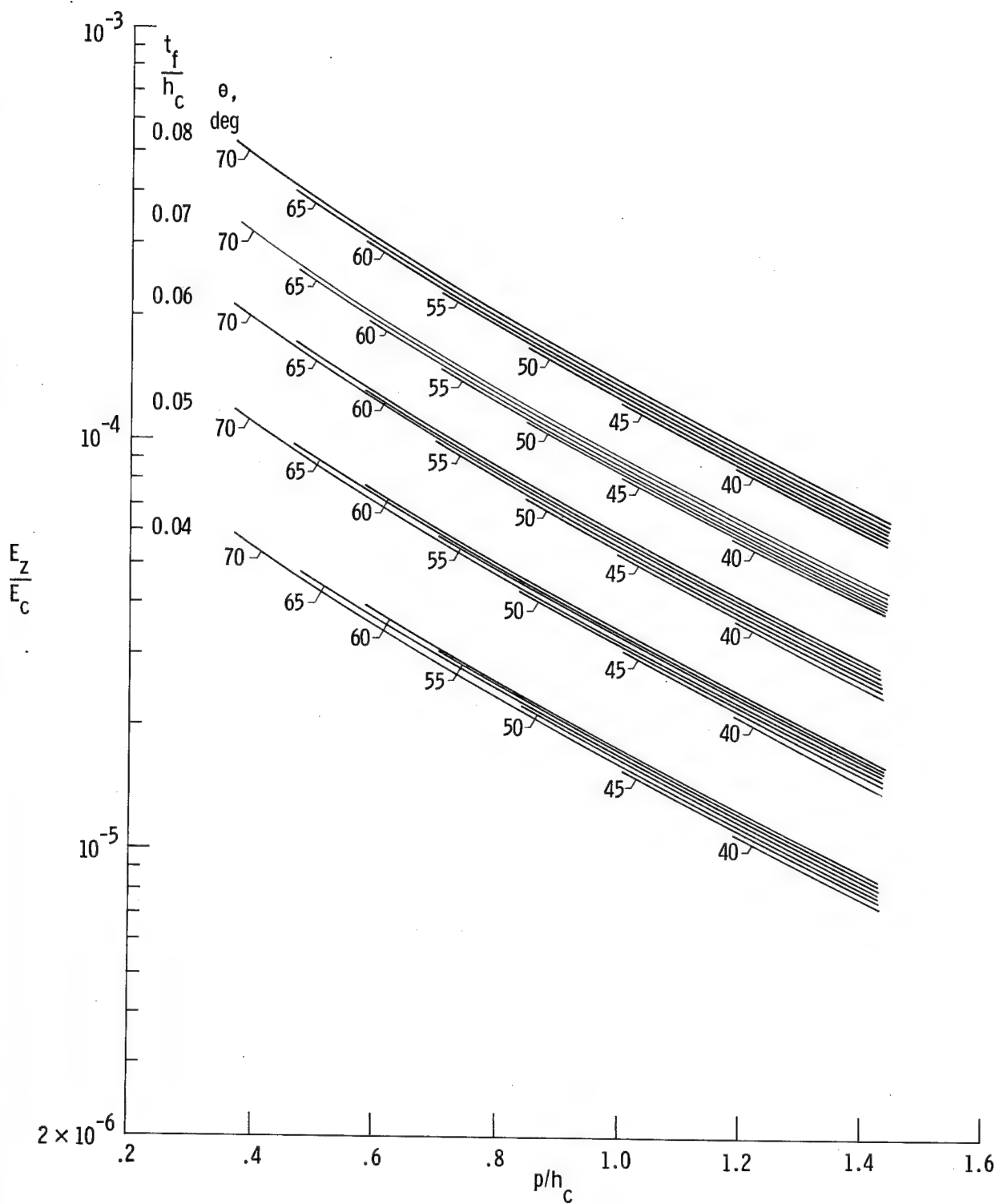
Figure 9. Concluded.
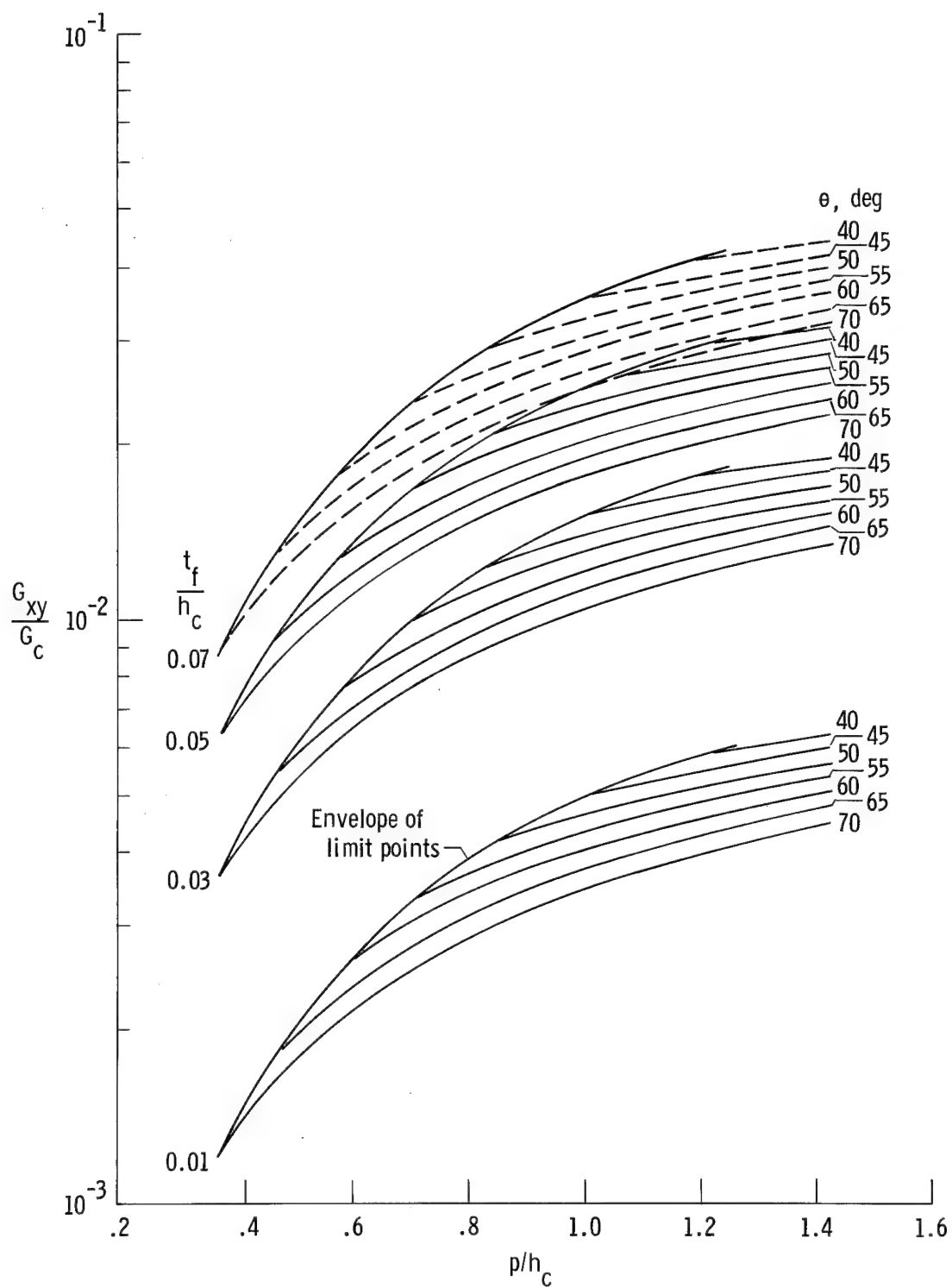
Figure 10. Shear modulus G_{xy} for SPF/DB corrugated core. $R = t_f$.
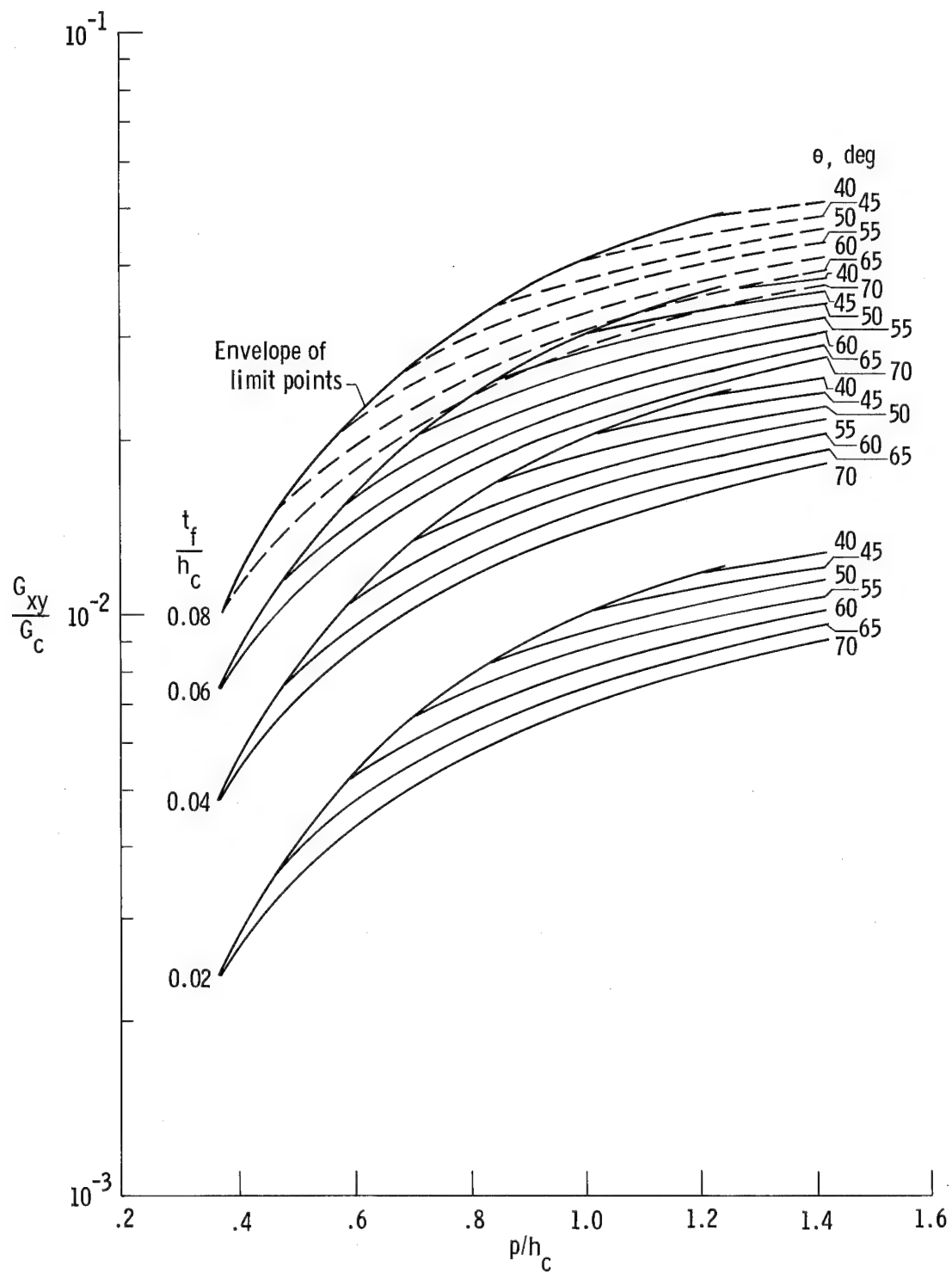
Figure 10. Concluded.
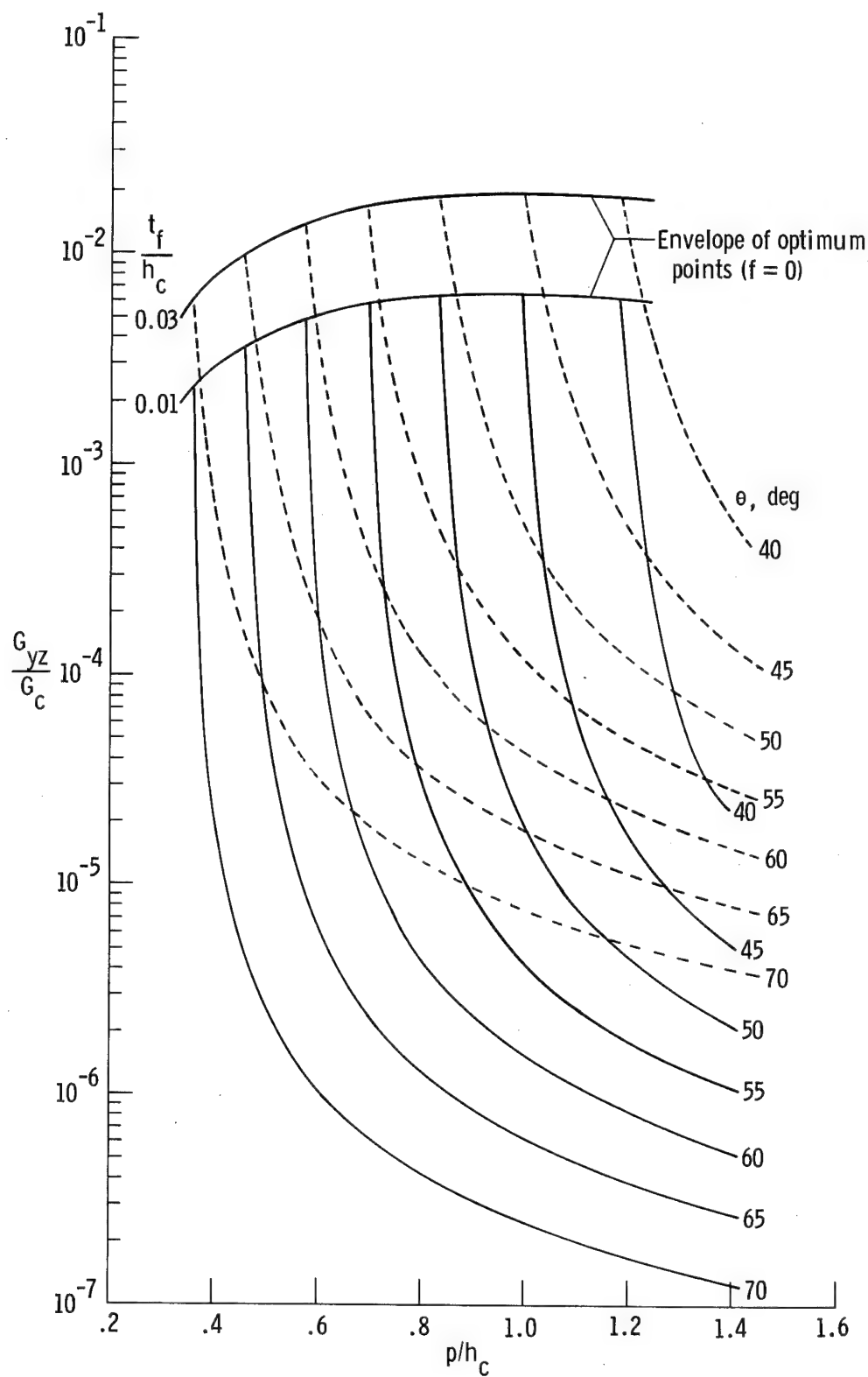
Figure 11. Shear modulus G_{yz} for SPF/DB corrugated titanium core. $R = t_f$.
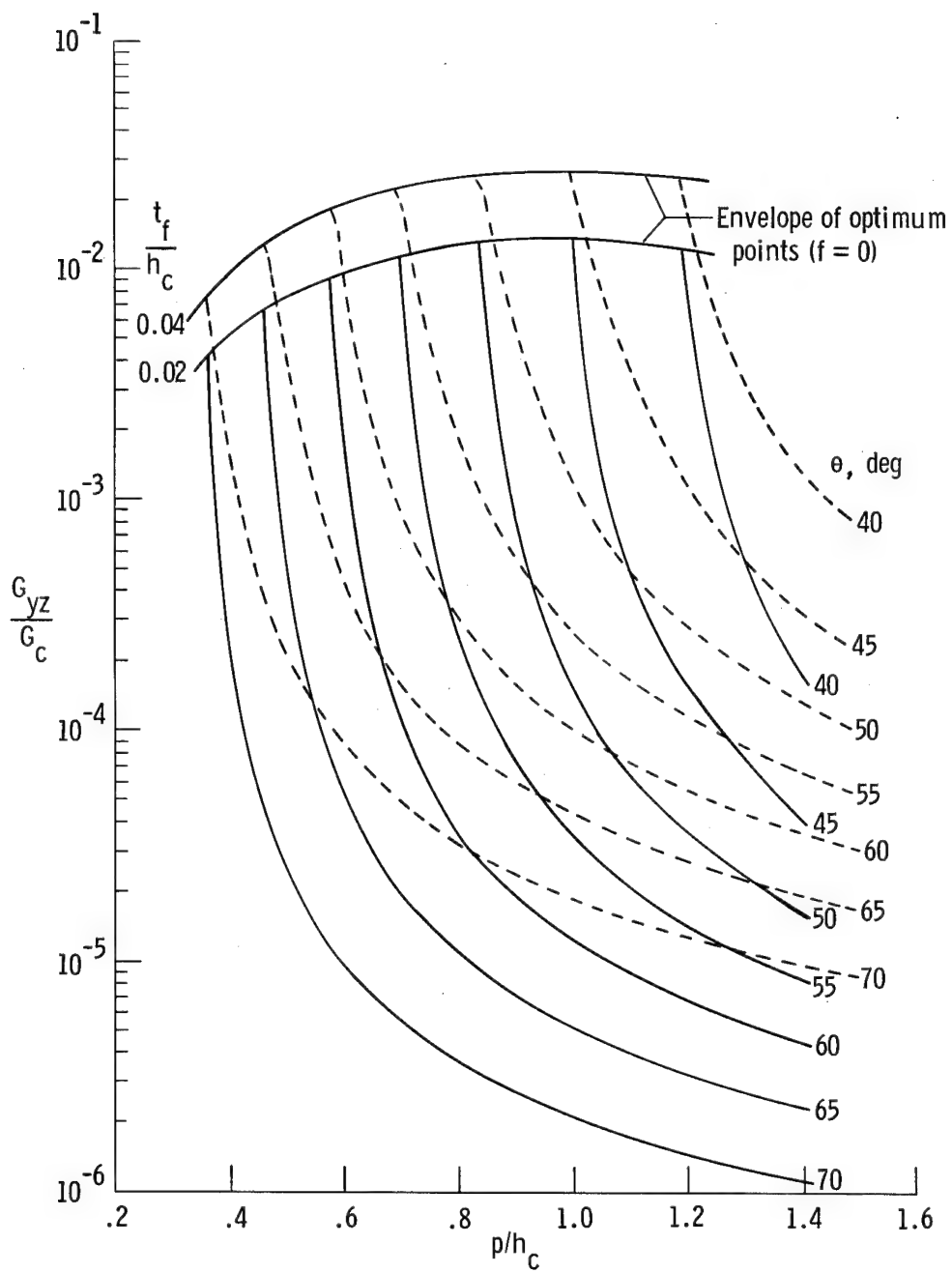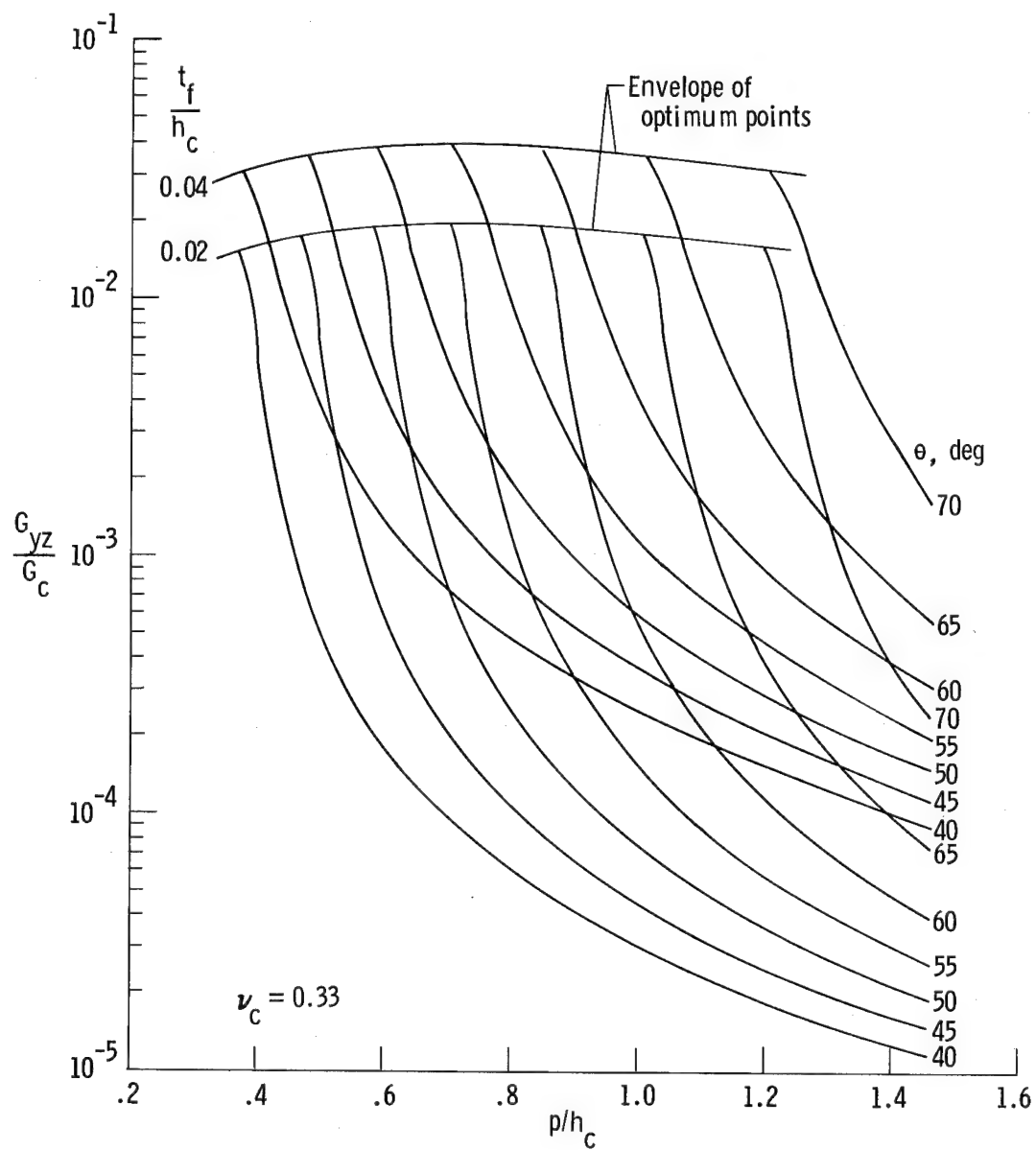
Figure 11.   Continued.
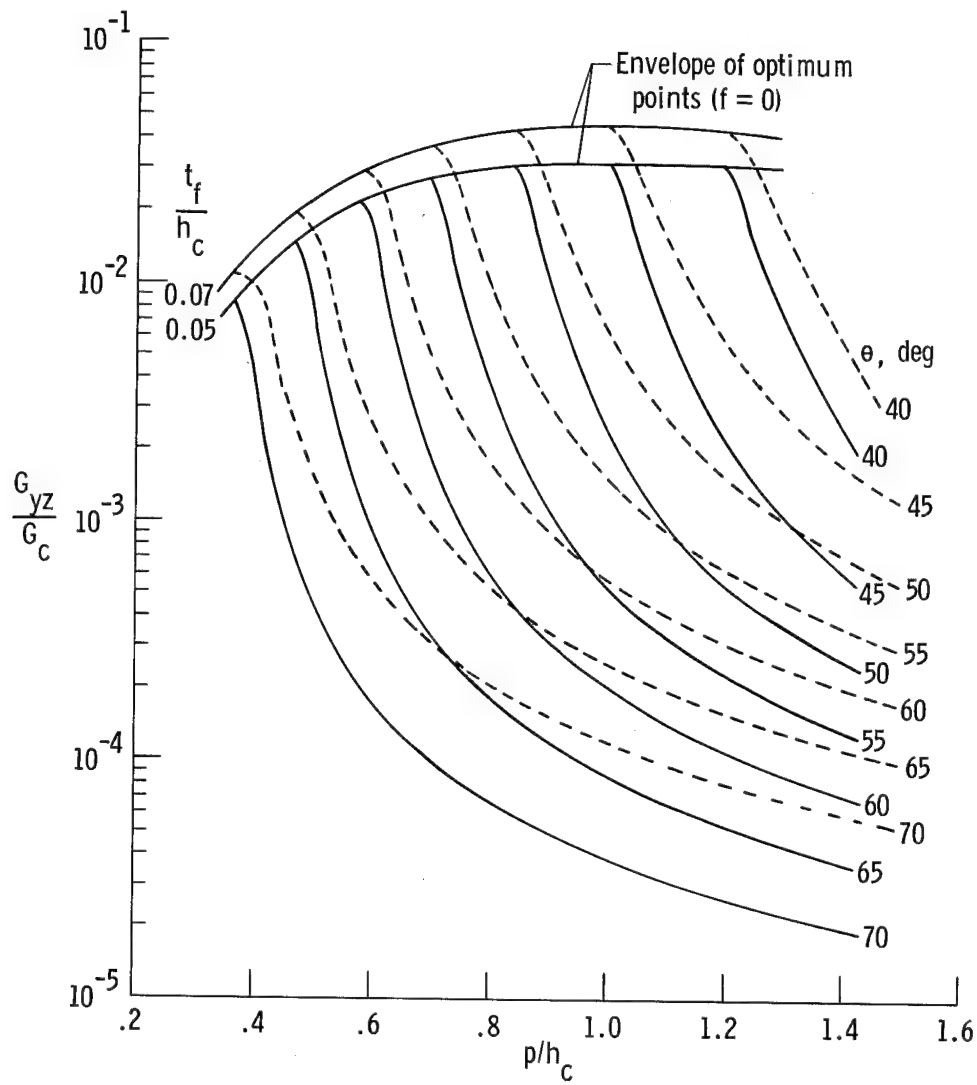
Figure 11. Continued.
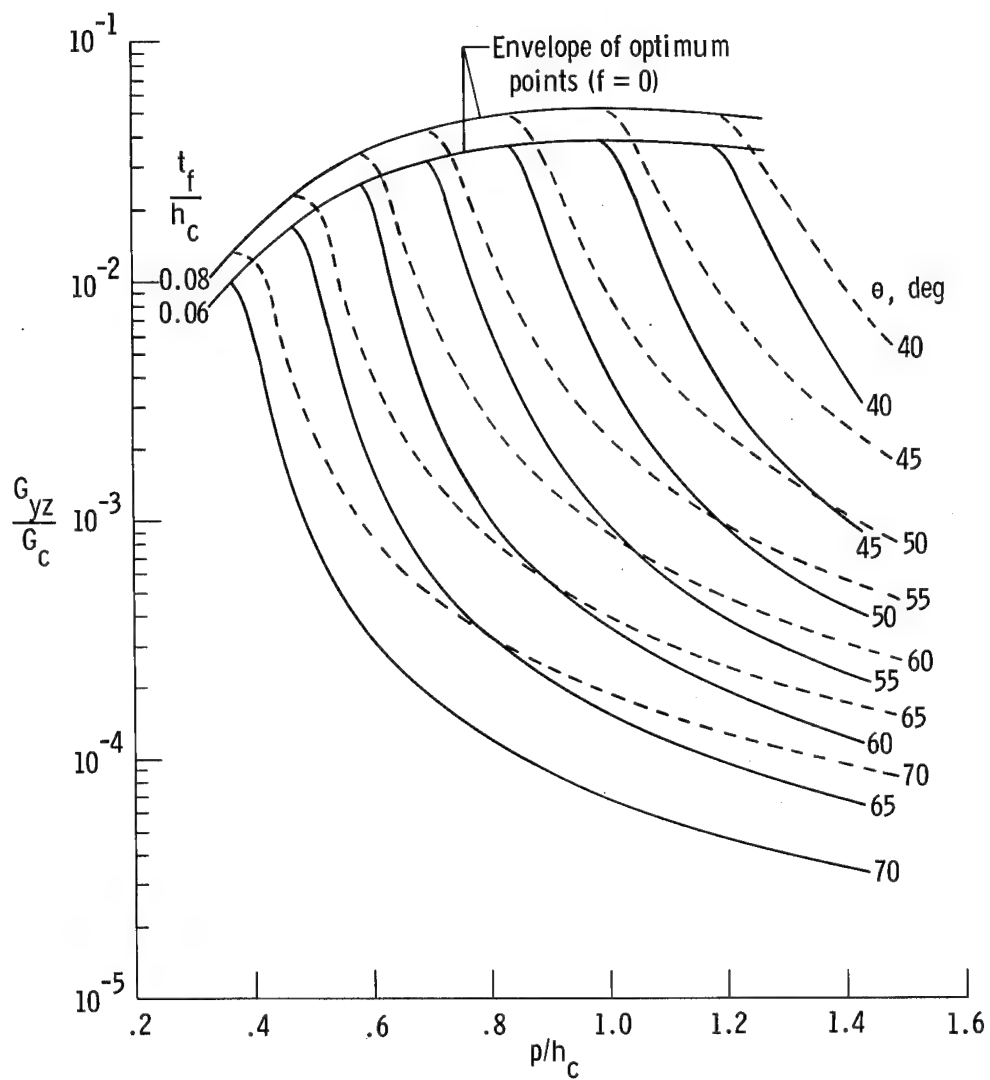
Figure 11. Concluded.

41
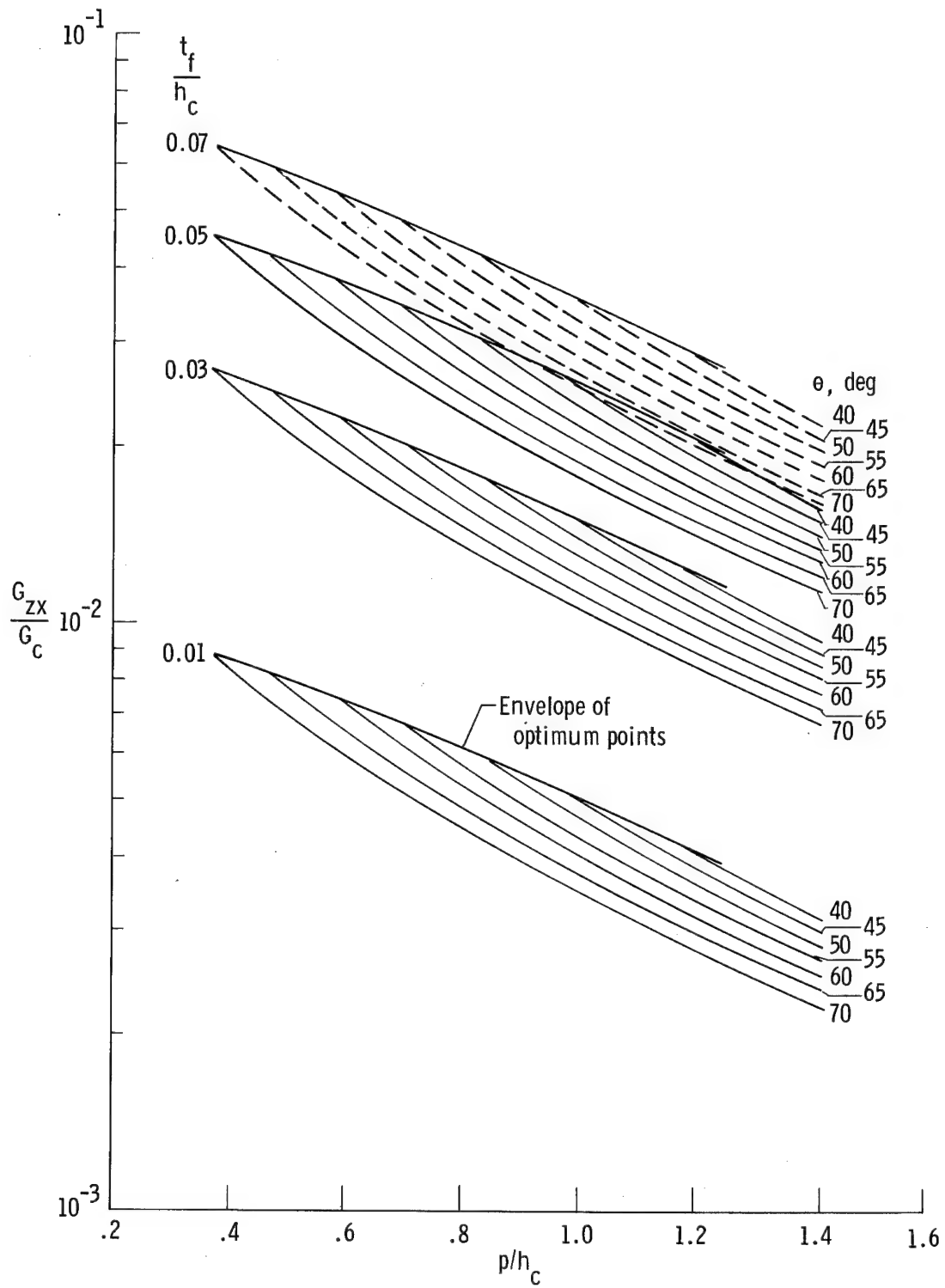
Figure 12. Shear modulus G_{zx} for SPF/DB corrugated core. $R = t_f$.
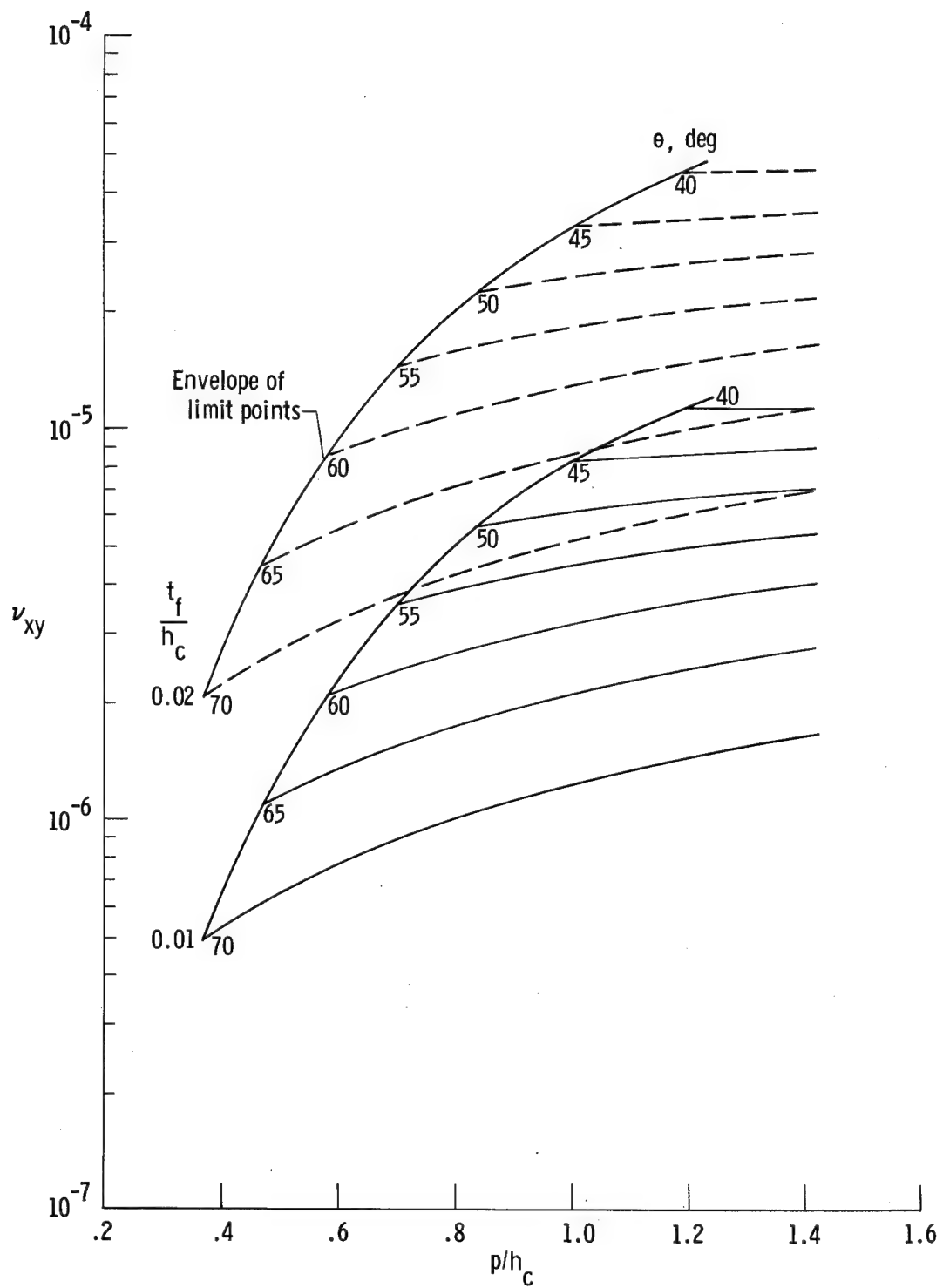
Figure 13. Poisson ratio ν_{xy} for SPF/DB corrugated core. $R = t_f$.
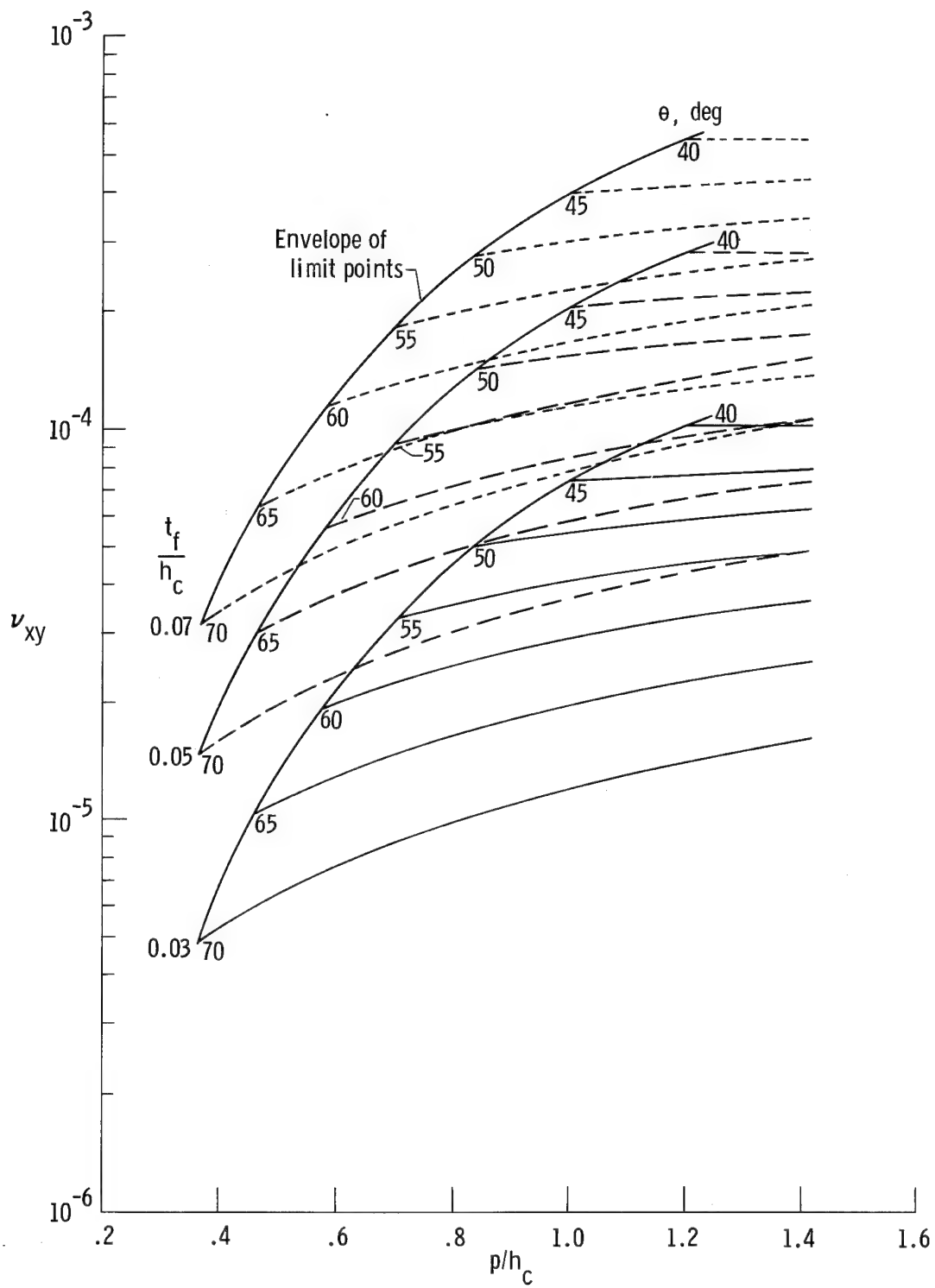
Figure 13. Continued.
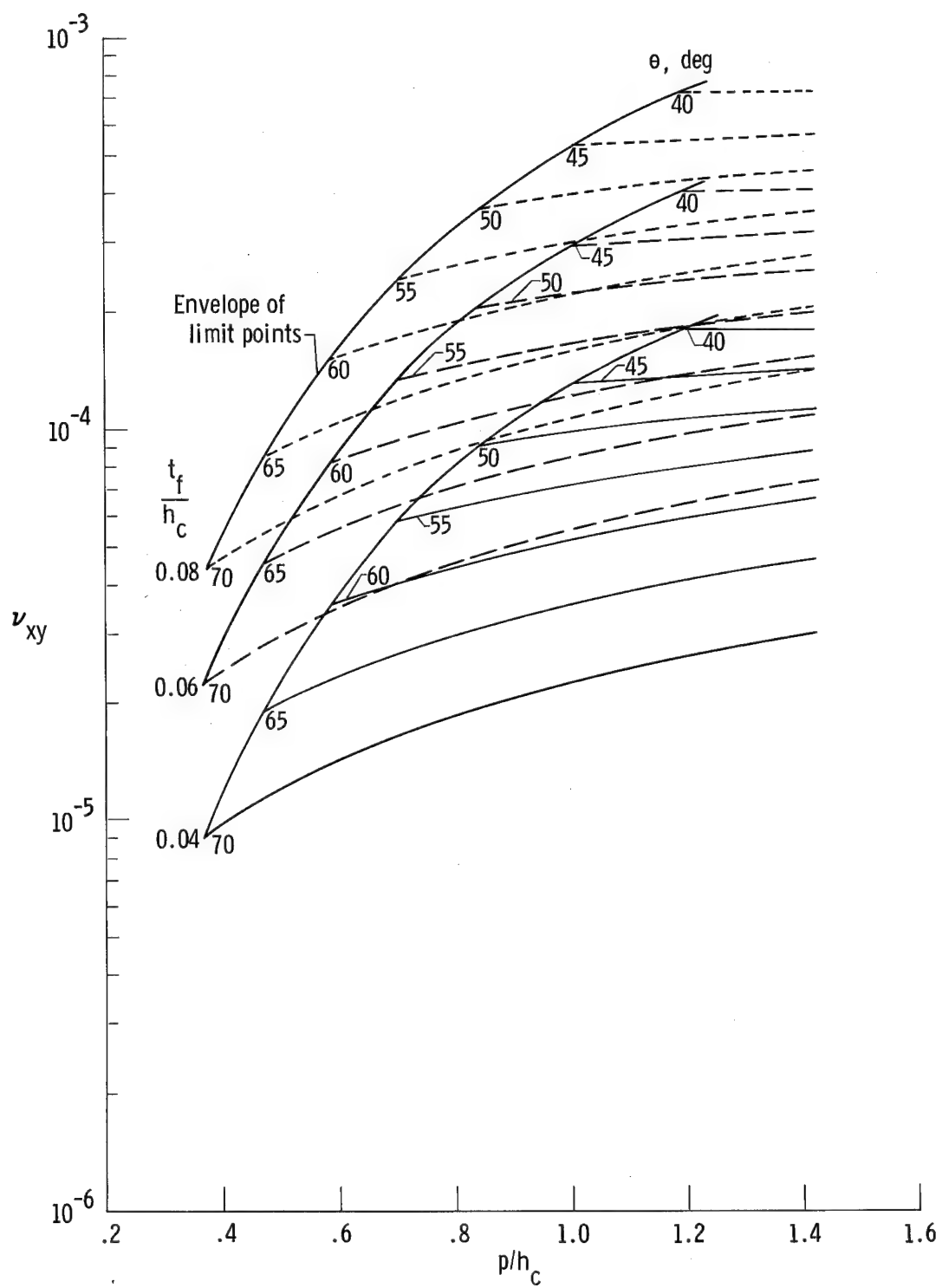
Figure 13. Concluded.

45
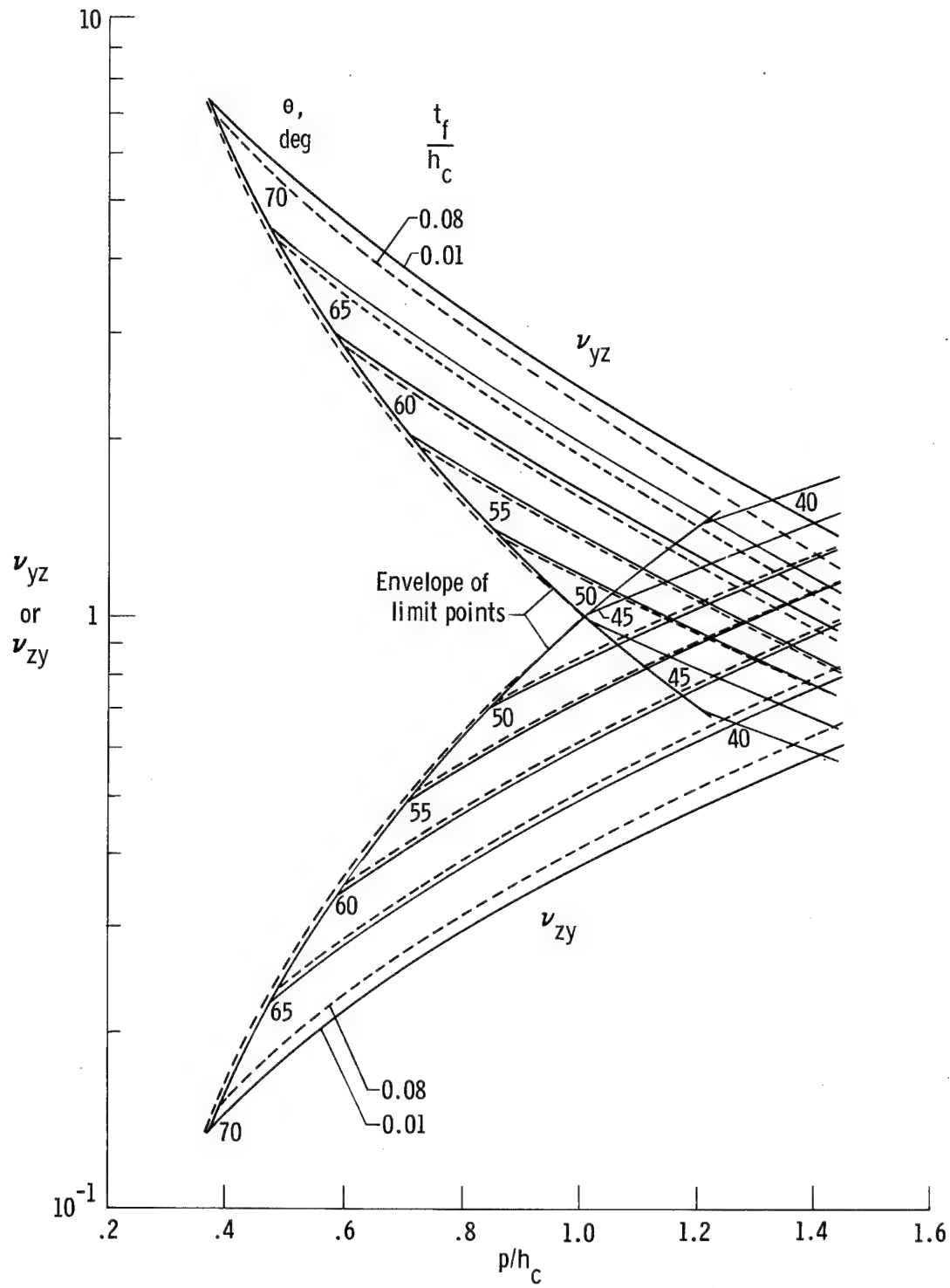
Figure 14. Poisson ratios ν_{yz} and ν_{zy} for SPF/DB corrugated core. $R = t_f$.
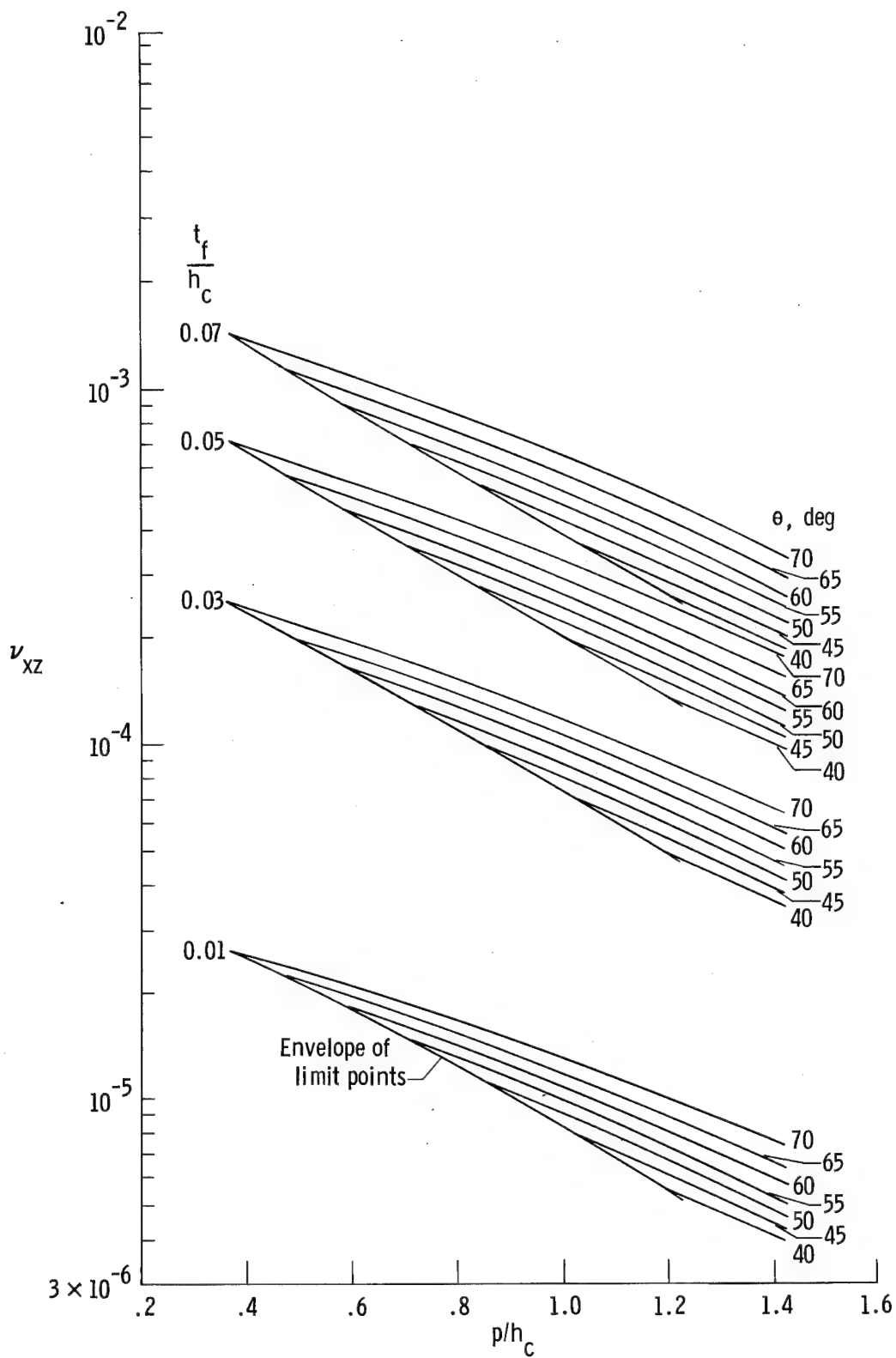
Figure 15. Poisson ratio ν_{xz} for SPF/DB corrugated core. $R = t_f$.
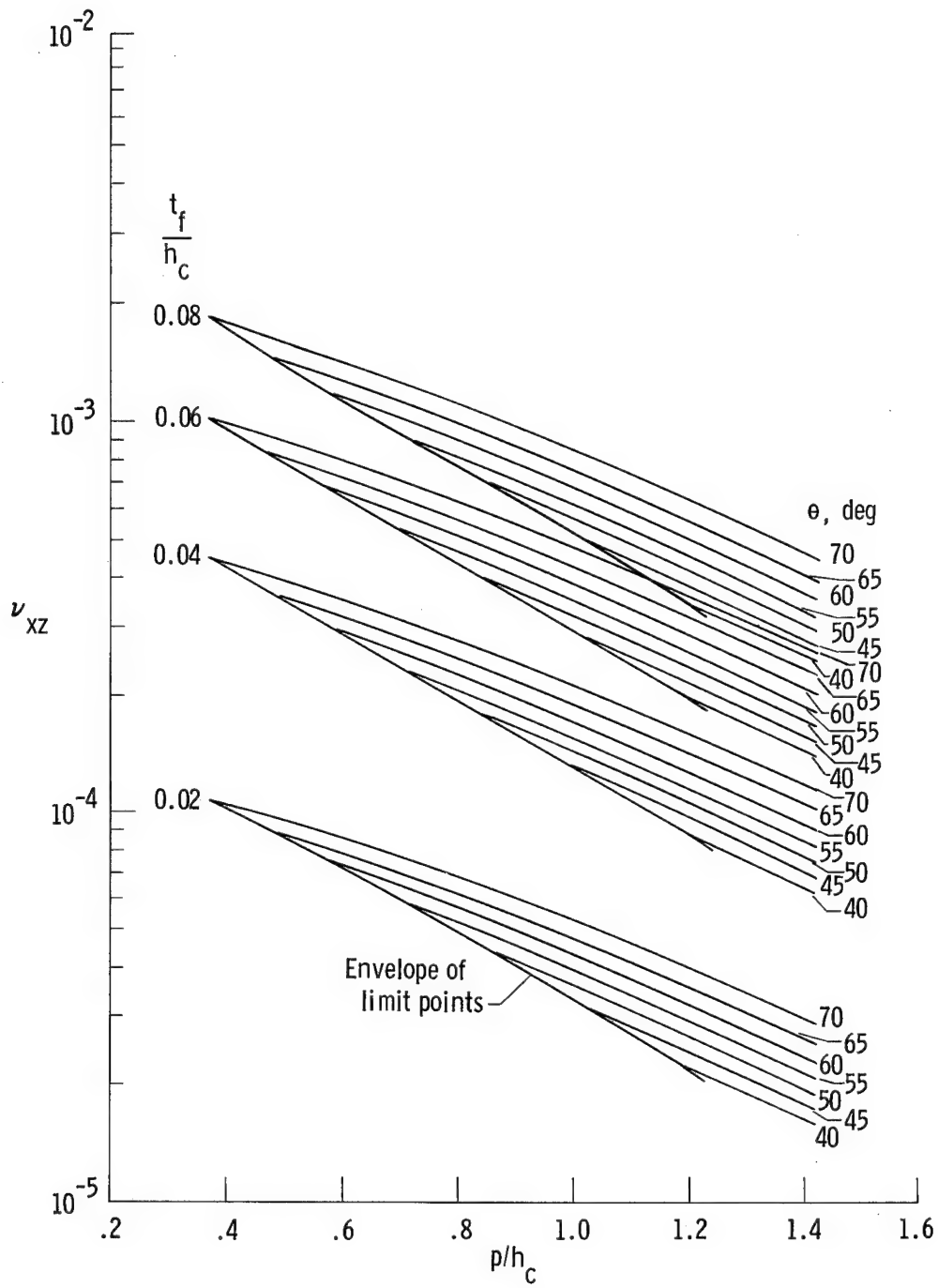
Figure 15.   Concluded.
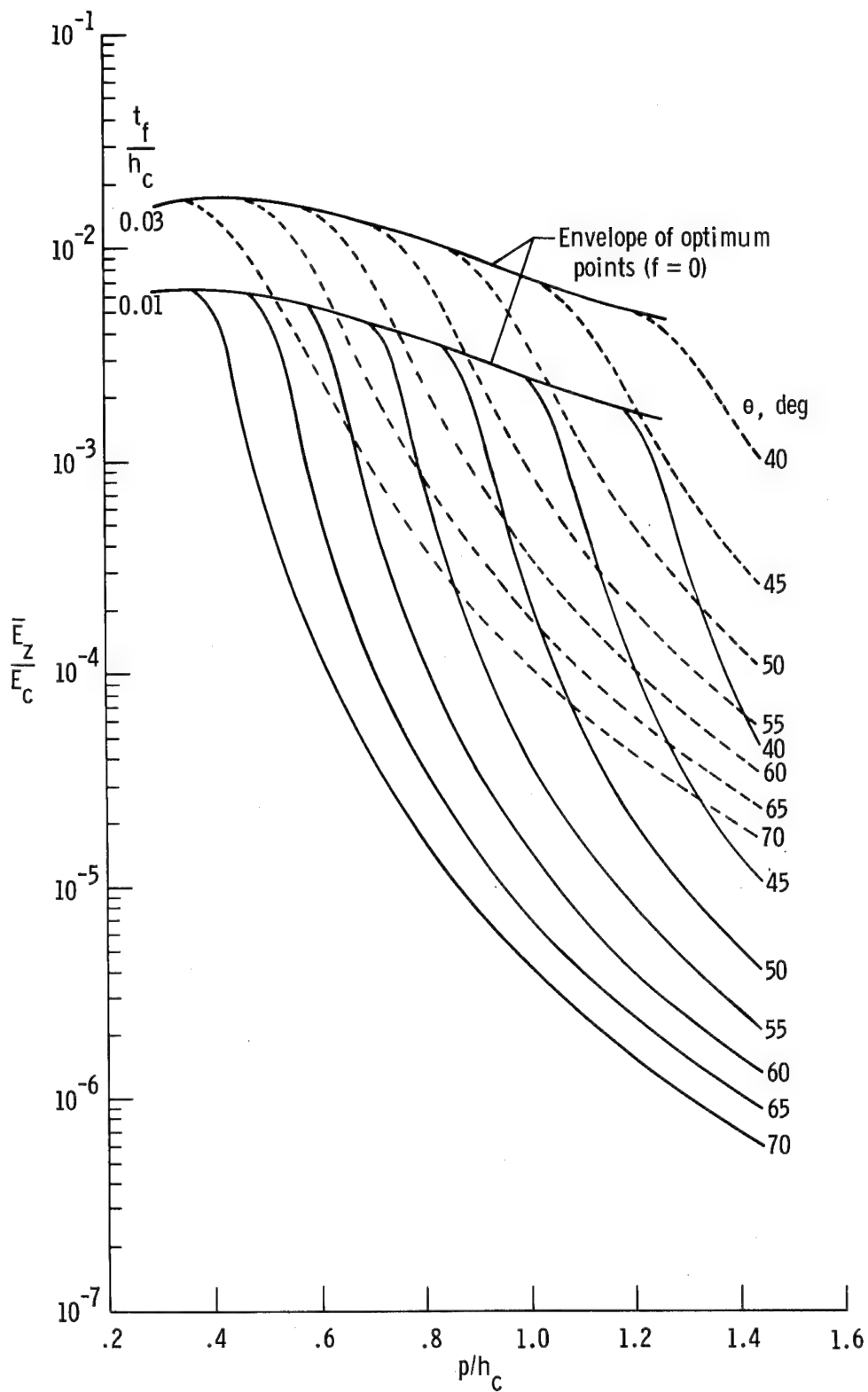
Figure 16. Modulus of elasticity $\bar{E}_z$ for SPF/DB corrugated core. $R = t_f$.

49
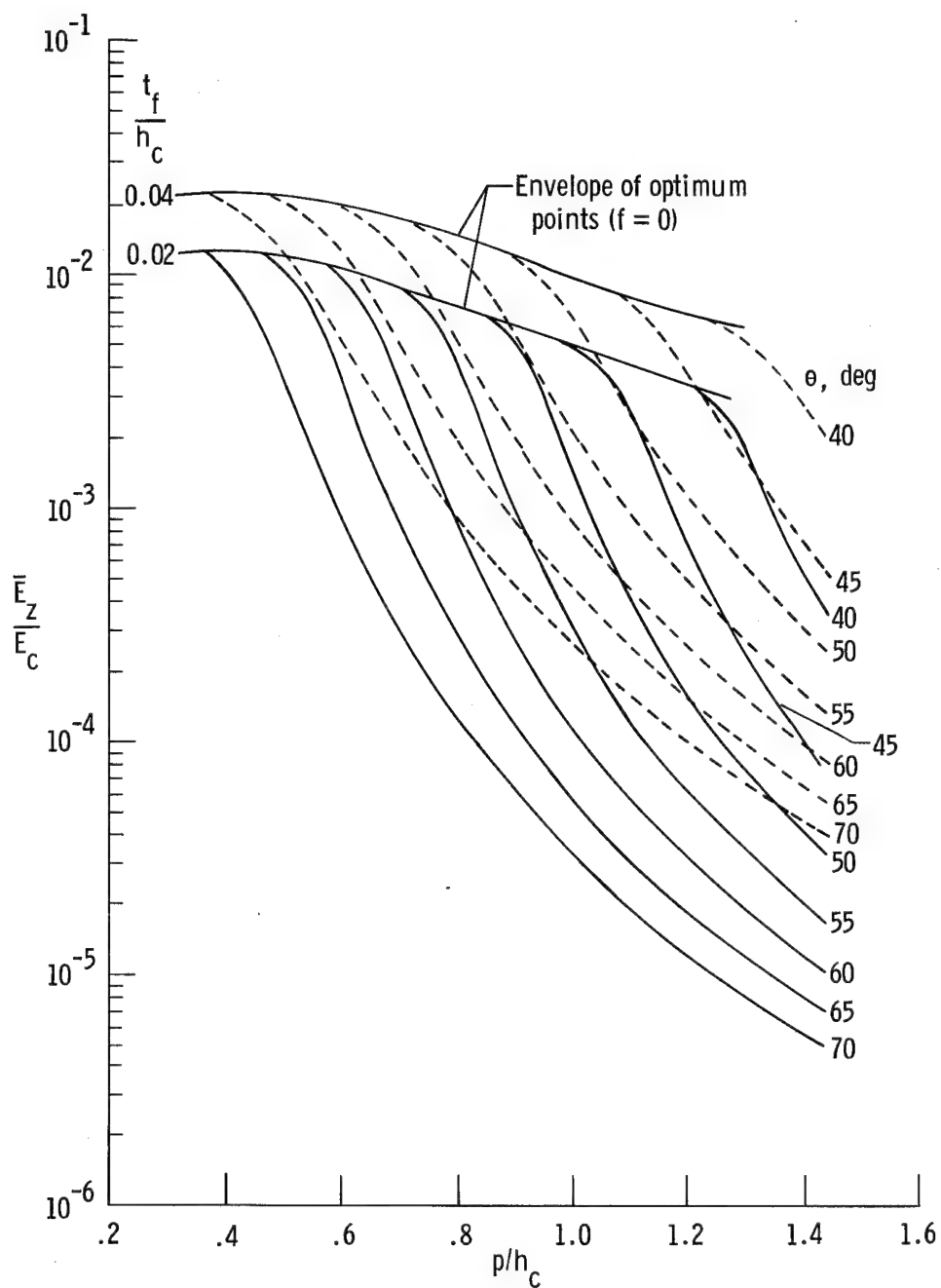
Figure 16. Continued.
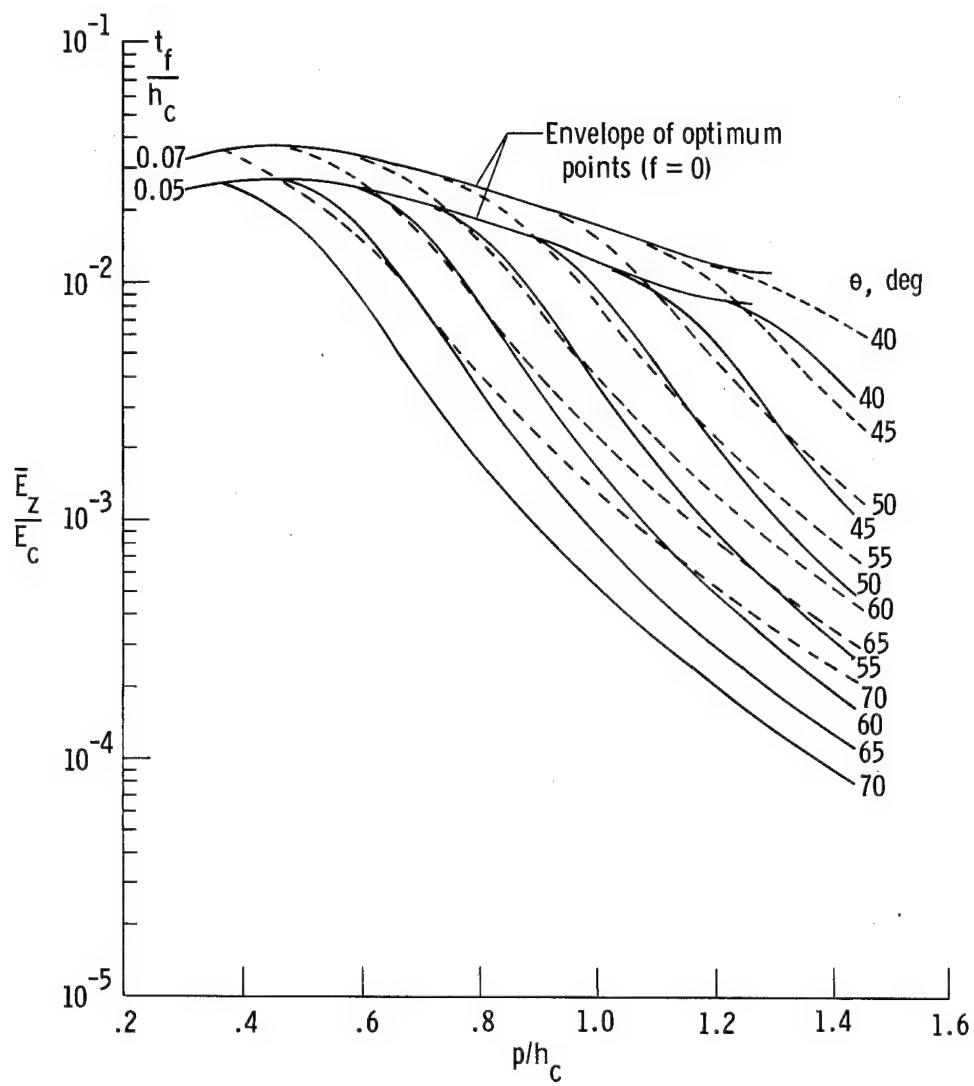
Figure 16.   Continued.
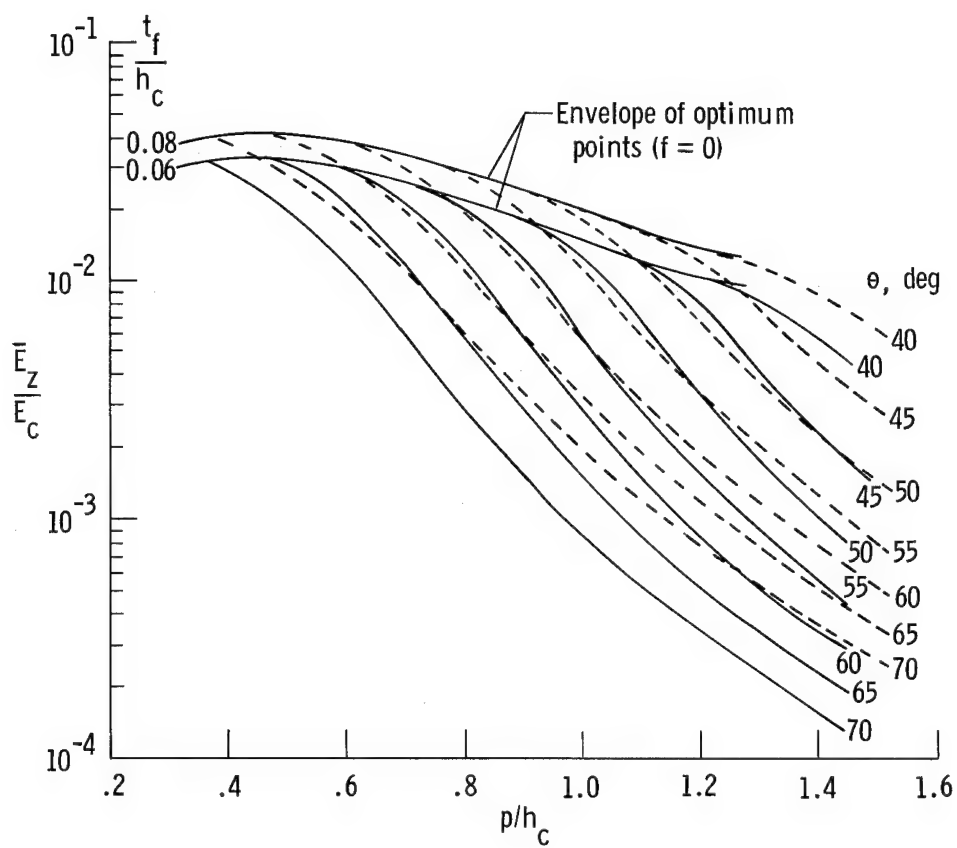
Figure 16. Concluded.
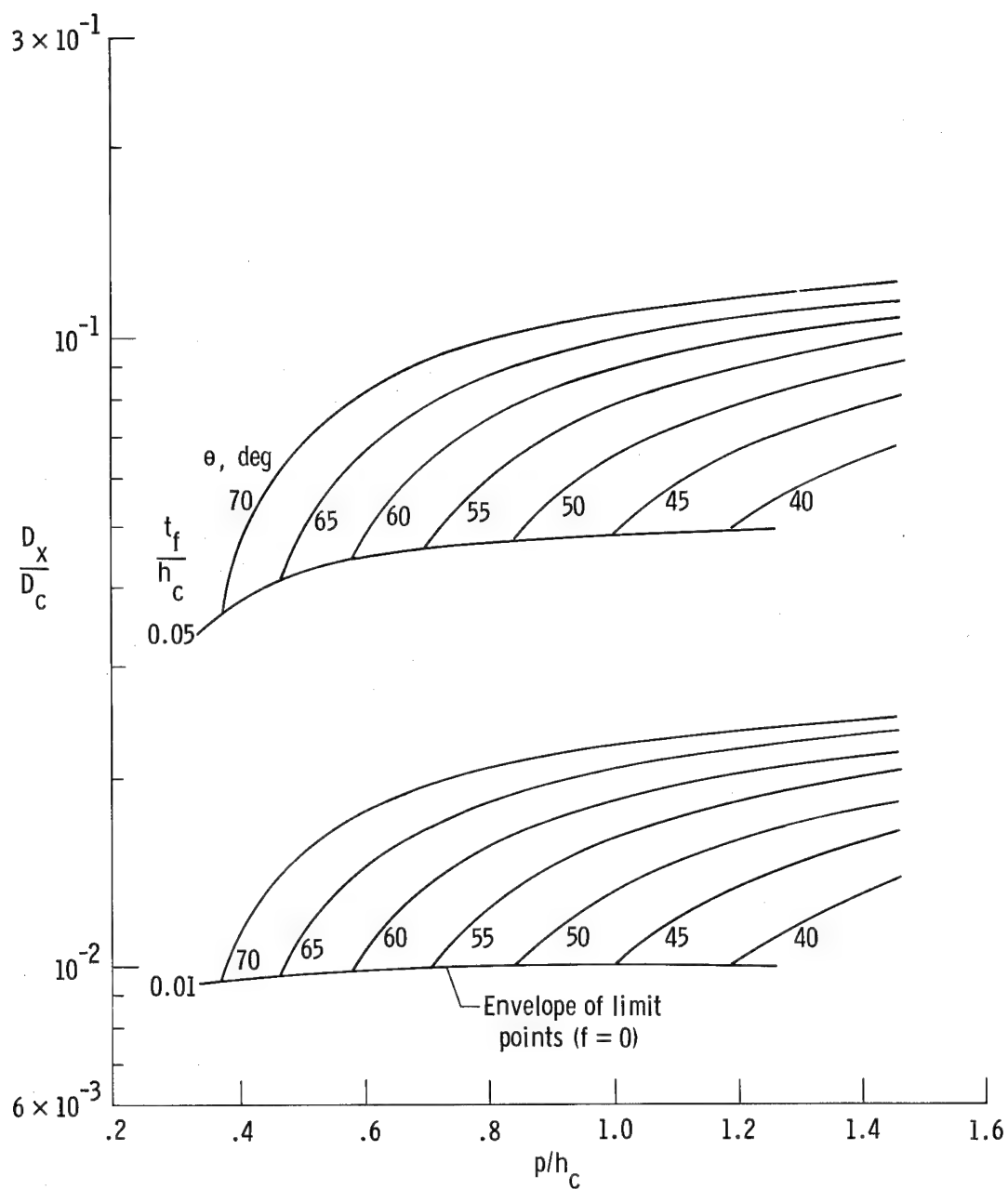
Figure 17. Bending stiffness D_x for SPF/DB corrugated
sandwich core. $R = t_f$; $D_c = E_c h_c^3/12$.
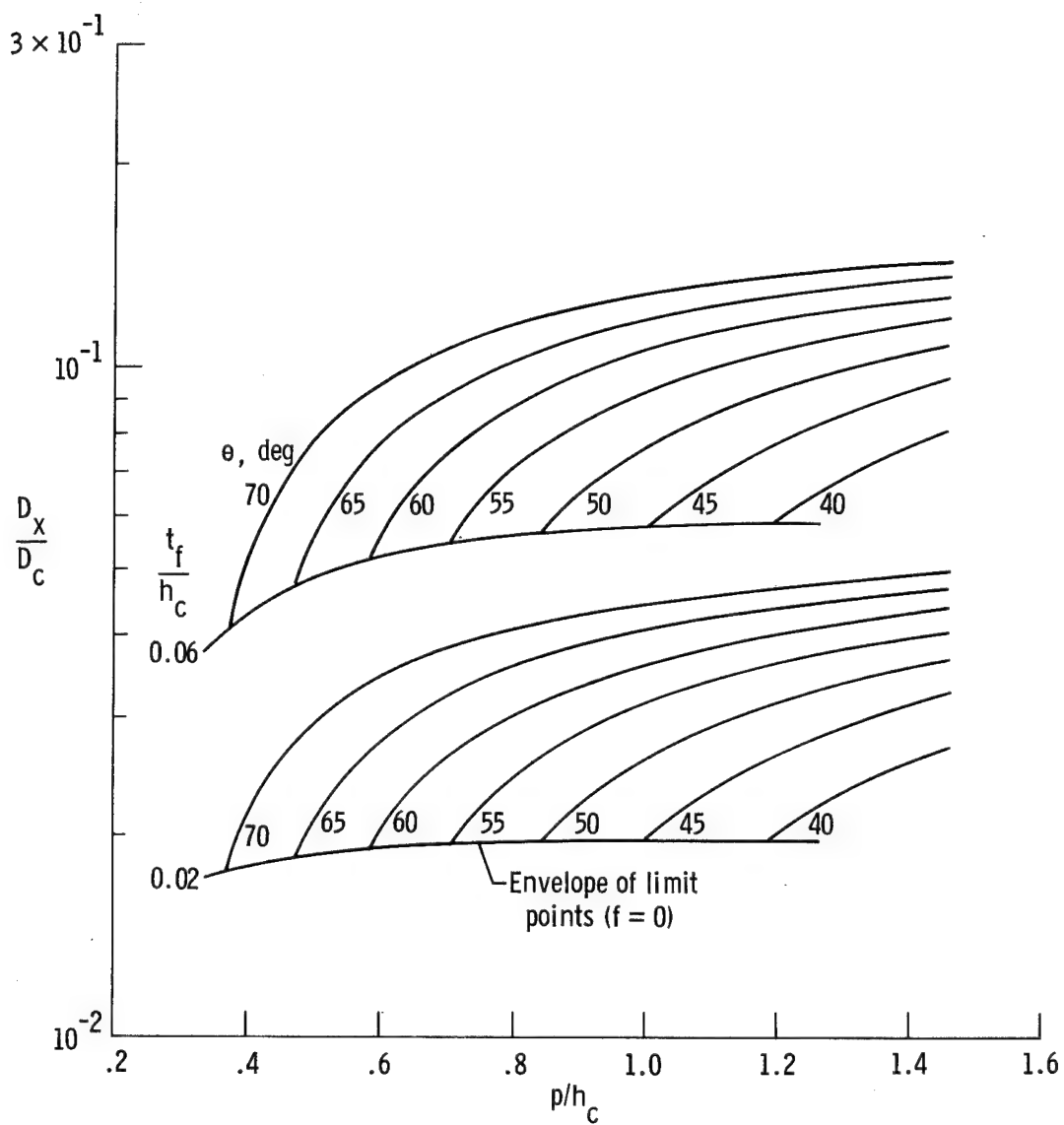
Figure 17. Continued.
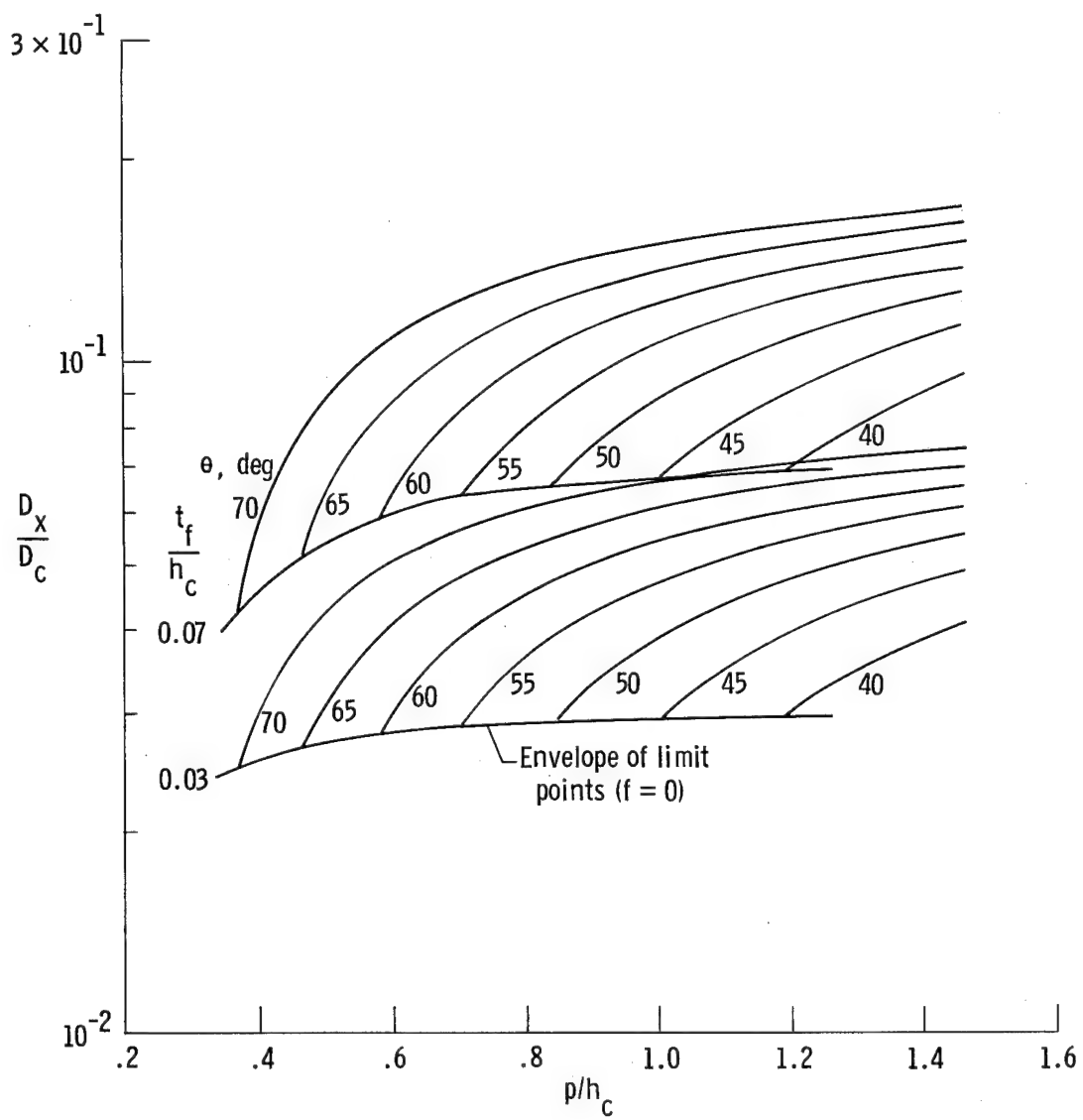
Figure 17.   Continued.
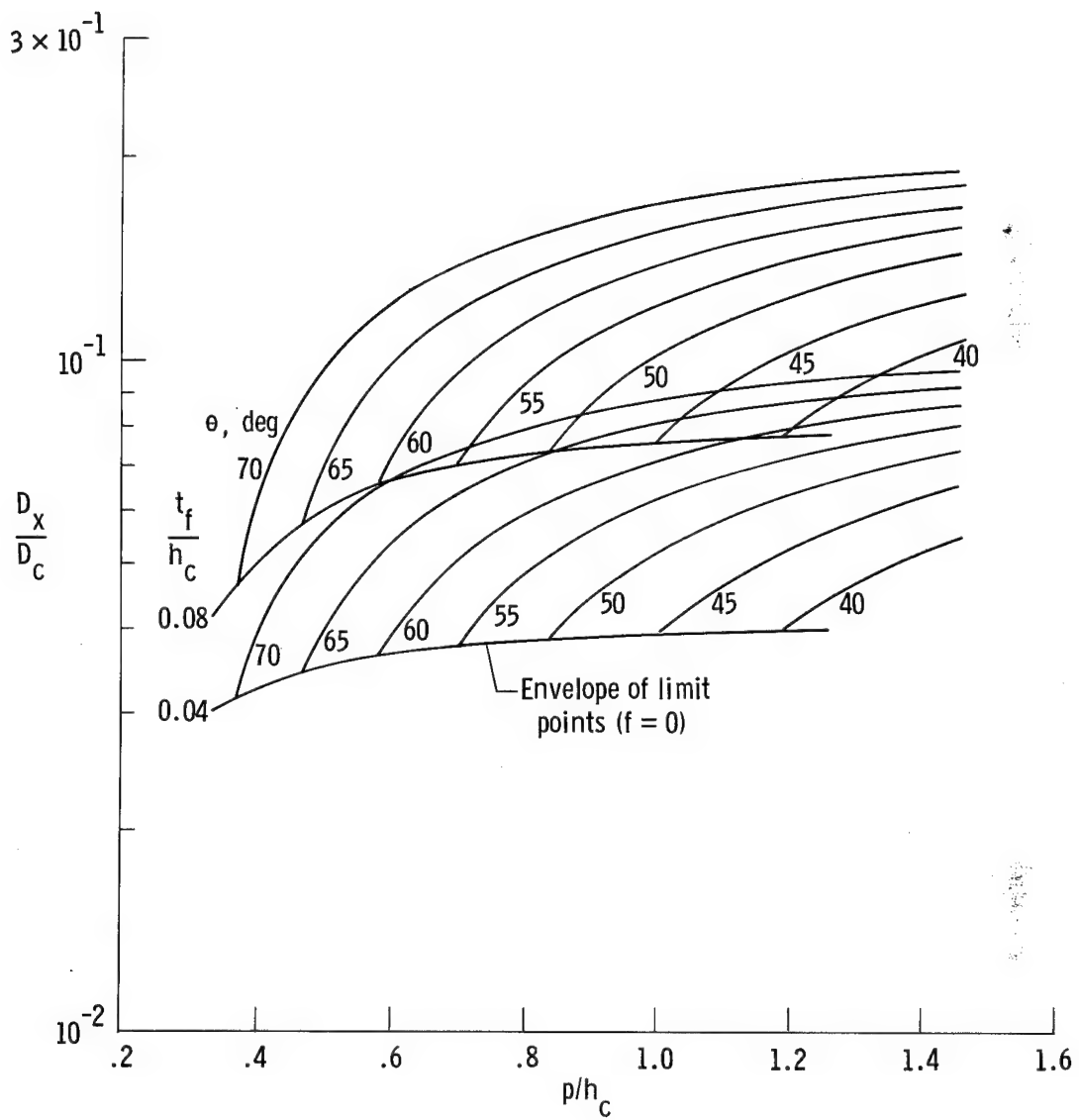
Figure 17. Concluded.
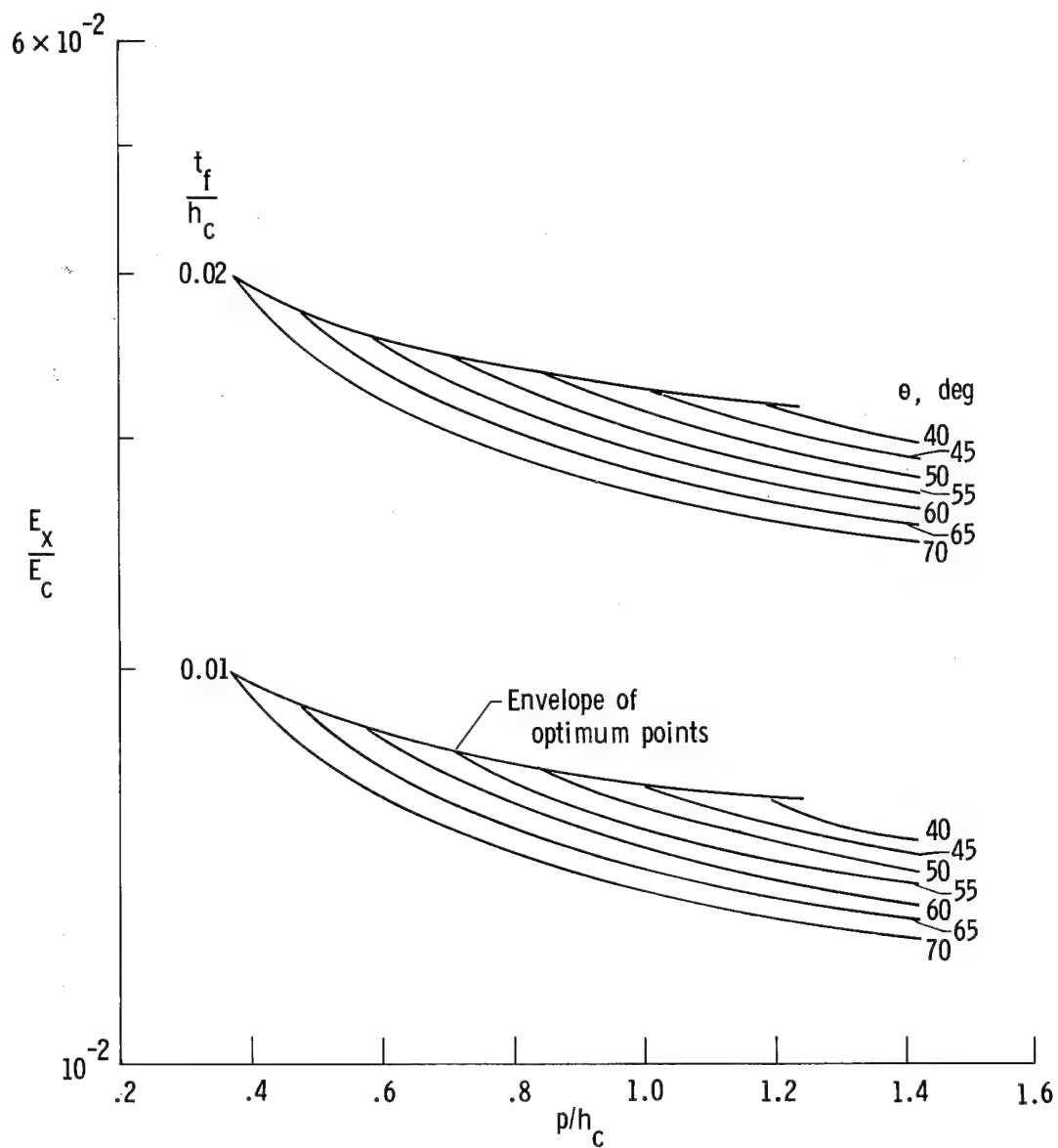
Figure 18. Modulus of elasticity E_x for honeycomb
core. $R = t_c = t_f$.
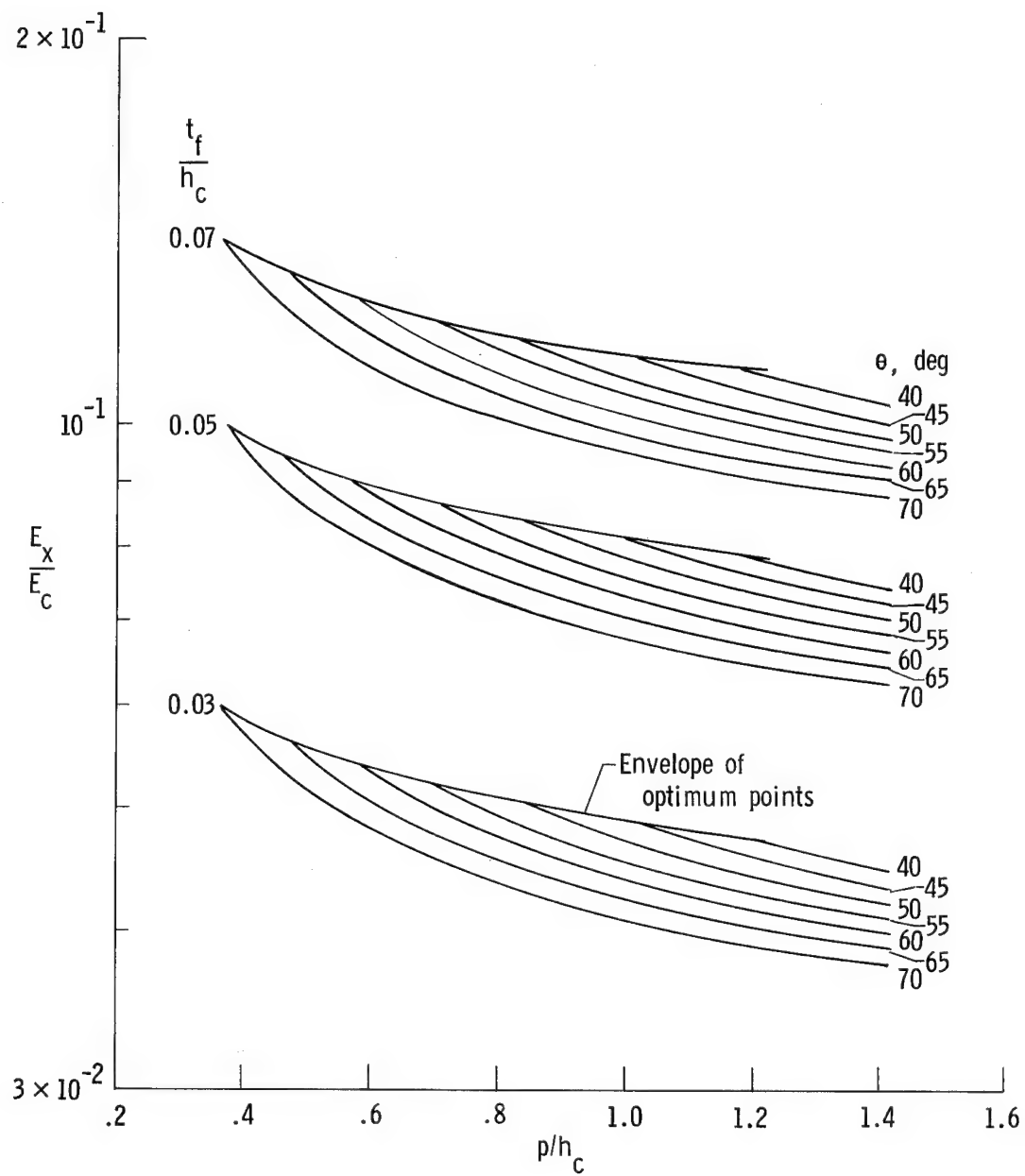
Figure 18. Continued.
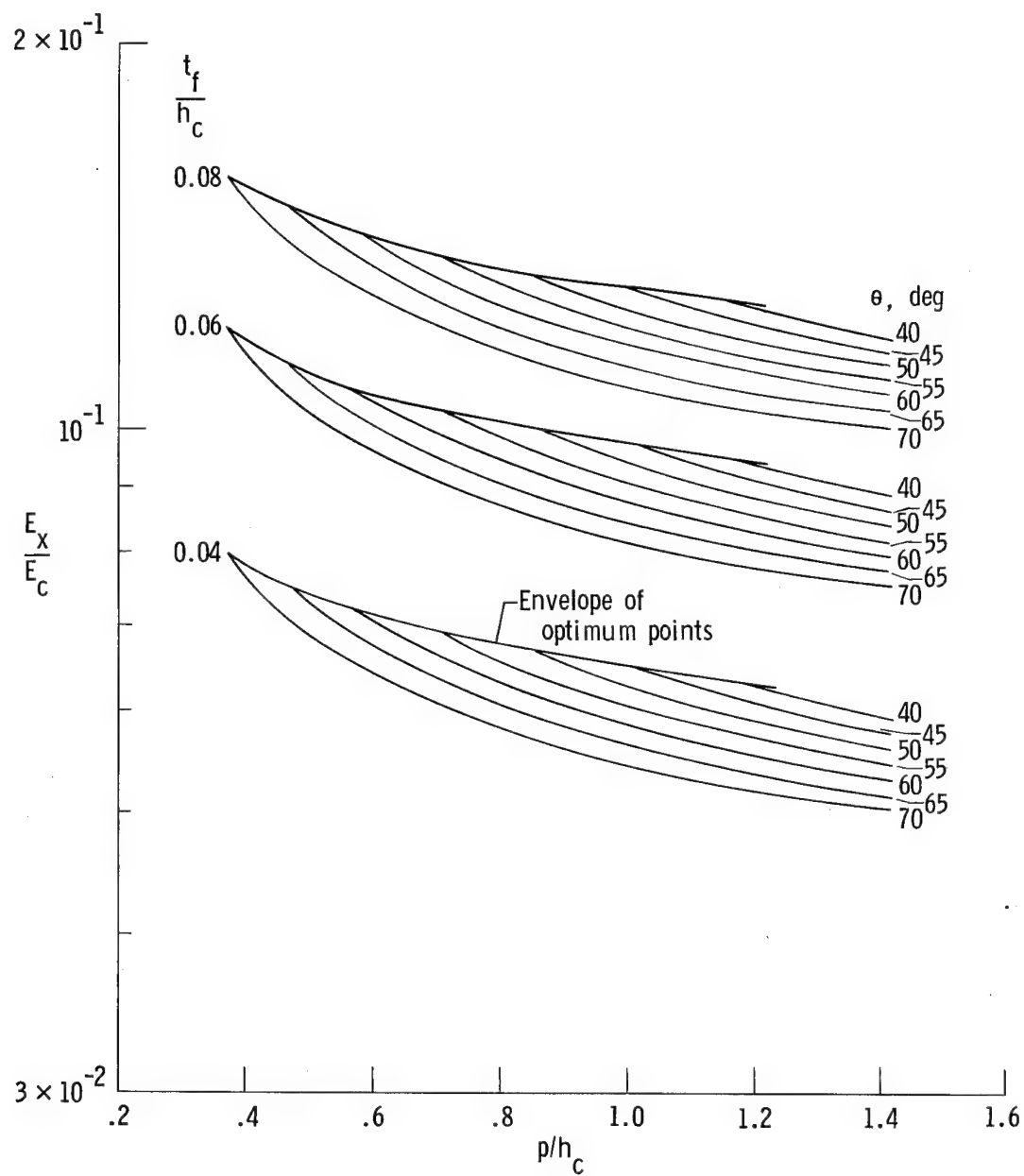
Figure 18. Concluded.
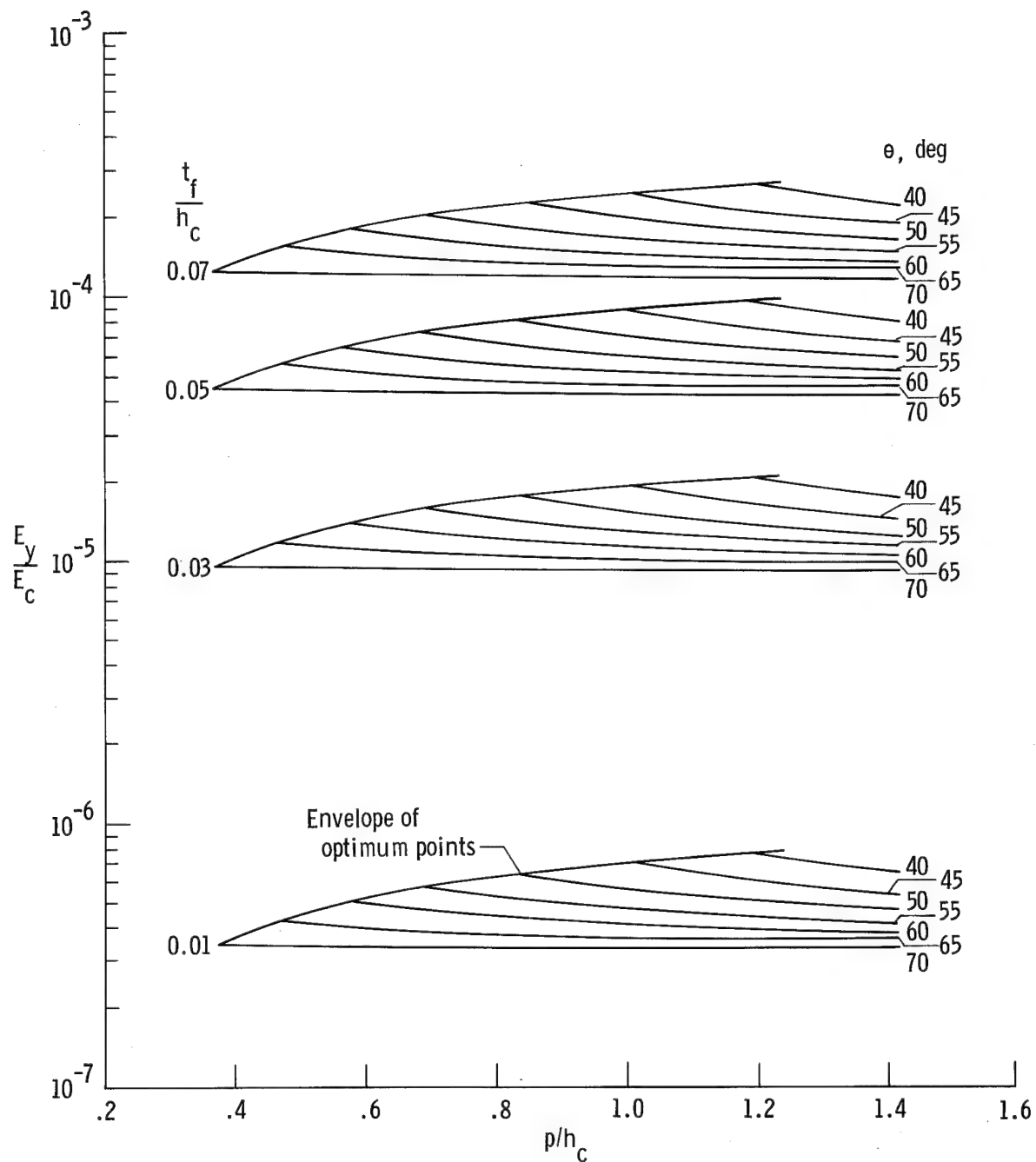
Figure 19. Modulus of elasticity E_y for honeycomb core. $R = t_c = t_f$.
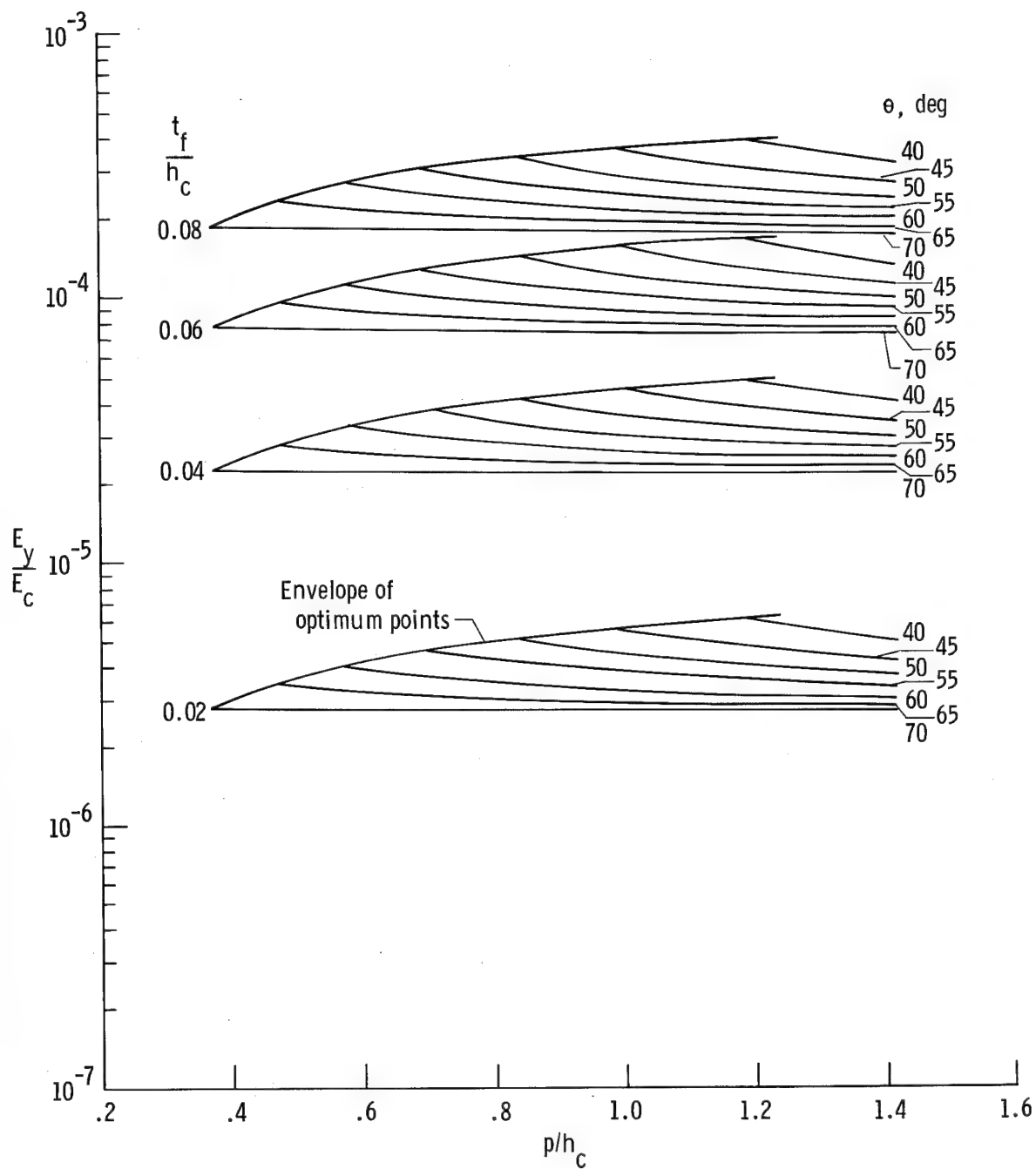
Figure 19. Concluded.
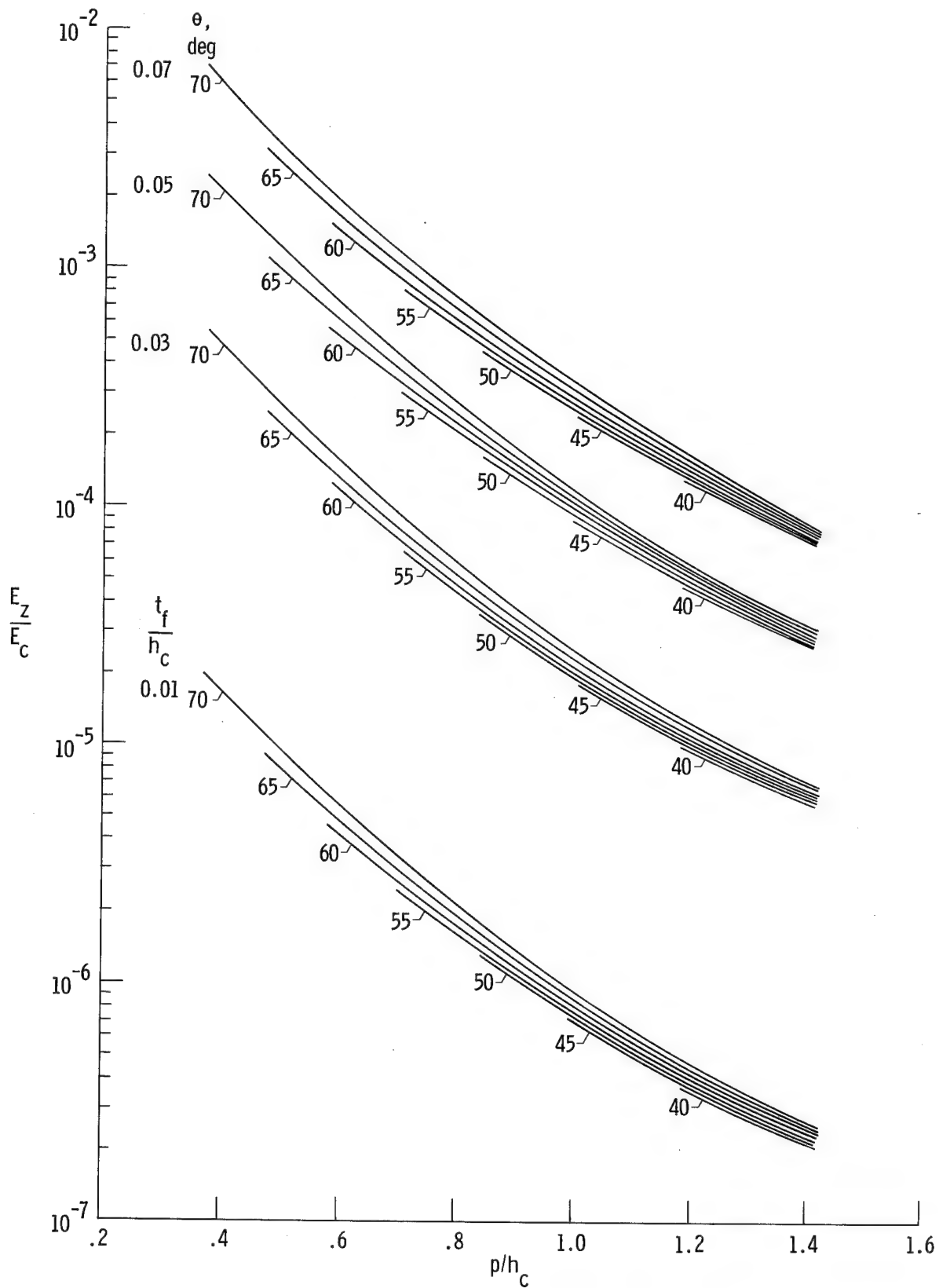
Figure 20. Modulus of elasticity E_z for honeycomb core. $R = t_c = t_f$.
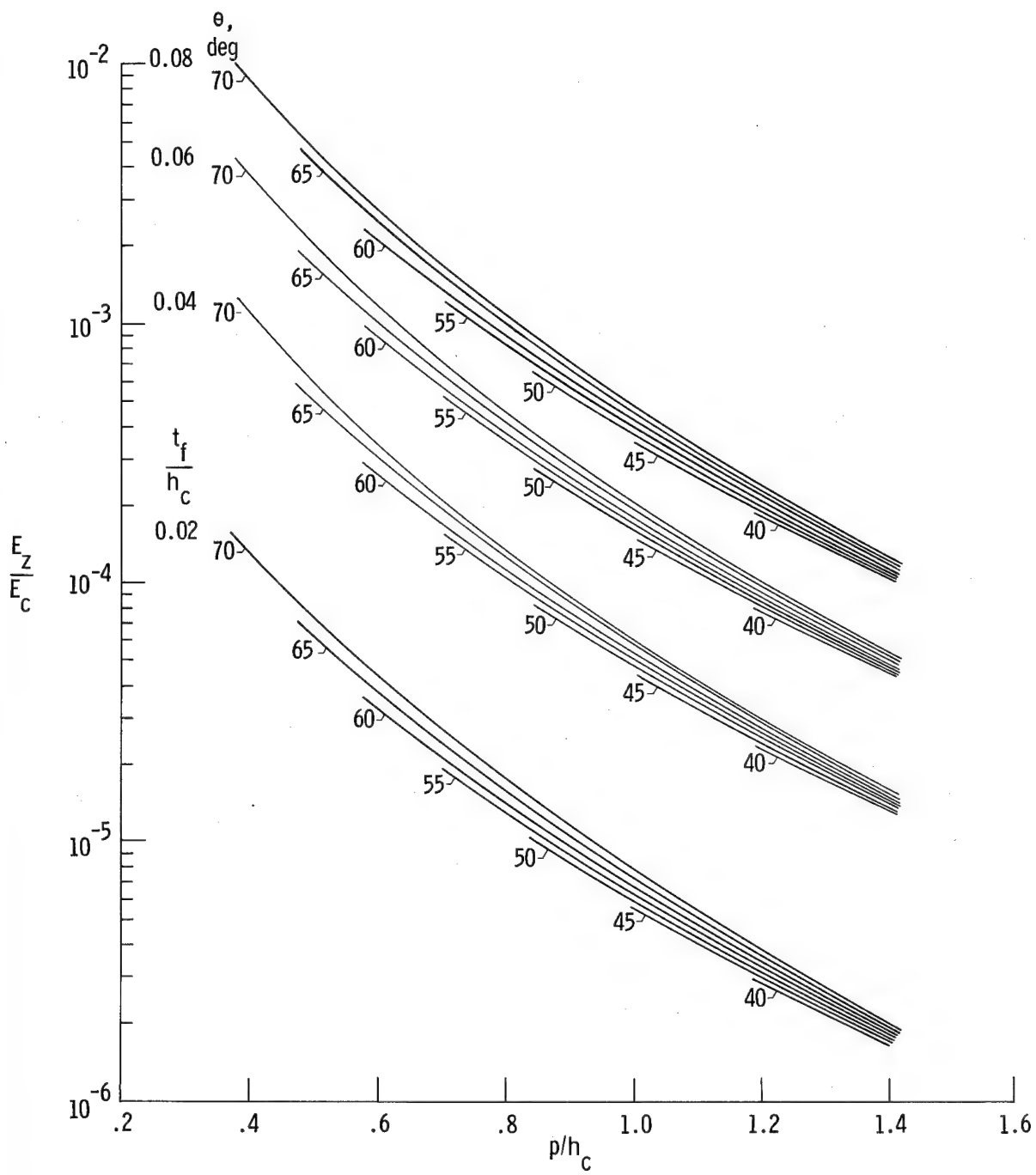
Figure 20.   Concluded.
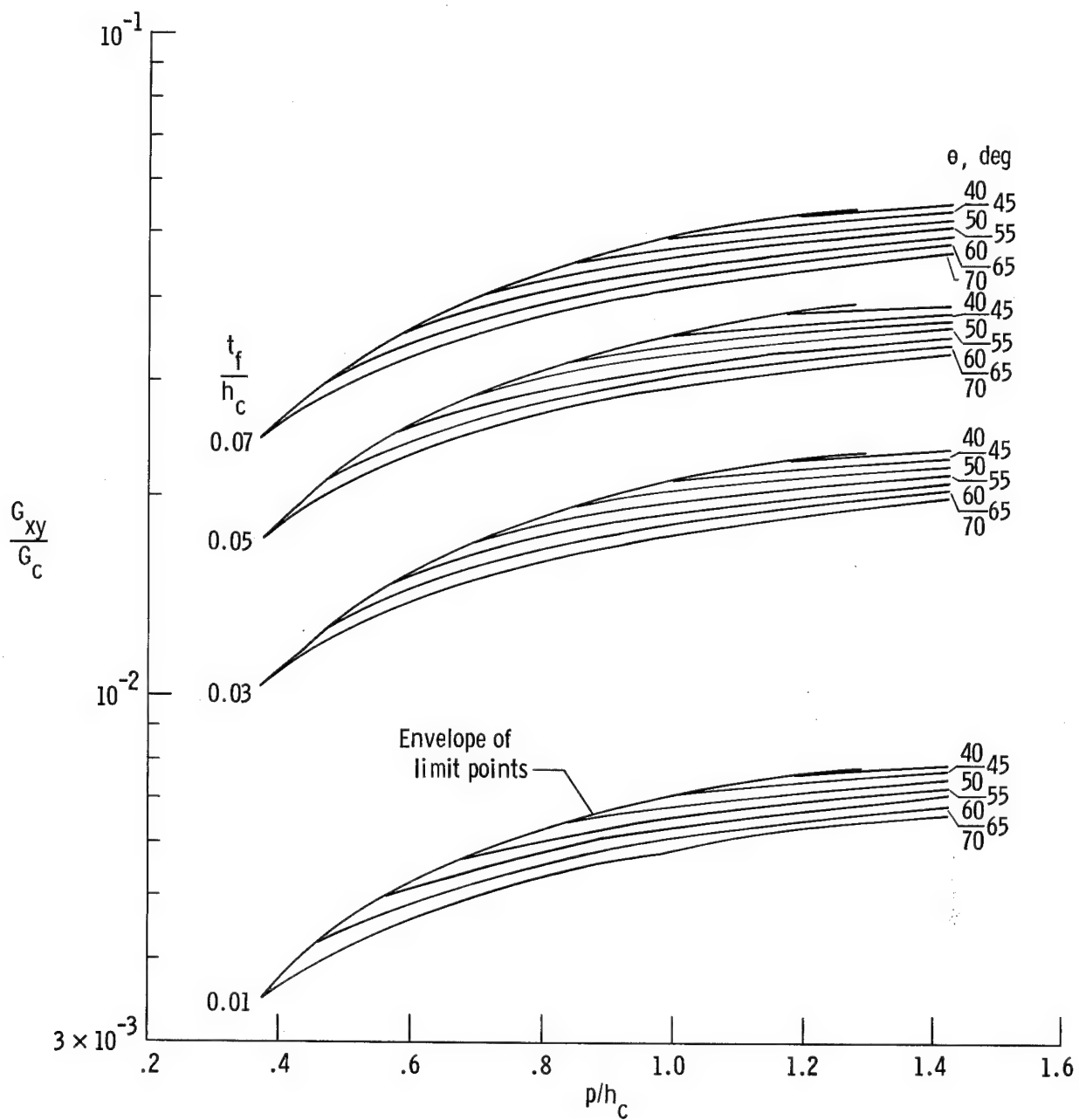
Figure 21. Shear modulus G_{xy} for honeycomb core. $R = t_c = t_f$.
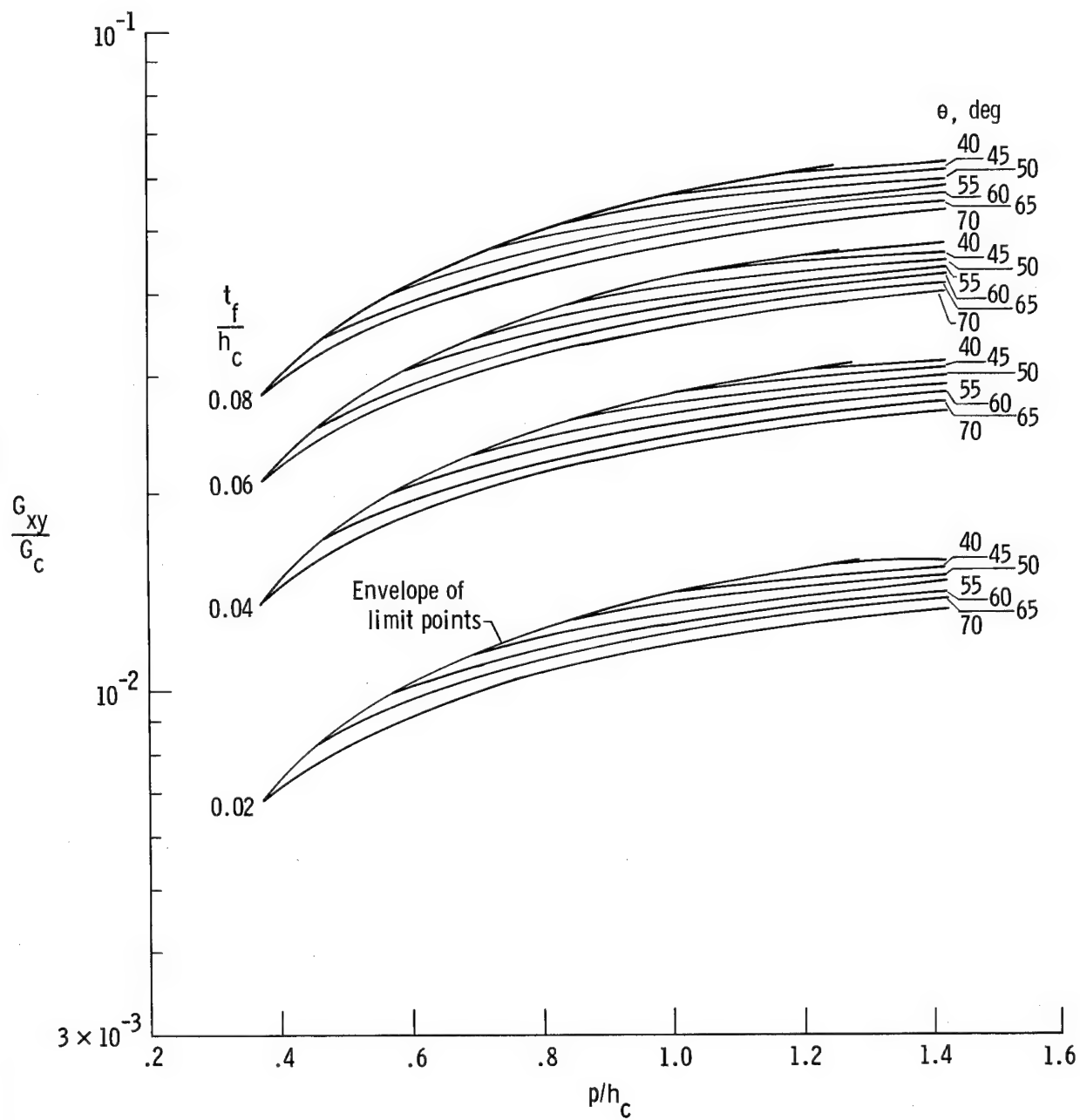
Figure 21.   Concluded.
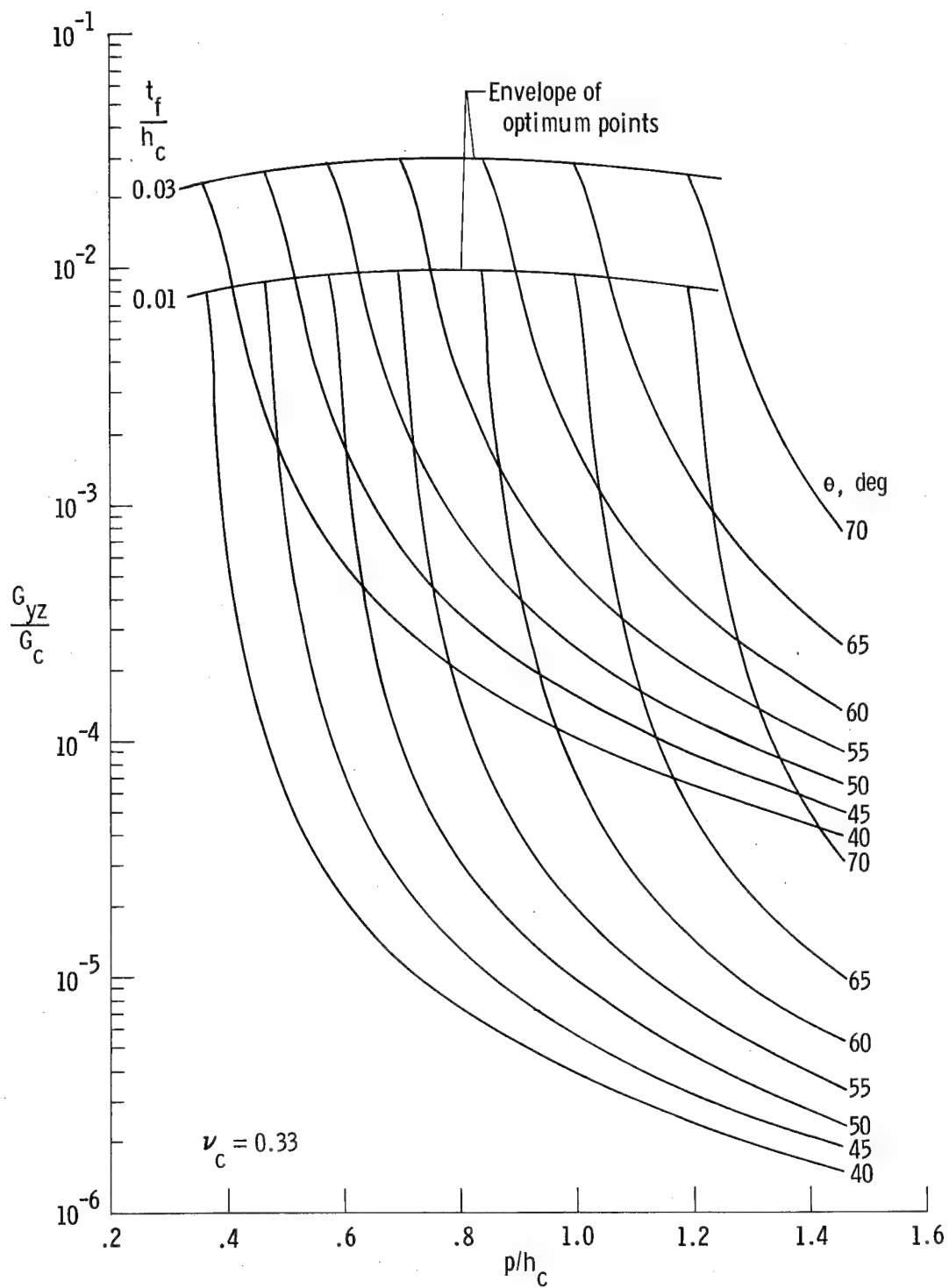
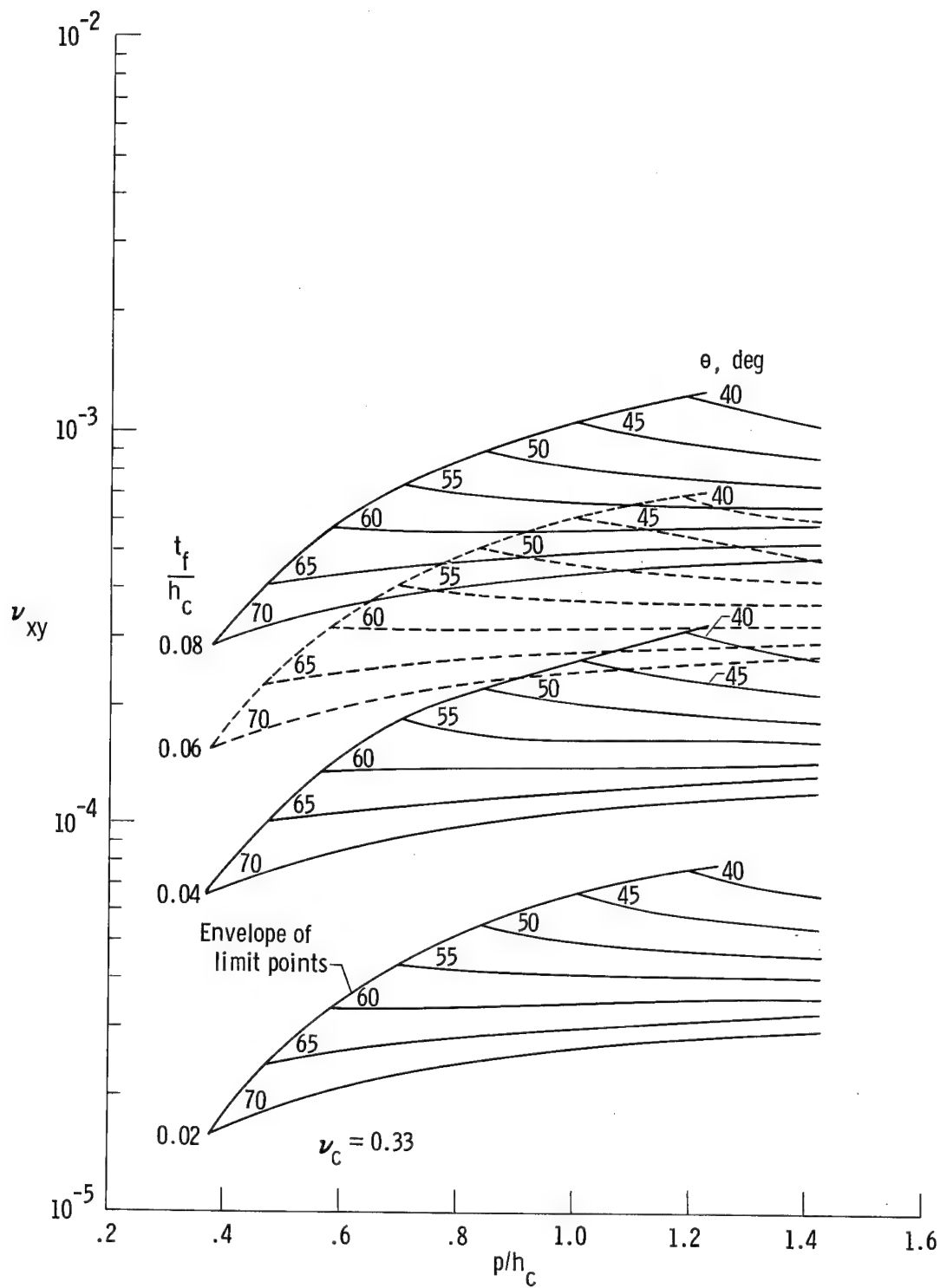Figure 22. Shear modulus G_{yz} for honeycomb core.
$R = t_c = t_f$.

Figure 22.   Continued.

67
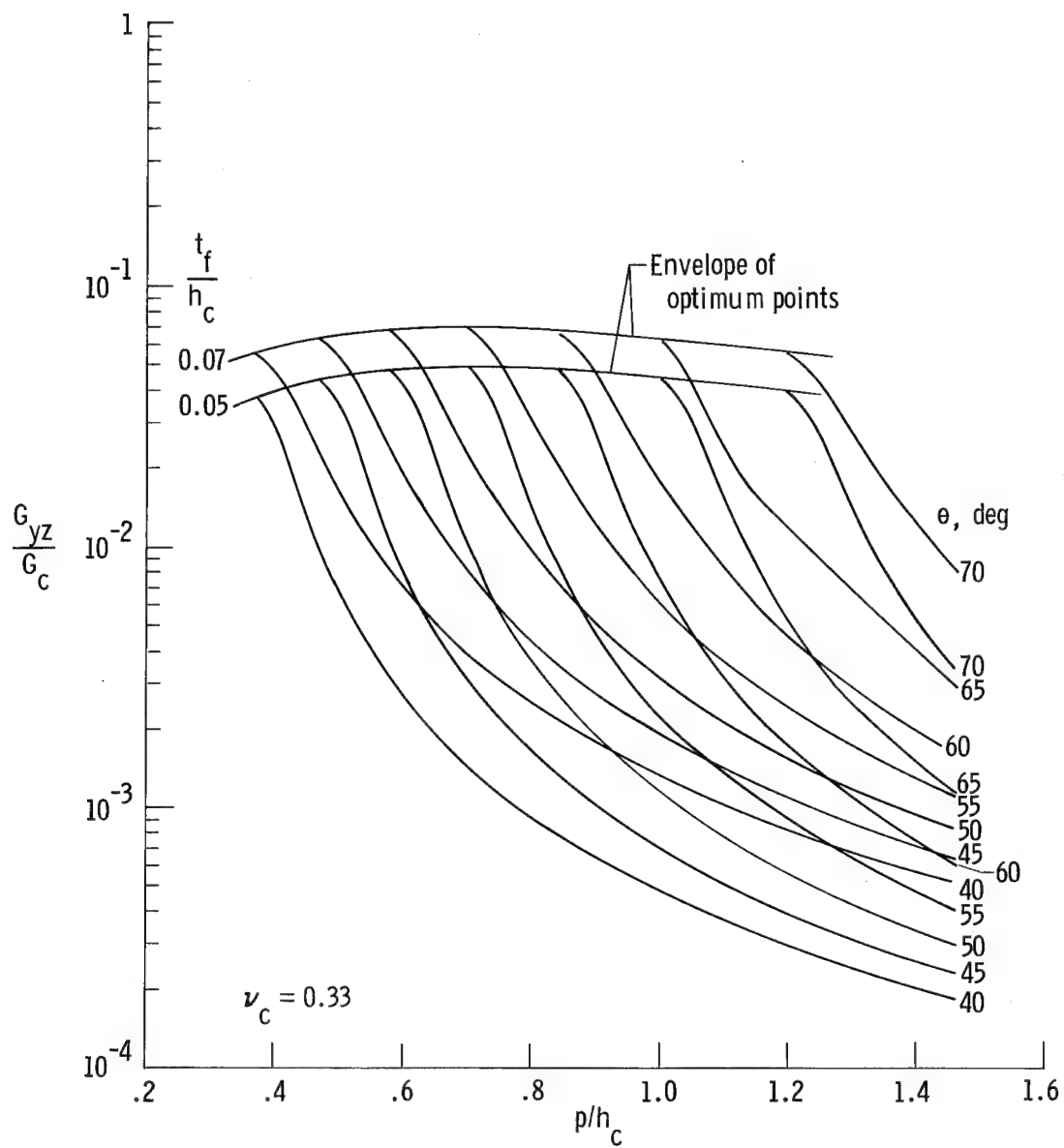
Figure 22.   Continued.
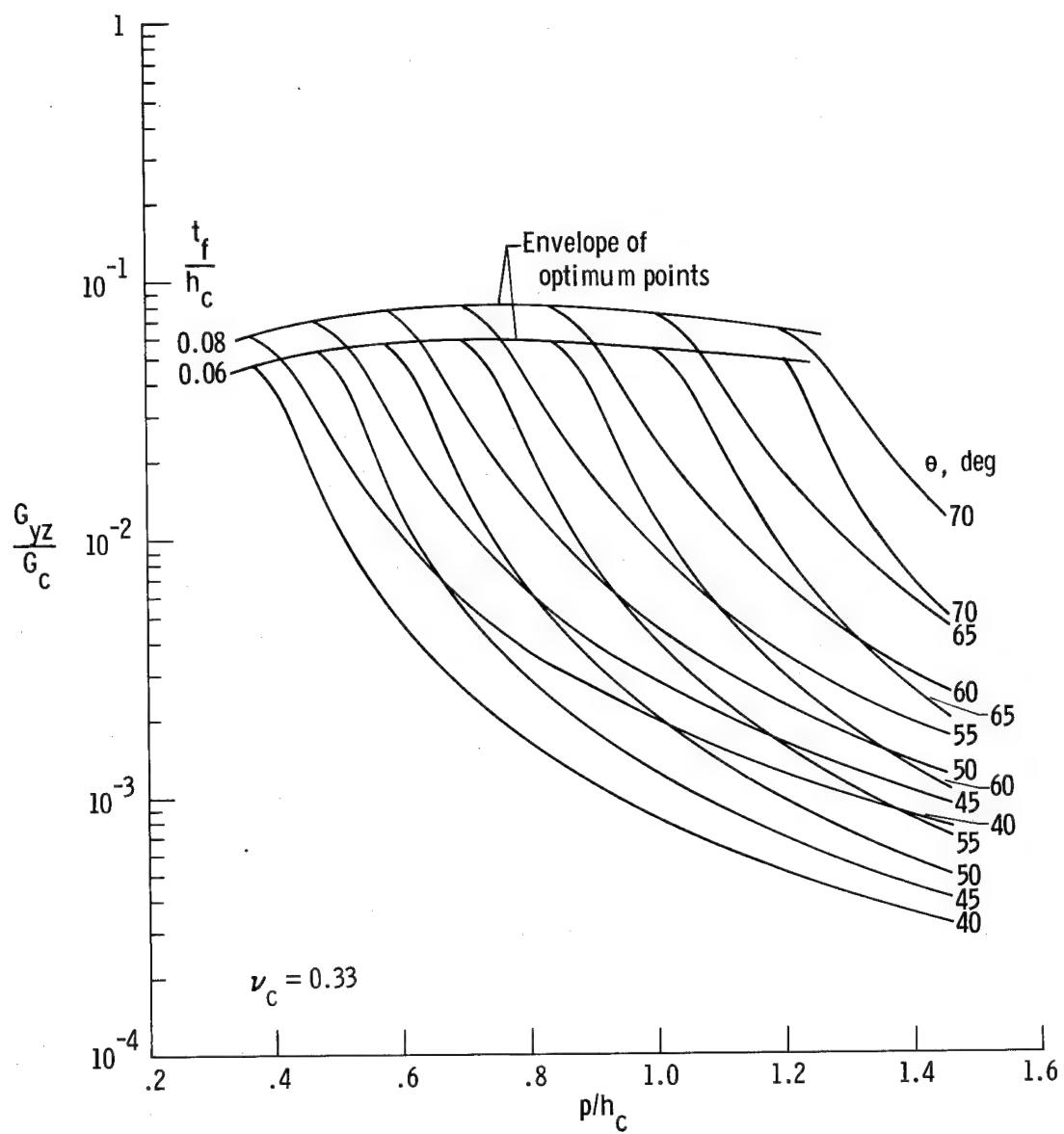
Figure 22.   Concluded.
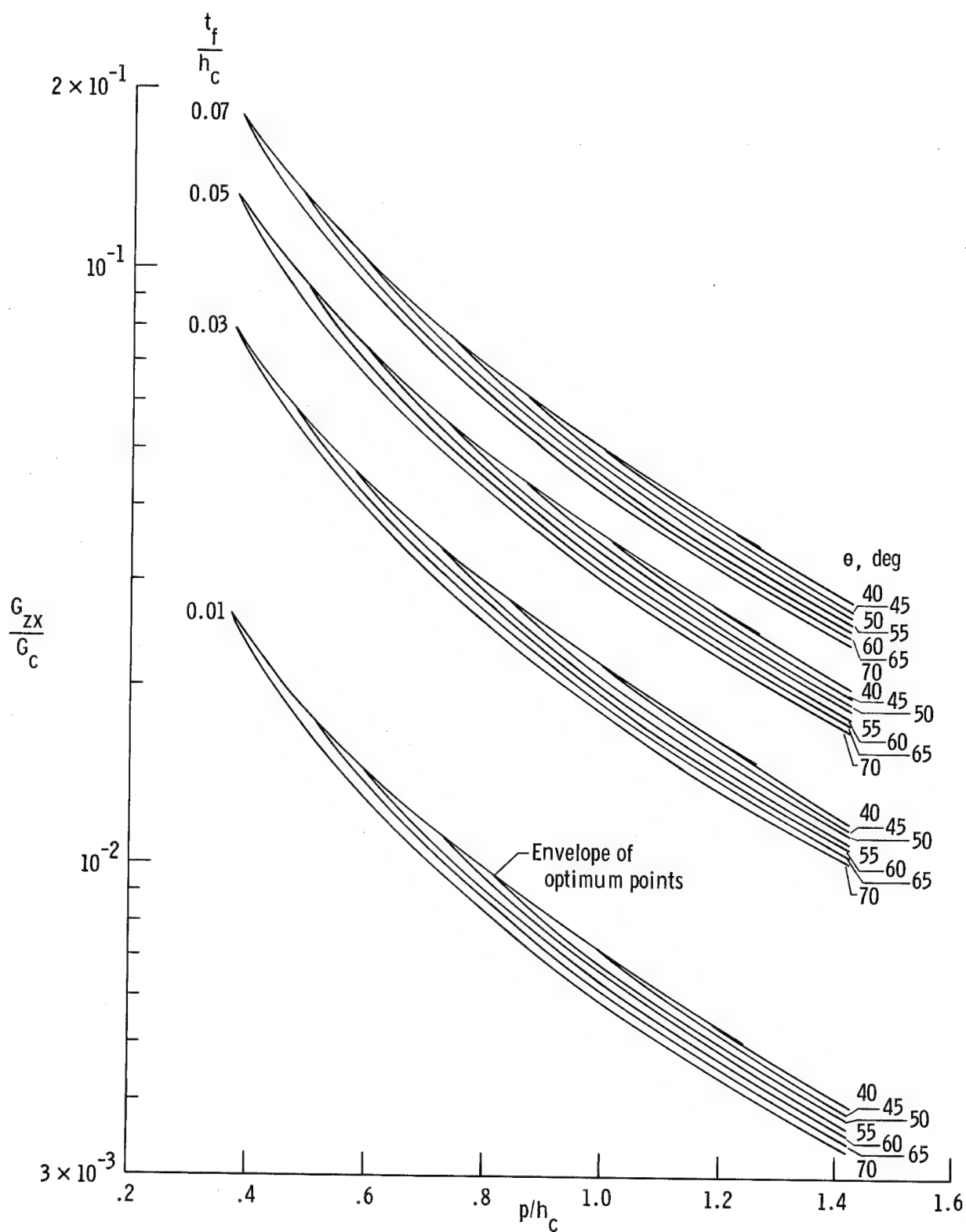
Figure 23. *Shear modulus G_{zx} for honeycomb core. $R = t_c = t_f$.*
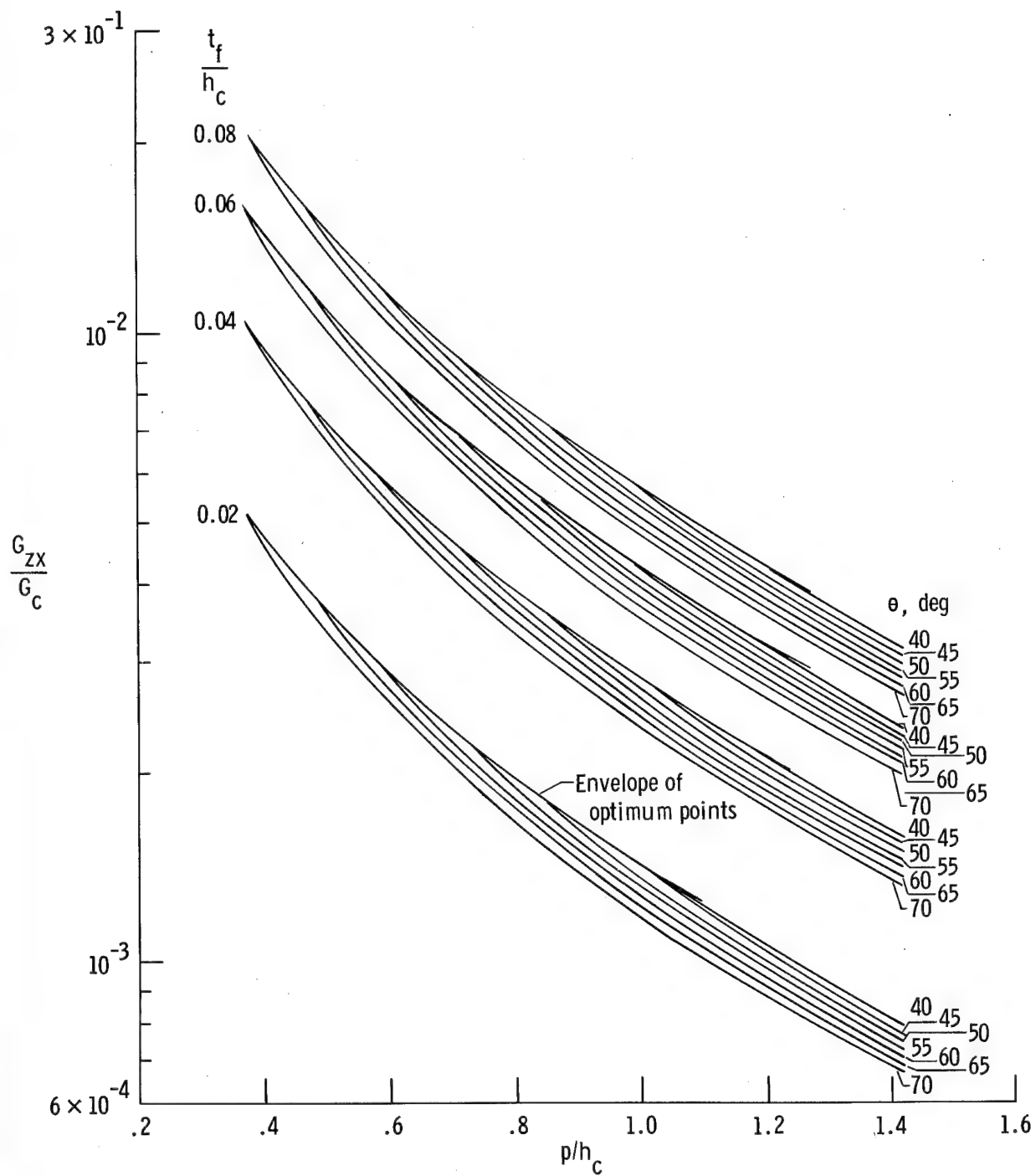
Figure 23. Concluded.
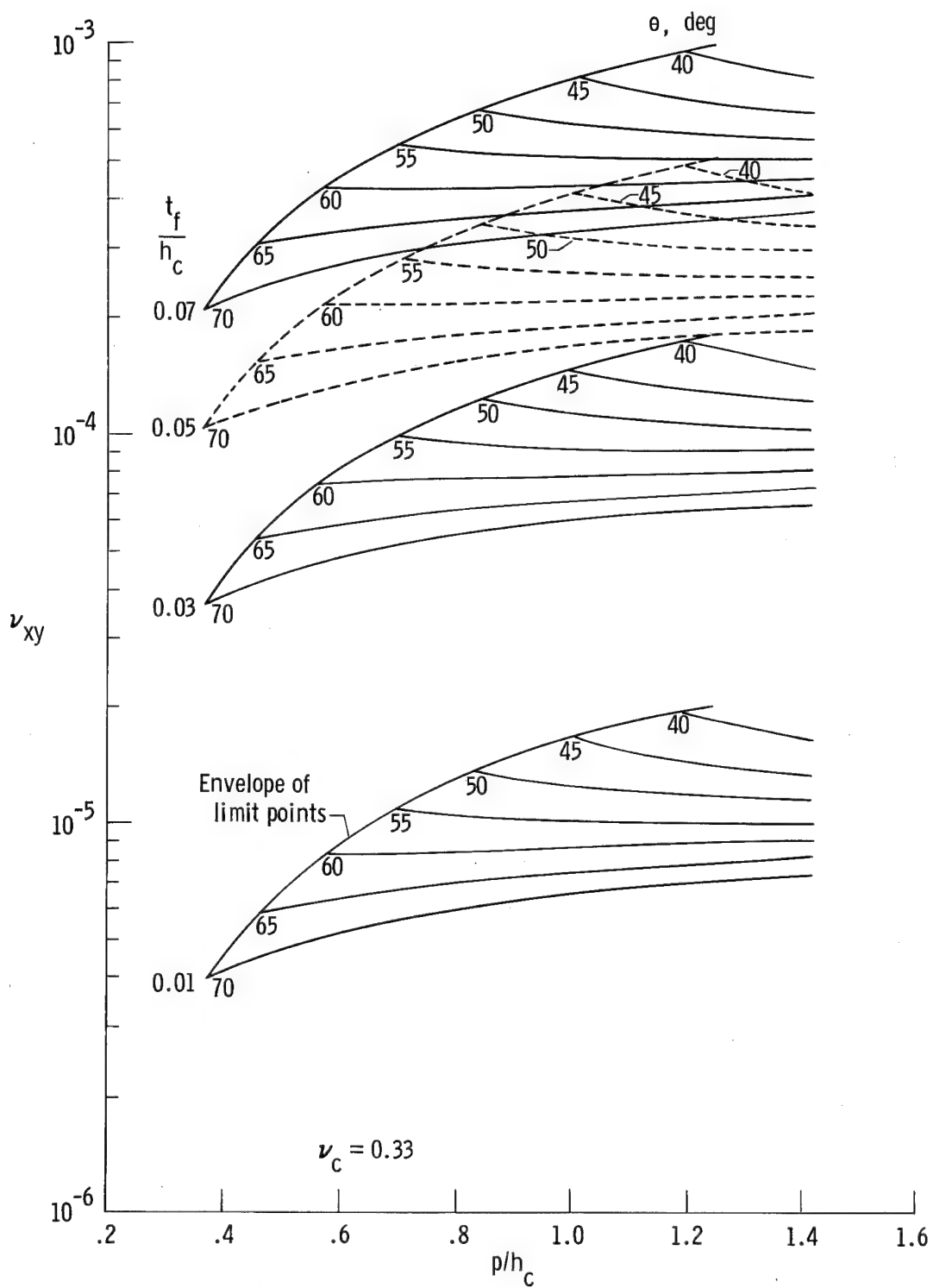
Figure 24. Poisson ratio ν_{xy} for honeycomb core. $R = t_c = t_f$.

Figure 24.   Concluded.

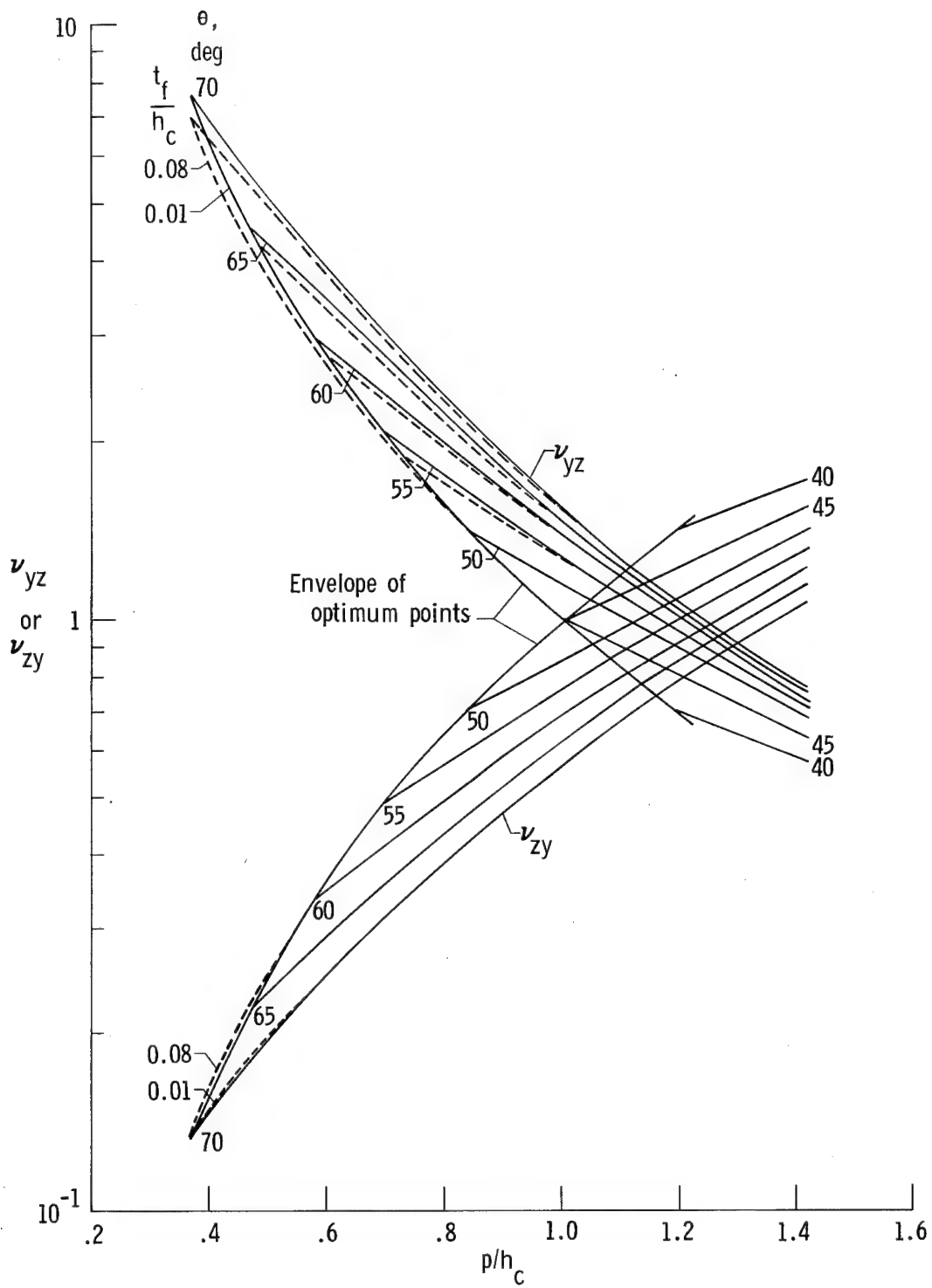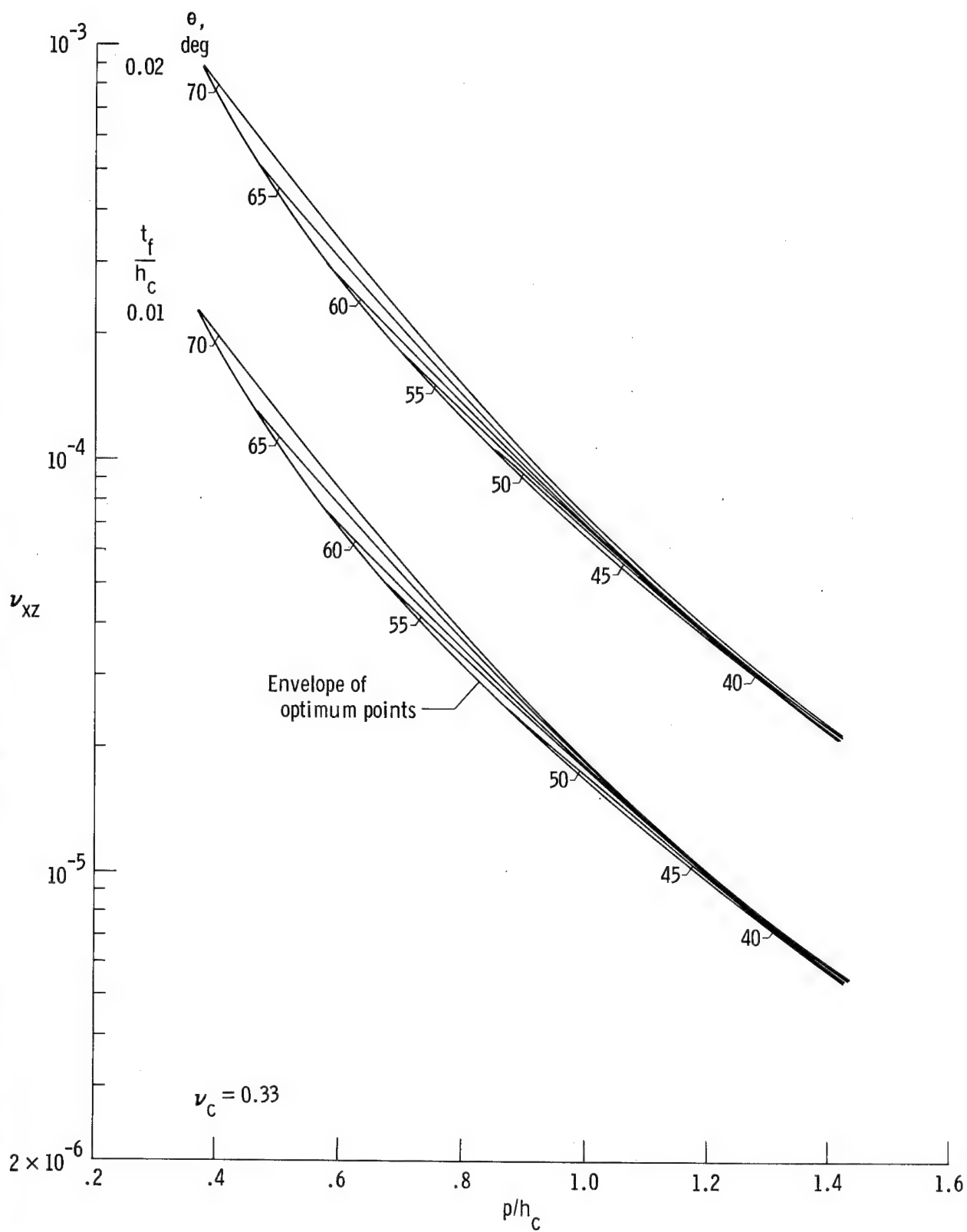Figure 25. Poisson ratios ν_{yz} and ν_{zy} for honeycomb core. $R = t_c = t_f$.

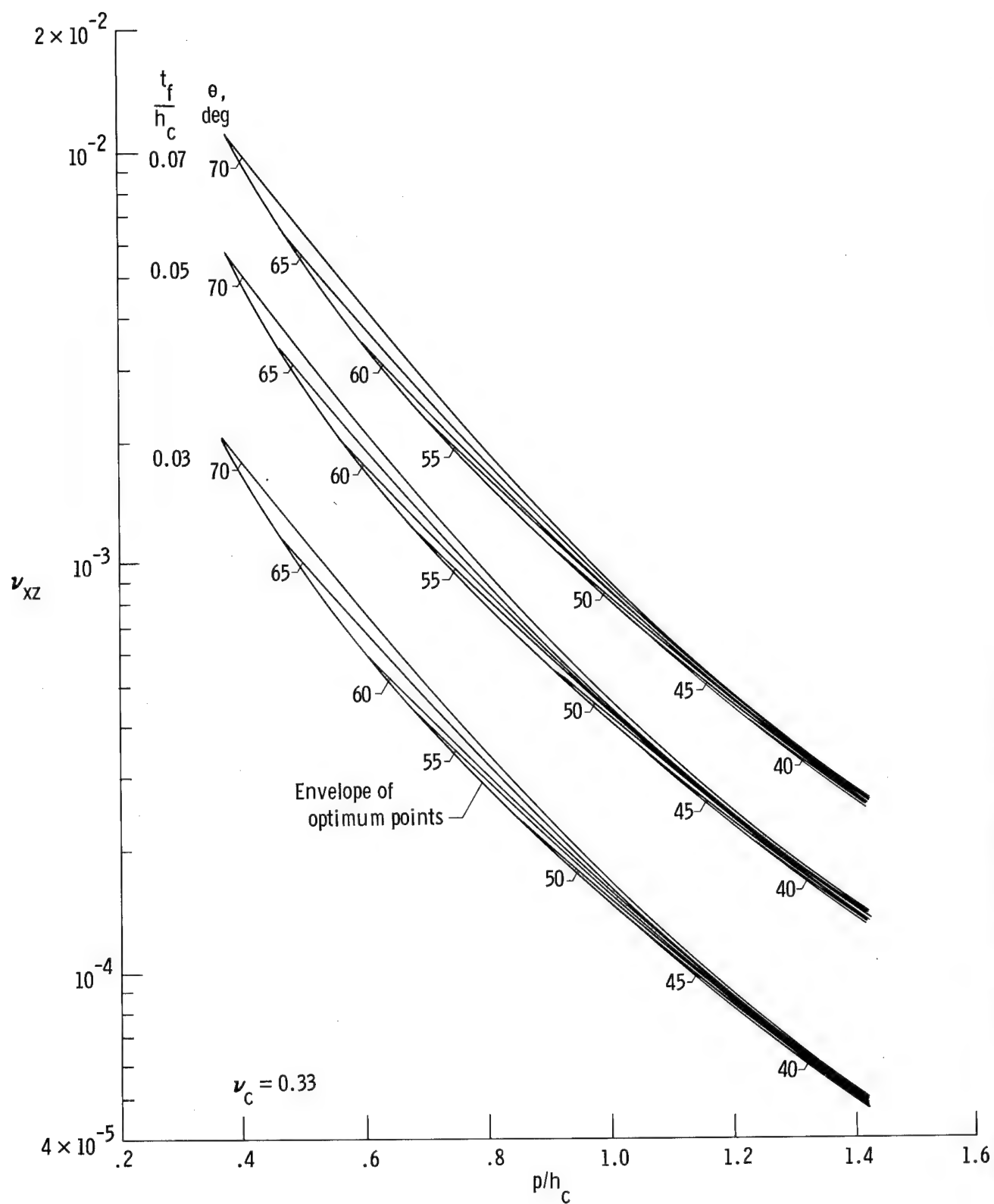Figure 26. Poisson ratio ν_{xz} for honeycomb core. $R = t_c = t_f$.

Figure 26.   Continued.
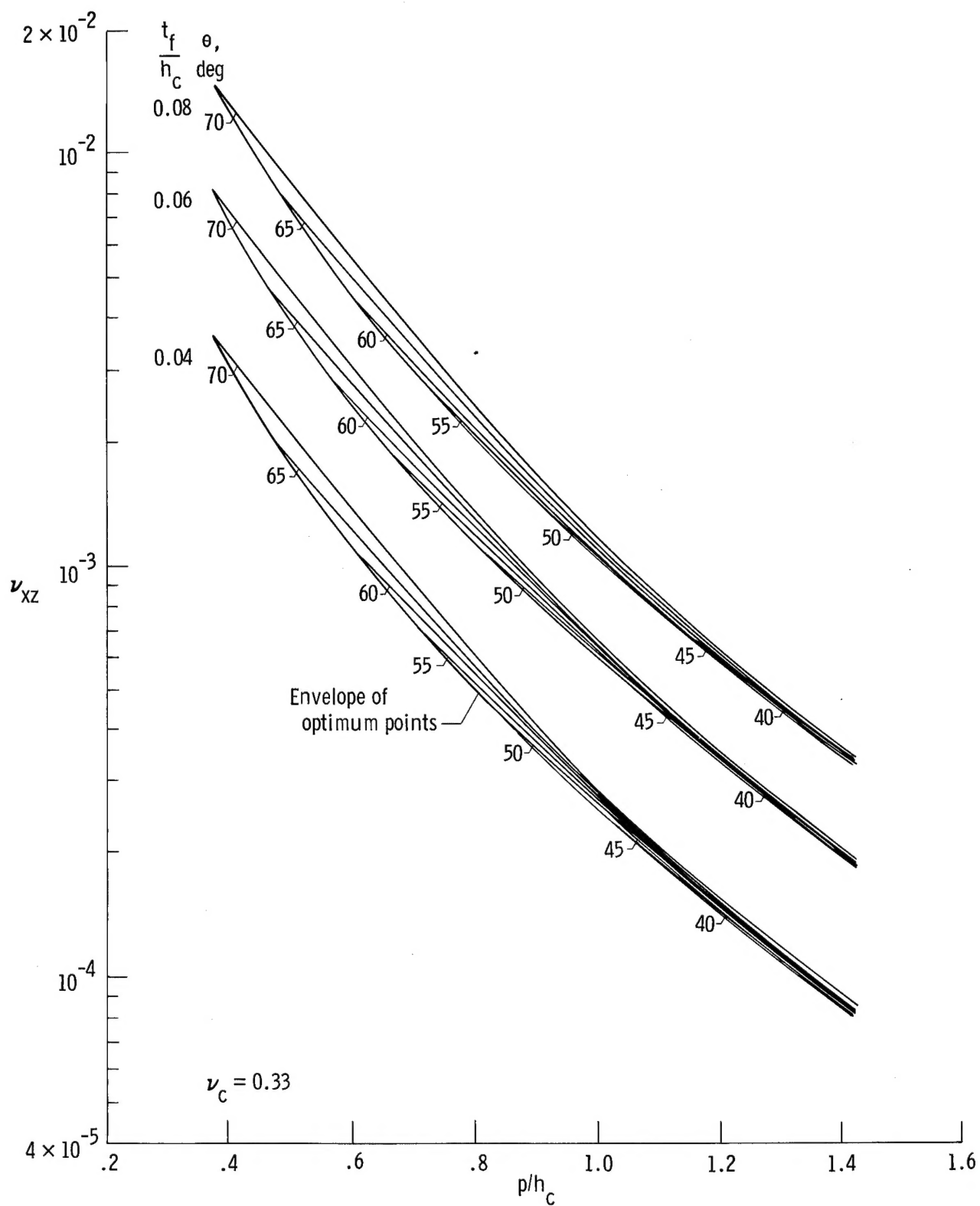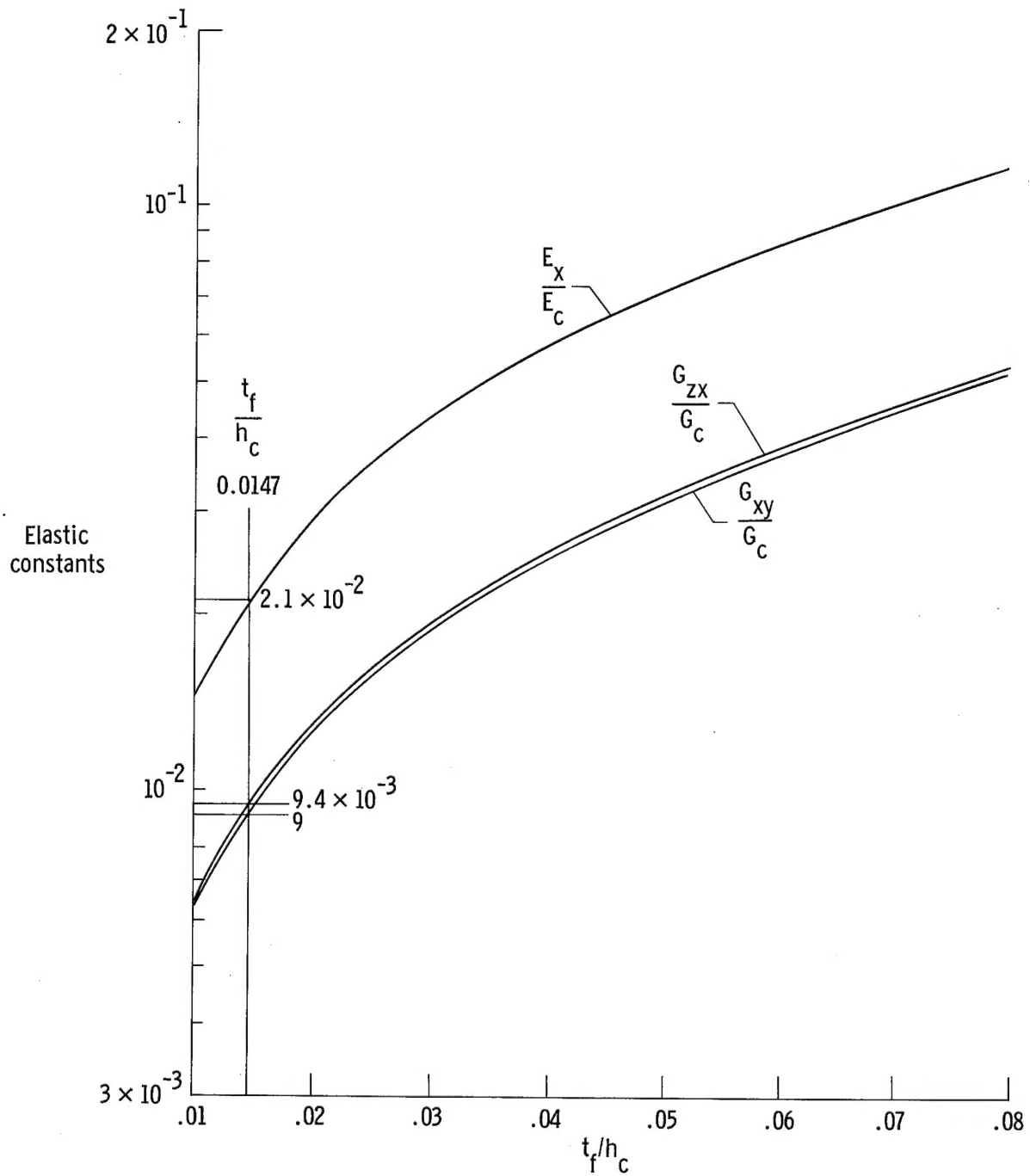
Figure 26. Concluded.

Figure 27. Variations of elastic constants with t_f/h_c for honeycomb core. $p/h_c = 0.9825$; $\theta = 60°$; $R = t_c = t_f$.

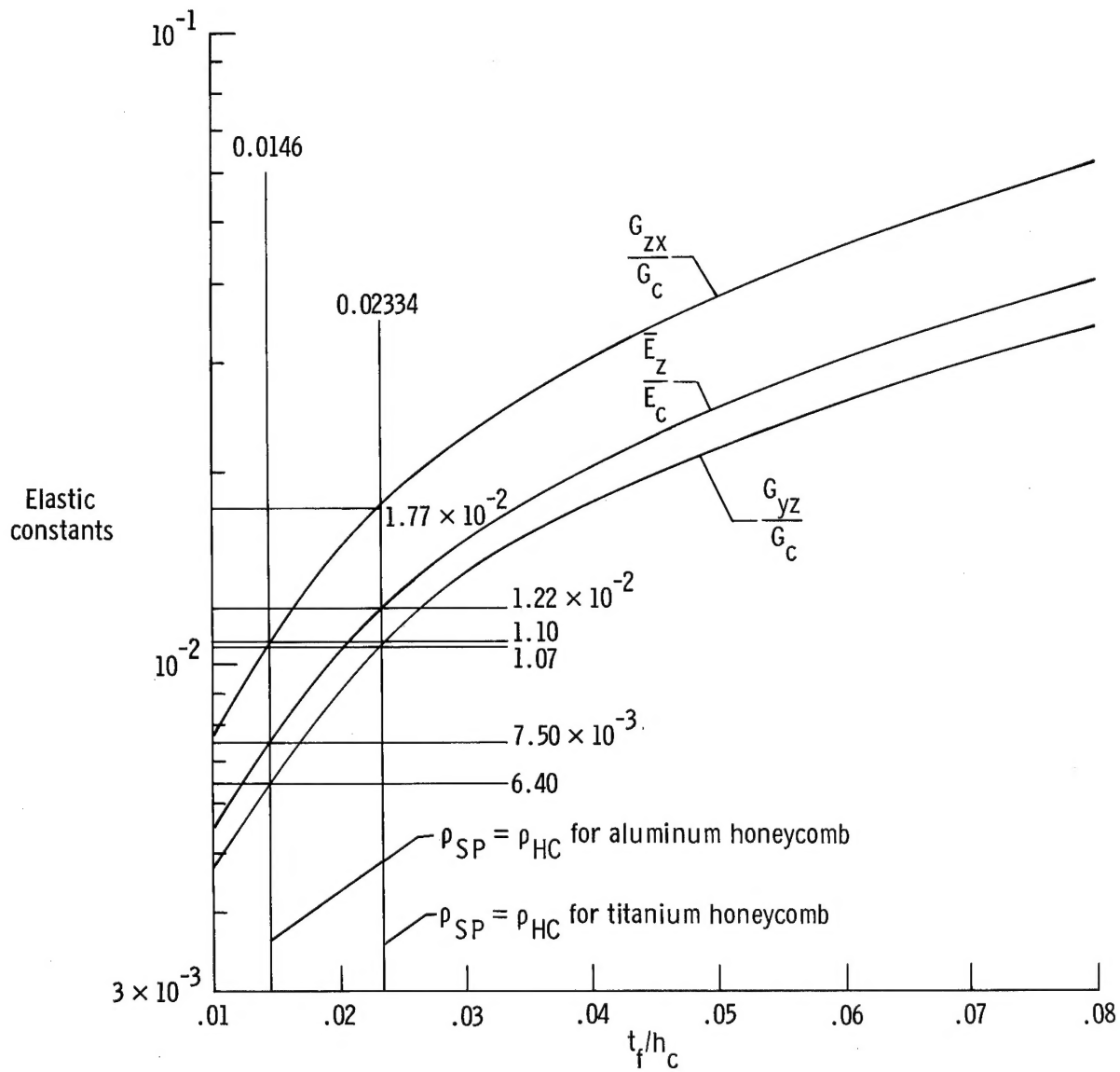Figure 28. Variations of elastic constants with t_f/h_C for SPF/DB corrugated sandwich core. $f = 0$; $\theta = 60°$; $R = t_f$.

1. Report No. NASA TP-1562	2. Government Accession No.	3. Recipient's Catalog No.
4. Title and Subtitle ELASTIC CONSTANTS FOR SUPERPLASTICALLY FORMED/DIFFUSION-BONDED CORRUGATED SANDWICH CORE		5. Report Date May 1980
		6. Performing Organization Code
7. Author(s) William L. Ko		8. Performing Organization Report No. H-1094
		10. Work Unit No.
9. Performing Organization Name and Address NASA Dryden Flight Research Center P.O. Box 273 Edwards, California 93523		
		11. Contract or Grant No.
		13. Type of Report and Period Covered Technical Paper
12. Sponsoring Agency Name and Address National Aeronautics and Space Administration Washington, D.C. 20546		
		14. Sponsoring Agency Code

15. Supplementary Notes

This report is an expanded version of "Elastic Constants for Superplastically Formed/Diffusion-Bonded Sandwich Structures" by the same author (AIAA Paper No. 79-0756).

16. Abstract

This paper presents formulae and associated graphs for evaluating the effective elastic constants for a superplastically formed/diffusion-bonded (SPF/DB) corrugated sandwich core.

The results were used in the comparison of structural stiffnesses of the above sandwich core and a honeycomb core under conditions of equal sandwich core density.

It was found that the stiffness in the thickness direction of the optimum SPF/DB corrugated core (that is, triangular truss core) was lower than that of the honeycomb core, and that the former had higher transverse shear stiffness than the latter.

17. Key Words (Suggested by Author(s)) Stiffness Structural properties	18. Distribution Statement Unclassified—Unlimited Category: 39

19. Security Classif. (of this report) Unclassified	20. Security Classif. (of this page) Unclassified	21. No. of Pages 83	22. Price* $4.75

For sale by the National Technical Information Service, Springfield, Virginia 22161